

Quote

"To build may have to be the slow and laborious task of years. To destroy can be the thoughtless act of a single day."

Winston Churchill

University of Alberta

Flammability Hazards of Fuel System Leak Testing

by

Kevin Michael Frank



A thesis submitted to the Faculty of Graduate Studies and Research in
partial fulfillment of the requirements for the degree of

Master of Science

Department of Mechanical Engineering

Edmonton, Alberta

Fall 2006



Library and
Archives Canada

Bibliothèque et
Archives Canada

Published Heritage
Branch

Direction du
Patrimoine de l'édition

395 Wellington Street
Ottawa ON K1A 0N4
Canada

395, rue Wellington
Ottawa ON K1A 0N4
Canada

Your file *Votre référence*

ISBN: 978-0-494-22266-9

Our file *Notre référence*

ISBN: 978-0-494-22266-9

NOTICE:

The author has granted a non-exclusive license allowing Library and Archives Canada to reproduce, publish, archive, preserve, conserve, communicate to the public by telecommunication or on the Internet, loan, distribute and sell theses worldwide, for commercial or non-commercial purposes, in microform, paper, electronic and/or any other formats.

The author retains copyright ownership and moral rights in this thesis. Neither the thesis nor substantial extracts from it may be printed or otherwise reproduced without the author's permission.

AVIS:

L'auteur a accordé une licence non exclusive permettant à la Bibliothèque et Archives Canada de reproduire, publier, archiver, sauvegarder, conserver, transmettre au public par télécommunication ou par l'Internet, prêter, distribuer et vendre des thèses partout dans le monde, à des fins commerciales ou autres, sur support microforme, papier, électronique et/ou autres formats.

L'auteur conserve la propriété du droit d'auteur et des droits moraux qui protègent cette thèse. Ni la thèse ni des extraits substantiels de celle-ci ne doivent être imprimés ou autrement reproduits sans son autorisation.

In compliance with the Canadian Privacy Act some supporting forms may have been removed from this thesis.

Conformément à la loi canadienne sur la protection de la vie privée, quelques formulaires secondaires ont été enlevés de cette thèse.

While these forms may be included in the document page count, their removal does not represent any loss of content from the thesis.

Bien que ces formulaires aient inclus dans la pagination, il n'y aura aucun contenu manquant.


Canada

University of Alberta

Library Release Form

Name of Author: Kevin Michael Frank

Title of Thesis: Flammability Hazards of Fuel System Leak Testing

Degree: Master of Science

Year this Degree Granted: 2006

Permission is hereby granted to the University of Alberta to reproduce single copies of this thesis and to lend or sell such copies for private, scholarly, or scientific research purposes only.

The author reserves all other publication and other rights in association with the copyright in the thesis, and except as hereinbefore provided, neither the thesis nor any substantial portion thereof may be printed or otherwise reproduced in any material form whatever without the author's prior written permission.

Kevin Michael Frank

RR # 3

Rimbey, Alberta

Canada T0C 2J0

University of Alberta

Faculty of Graduate Studies and Research

The undersigned certify that they have read, and recommend to the Faculty of Graduate Studies and Research for acceptance, a thesis entitled Flammability Hazards of Fuel System Leak Testing submitted by Kevin Michael Frank in partial fulfillment of the requirements for the degree of Master of Science .

Dr. M. D. Checkel

Dr. C. R. Koch

Dr. R. E. Hayes

Date _____

ABSTRACT

To meet current emission regulations, automotive evaporative emissions systems must meet maximum leak rate specifications. Leaks exceeding the required rate must be located and repaired. Evaporative emissions systems are commonly leak tested with smokes or aerosols. Under normal conditions, the contents of automotive fuel tanks are inherently safe from fire and explosions because the gasoline vapour contained within is too rich to burn. Introducing a typical leak testing flow will dilute the over-rich mixture, creating flammable volumes within the tank if air is used as the carrier gas for the leak test fluid.

This thesis considers the gasoline vapour behaviour in an automotive gasoline tank under leak testing conditions. An experimental study was performed on a typical gas tank and was used to verify the results obtained from a numerical model. Significant flammable volumes were found under some conditions. Recommendations for preventing flammable mixture formation during leak testing are included.

ACKNOWLEDGEMENTS

I would like to thank to following people for their contribution to this project:

Dr. M.D. Checkel for his supervision and guidance.

Richard Banyard and Star Envirotech Inc. for providing funding and assistance throughout the project.

Kelvin Lien for his assistance with sampling methods and gas chromatograph work.

Phil Malanchuk for his help with all things electrical.

Machine Shop staff who contributed to this project including Roger Marchand, Bernie Faulkner, and Rick Bubenko.

Natural Science and Engineering Research Council (NSERC), Faculty of Engineering, Alberta Heritage Scholarship Fund, and Walter Johns for their financial contribution.

The Combustion & Environment Research Group for providing technical and non-technical support.

Finally, my family, who have supported me throughout my education and have kept the farm going with minimal assistance.

DEDICATION

To Kayda

TABLE OF CONTENTS

1	Introduction	1
	References	5
2	Evaporative Emissions System Background	6
2.1	Introduction	6
2.2	Gas Mixtures and Fuel Volatility	7
2.3	A History of Gasoline RVP Requirements	10
2.4	Evaporative Emissions System Overview	11
2.5	Leak Testing Procedures	14
2.6	Potential Leak Locations	15
2.7	Potential Ignition Sources	15
	2.7.1 Internal Ignition Sources	16
	2.7.2 External Ignition Sources	17
2.8	Previous Fuel System Flammability Research	18
	2.8.1 Aviation Fuel Tank Research	20
	2.8.2 Automotive Research	20
2.9	Summary and Conclusions	21
	References	22

3	Fuel Tank Vapour Fraction Under Imposed Flow Conditions	26
3.1	Introduction	26
3.2	Methodology	27
3.3	Experimental Setup	29
3.3.1	Equipment	29
3.3.2	Gasoline Samples	31
3.3.3	Oxygen Sensor Calibration Procedures	34
3.3.4	Test Procedures	35
3.4	Results	38
3.4.1	Inlet Condition Effects	38
3.4.2	Inlet Flow Rate Effects	39
3.4.3	Initial Volatility Effects	40
3.4.4	Weathering Effects	44
3.4.5	Weathering and Volatility Comparison	46
3.4.6	Fuel Tank Flammable Mixture Ignition	48
3.5	Conclusion	48
	References	50
4	Numerical Simulation of Vapour Composition In Nearly-Empty Fuel Tanks Under Imposed Flow Conditions	52
4.1	Introduction	52
4.2	Physical Description	53
4.2.1	Geometry	53
4.2.2	Fuel Tank Contents	53
4.2.3	Initial Conditions	53

4.2.4	Leak Testing Flow Regimes	55
4.3	Model Characteristics	55
4.3.1	Model Theory	56
4.3.2	Reynolds Averaged Governing Equations	57
4.3.3	Turbulence Model	58
4.3.4	Fluid Properties	58
4.3.5	Density Considerations	58
4.3.6	Boundary Conditions	59
4.4	Solution Strategy	60
4.5	Results	61
4.5.1	Air Flow Characteristics	61
4.5.2	Comparison to Experimental Results	61
4.5.3	Flammable Mixtures	61
4.6	Summary And Conclusions	67
	References	69
5	Conclusions and Recommendations	71
5.1	Hazard Reduction Analysis	71
5.2	Summary and Conclusions	73
5.3	Recommendations	76
5.4	Future Work	76
	References	78
A	Equilibrium Vapor Pressure Measurements	79
A.1	Introduction	79

A.2	Vapour Pressure Measurement Standards	79
A.3	Test Equipment and Procedure	80
A.4	Vapour Pressure Measurement Uncertainty	82
A.4.1	Pentane Vapour Pressure Measurement	83
A.4.2	Gasoline Vapour Pressure Measurement	83
A.4.3	Repeatability	84
	References	86
B	Gas Chromatograph Measurements	87
B.1	Introduction	87
B.2	GC Measurement Procedure	87
B.3	Uncertainty in GC Measurements	88
	References	93
C	EnviteC® O₂ Sensor Calibration	94
C.1	Introduction	94
C.2	Sensor Description and Theory	94
C.3	Signal Conditioning	96
C.4	Sensor Calibration	97
C.4.1	N ₂ -Air Calibration	97
C.4.2	Butane Calibration	98
C.4.3	Gasoline Vapour Calibration	98
C.5	Sensor Transient Response	100
C.5.1	Oxygen Concentration Response	100
C.5.2	Total Pressure Response	103

C.5.3	Moving Average Filter Effects on Transient Response	104
C.6	Measurement Uncertainty	105
C.6.1	Transient Response Uncertainty	105
C.6.2	Non-linear Sensor Response Uncertainty	106
	References	107
D	CFX Model	108
D.1	Introduction	108
D.2	Fluid Properties	108
D.3	Fuel Species Sensitivity Study	109
D.4	Mesh Refinement Study	109
D.5	Sample CFX Input File	113
	References	122
E	Fuel Tank Flammable Mixture Ignition: Field Testing	123
E.1	Introduction	123
E.2	Equipment and Procedure	123
E.3	Results	124
E.4	Conclusions	124

LIST OF TABLES

3.1	Oxygen Sensor Locations	31
3.2	Tested Gasoline Volatilities	34
3.3	Weathered Gasoline Vapour Fractions	34
4.1	Initial Conditions Considered for Modeling	55
B.1	Nitrogen Sample Statistics	89
C.1	Oxiplus A Sensor Specifications	95
D.1	Coarse Mesh Statistics	111
D.2	Fine Mesh Statistics	111

LIST OF FIGURES

1.1	US Public Service Station Fires (1980-1998)	2
2.1	Certification Fuel Composition	9
2.2	Certification Fuel Vapour Composition	10
2.3	Gasoline Vapour Pressure vs. Temperature	12
2.4	Common Evaporative Emissions System Components	13
2.5	Typical Distribution of Leak Locations	16
2.6	Quench Distances for Typical Gasoline Vapour Components	18
2.7	Iso-octane Flame Speed at Ambient Conditions	19
2.8	Critical Diameter for Backward Flame Propagation	19
3.1	Automotive Fuel Tank Configuration	30
3.2	Oxygen Sensor Locations	32
3.3	Flow Diagram	33
3.4	Gasoline Vapour/ Air Calibration of Sensor 1	35
3.5	Butane-Air Calibration of Sensor 1	36
3.6	Typical Test Timeline	37
3.7	Gasoline Vapour Profiles	38
3.8	Comparison of Service Port and Filler Cap Inlet Flows	40

3.9	Service Port Inlet Flow Rates	41
3.10	Filler Cap Flow Rates	42
3.11	Volatility Effects	43
3.12	Return to Equilibrium After Flow	44
3.13	Liquid Volume Effect on Weathering	45
3.14	Weathering Effects	46
3.15	Volatility - Weathering Comparison	47
4.1	Fuel Tank Model Geometry	54
4.2	Velocities During Service Port Inlet Flow	62
4.3	Comparison of Model and Experimental Gasoline Vapour Mole Fraction, Weathered Gas	63
4.4	Comparison of Model and Experimental Gasoline Vapour Mole Fraction, Low Volatility Gas	64
4.5	Comparison of Model and Experimental Gasoline Vapour Mole Fraction	65
4.6	Effect of Initial Composition on Flammable Volume	66
4.7	Effect of Flow Rate on Flammable Volume	67
4.8	Low Volatility Flammable Vapour Formation	68
5.1	Nitrogen as Test Fluid	74
A.1	Vapour Pressure Test Bomb Construction	81
A.2	Vapour Pressure Test Procedure	82
A.3	Pentane Vapour Pressure Measurement	84
A.4	Vapour Pressure Measurements for Two Gasoline Blends	85

B.1	Nitrogen GC Sample	90
B.2	Lab Air GC Sample	91
B.3	Fuel Tank GC Sample	92
C.1	O ₂ Sensor Schematic	95
C.2	Sensor Output Amplification	96
C.3	N ₂ -Air Calibration	98
C.4	Butane-Air Calibration	99
C.5	Calibration Method Comparison	100
C.6	Transfer Functions for Sensors 1-4.	101
C.7	Transfer Functions for Sensors 5-7.	102
C.8	Air to Nitrogen Transient Response	103
C.9	Transient Response to Pressure Step Input	104
C.10	Filtered Transient Response	105
D.1	Saturated Hydrocarbon Binary Diffusivity in Air	109
D.2	Fuel Species Sensitivity Study	110
D.3	CFD Model Mesh	111
D.4	Fine CFD Model Mesh	112
D.5	Mesh Sensitivity Study	112
E.1	Flammable Mixture Ignition Illustration	125

LIST OF NOMENCLATURE

D_{AB}	Binary diffusivity for gasoline into air
$DVPE$	Dry vapor pressure equivalent
k_B	Boltzman constant
LFL	Lower flammable limit
\dot{m}''_{air}	Air mass flux
$\dot{m}''_{gasoline}$	Gasoline mass flux
$\dot{m}_{gasoline}$	Gasoline mass flow
M	Molar mass
M_A	Molar mass of species A
P	Pressure
P_m	Mixture pressure
P_T	Total pressure
P_i	Partial pressure of mixture component i
P_{O_2}	Oxygen partial pressure
$P_{gasoline}$	Gasoline vapour partial pressure
P_{atm}	Atmospheric pressure
P_{sat}	Saturated vapour pressure

R	Gas constant
\bar{R}	Universal gas constant
RVP	Reid vapour pressure
S_M	Momentum source term
T	Temperature
T_m	Mixture temperature
T_{amb}	Ambient temperature
UFL	Upper flammable limit
\mathbf{U}	Velocity vector
$\bar{\mathbf{U}}$	Reynolds-averaged velocity vector
\mathbf{u}	Fluctuating velocity vector
V_{out}	Sensor output voltage
V_m	Mixture volume
V_i	Partial volume of mixture component i
$Y_{gasoline}$	Gasoline vapour mass fraction
Y_{O_2}	Oxygen mass fraction
$\chi_{gasoline}$	Gasoline vapour mole fraction
χ_{O_2}	Oxygen mole fraction
ϵ_A	Lennard-Jones energy for species A
Ω_D	Collision integral
ρ	Density
ρ_{ref}	Reference density
σ_A	Hard sphere diameter of species A
μ	Absolute viscosity

CHAPTER 1

INTRODUCTION

VEHICLE emissions are a major source of pollution today. Passenger cars were the third largest source of air emissions in California in 1995.¹ One of the major components is evaporative emissions from evaporating fuel.² Most vehicles have systems to contain the fuel vapours that comprise these emissions, but leaks in aging or poorly maintained systems will allow the fuel vapour to enter the environment.

The requirement for evaporative emissions system testing is a result of air quality regulations introduced in the past decade. The regulations for testing evaporative emissions systems are fairly recent. Evaporative emissions leak testing is only now becoming prevalent in the automotive repair environment, and therefore the research into the potential hazards associated with evaporative emissions system leak testing is limited.

New vehicles typically include an on-board diagnostics system that indicates excessive leakage in these systems, but provide only indication and not the location of the leak required for repair. An additional test is required to identify the location of the leak, where a test fluid is introduced to the system and provides some form of indication where the fluid exits the system through the leak.

The driving component of the test fluid is usually air or nitrogen. Fluid introduced to the system mixes with the fuel vapour - air mixture within, reducing the fuel vapour concentration. Gasoline is designed to produce

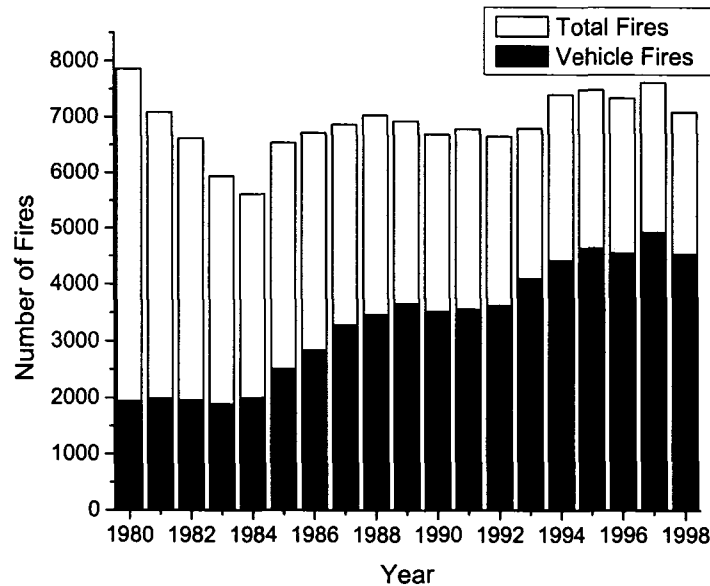


Figure 1.1: Vehicle and total fires for public service stations in the US, 1980-1998. Total fires have remained relatively constant while vehicle fires have a significant upward trend.

vapour - air mixtures in the system too rich to burn under normal circumstances. Introducing air to the system creates a range of gasoline vapour concentrations from too lean to too rich, encompassing the flammable range. The extent of the vapour volume that is flammable defines the hazard of leak testing with air. This project identifies the potential flammable volumes created in evaporative emissions systems when air is introduced to the system.

Most leak location testing is done at an automotive repair facility or service station. Information on fires at these facilities in the United States is available for the years 1980-1998 from the National Fire Protection Association (NFPA).³ A summary of service station fires over this period is shown in figure 1.1. Total service station fires have remained relatively constant, but vehicle fires at these facilities have shown a definite upward trend.

No statistics available point directly to evaporative emission system leak

testing as a source of vehicle fires at these facilities. However, of the fires listed, 77% were caused by mechanical or electrical problems. Part failures, leaks, or breaks were attributed as the ignition factor to 25% of the fires, and gasoline was the first material ignited in 32% of the fires. These statistics undoubtedly include other sources of fire not related to evaporative emissions testing. For example, a fire started by a broken liquid fuel line would qualify as a part failure, and gasoline would likely be the first material ignited. Regardless, the statistics currently available provide some evidence that further investigation is warranted.

This dissertation describes an experimental and modeling study carried out to evaluate the potential fire and explosion hazards associated with leak testing activities in automotive fuel and evaporative emission systems.

Chapter 2 provides a background on evaporative emissions systems and the requirements for leak testing. A summary of previous work on flammable mixtures in fuel tanks is included, as well as potential ignition sources that could ignite flammable mixtures formed inside the tank.

Chapter 3 describes experimental testing on a typical automotive fuel tank. The development of the test rig is included as well as results for typical leak detection scenarios. The results of this chapter are used for comparison to the model results of chapter 4.

Chapter 4 describes a simulation model that predicts flammable mixtures formed within evaporative emissions systems, and compares model results to experimental results. The major factors that affect flammable mixtures in fuel tanks are discussed.

Chapter 5 summarizes the work completed and the conclusions made. Recommendations are included for preventing flammable mixtures from forming in automotive fuel tanks during leak testing procedures, and suggestions for future work are presented.

The method used for measuring equilibrium gasoline vapour pressure is covered in appendix A. Appendix B describes the gas chromatograph sampling and analysis procedure used. Appendix C includes the use and calibration of oxygen sensors to determine the gasoline vapour composition

in the fuel tank during leak testing procedures. Appendix D contains an example of the computational fluid dynamics model for gasoline vapour in a gas tank during leak testing. Appendix E describes a fuel tank flammable mixture ignition test conducted in the field.

REFERENCES

- [1] Anonymous. Top 25 emissions report. Retrieved July 27, 2006, from http://www.arb.ca.gov/app/emsinv/t25cat/cat_top25.php. California Air Resources Board.
- [2] T. V. Johnson. Gasoline vehicle emissions - SAE 1999 in review. *SAE Paper No. 2000-01-0855*, 2000.
- [3] Anonymous. "Special data information package: Fires in or at service stations and motor vehicle repair and paint shops". National Fire Protection Association, 2002.

CHAPTER 2

EVAPORATIVE EMISSIONS SYSTEM BACKGROUND

Evaporative emissions systems are designed to contain vapour generated from volatile gasoline in automobiles. Any leaks within the system result in fuel emissions to the environment and recent regulations limiting evaporative emissions have resulted in a need to locate and repair leaks. Previous work on automotive fuel system flammability has either focused on low temperature conditions where the equilibrium gasoline vapour concentration was within the flammable range, or flammable conditions created by refueling vapour recovery systems. The aerospace industry, which uses less volatile fuels and operates under a wider range of conditions, has done a considerable amount of research into preventing fuel tank vapour space flammability. Potential ignition sources both inside and outside fuel tanks are surveyed.

2.1 Introduction

AT atmospheric temperature and pressure, gasoline is a volatile liquid. When liquid gasoline is exposed to air it will produce vapour through evaporation at the gas-liquid interface until an equilibrium vapour pressure is attained. As a fuel, gasoline vapour can be readily ignited when combined with sufficient oxygen in the presence of an ignition source. Flammable gasoline vapour/air mixtures within automotive fuel systems are prevented by blending gasoline to have sufficient volatility that it will produce a vapour fraction above the upper flammable limit (UFL) at equilibrium. While normal venting and air intake cycles encountered from temperature and liq-

uid volume variations within the fuel system do cause fluctuations from equilibrium, the volatility has an adequate margin of safety so the gasoline vapour fraction does not enter the flammable range.¹

Excess fuel vapour is produced from evaporation, temperature cycling, and refueling and is a major source of pollution if the vapour space is vented to the atmosphere. Modern vehicles are equipped with an evaporative emissions reduction system designed to capture any excess gasoline vapours and ultimately route them to the engine for combustion. However, the effectiveness is reduced if there are any leaks in the system.

Recent regulations requiring adequate evaporative emissions system performance have brought about the requirement for locating and repairing evaporative emissions system leaks and testing procedures have been developed to find such leaks. Many test methods introduce air to the system to find leaks, effectively disrupting the gasoline liquid-vapour equilibrium. The consequences of such an action have not been thoroughly investigated thus far, and to date the possibility of producing flammable mixtures during leak testing has been unclear.

2.2 Gas Mixtures and Fuel Volatility

The potential of a gas mixture to burn or its flammability is related to the properties of the gas mixture. Combustion requires 3 elements: fuel in sufficient quantities, oxygen in sufficient quantities, and energy to initiate the reaction. The relative fuel and oxygen quantities are a property of the mixture, while energy can come from a variety of sources, including flames, electrical sparks, or hot surfaces. The most common flammable mixtures are fuel/air mixtures, with air as the oxygen source.

The relative proportions of each species in a mixture can be described on either a mass basis or a molar (volumetric) basis. Flammable mixtures are typically quantified on a molar basis. The molar fraction of a mixture can be modeled on a partial pressure or partial volume model, known as Dalton's

Law and Amagat's Law, respectively.²

$$P_m = \sum_{i=1}^k P_i(T_m, V_m) \quad (2.1)$$

$$V_m = \sum_{i=1}^k V_i(T_m, P_m) \quad (2.2)$$

where P_i and V_i are the partial pressure and partial volume of the mixture component i , and T_m , P_m , and V_m are the total temperature, pressure, and volume of the mixture. Dalton's Law and Amagat's Law are exact for ideal gas mixtures, which follow the relationship below for density.

$$\rho = \frac{P}{RT} \quad (2.3)$$

where P is the mixture pressure, T is the mixture temperature, and

$$R = \frac{\bar{R}}{M} \quad (2.4)$$

where \bar{R} is the ideal gas constant and M is the mixture molar mass.

Typical hydrocarbon automotive fuels (gasoline, diesel) are comprised of a mixture of many hydrocarbon species that form a liquid-vapour interface at room temperature. The composition of a certification fuel commonly used for emissions testing is shown in figure 2.1.³ The majority of the components are in the C_5 - C_8 range, (ie. contain 5 to 8 carbon atoms per molecule), with small amounts of hydrocarbons outside this range.

Like water or other volatile liquids, some proportion of these fuels will evaporate or volatilize and form vapour until the space above the liquid is saturated. Lighter, more volatile hydrocarbons will tend to evaporate more readily than heavier hydrocarbons. Figure 2.2 lists the composition for the saturated vapour formed above the previously mentioned certification fuel. The lighter hydrocarbons such as butane form a much higher percentage of the vapour than the liquid, with isobutane, n-butane, and isopentane forming 78% of the vapour mixture.³ Subsequent research performed un-

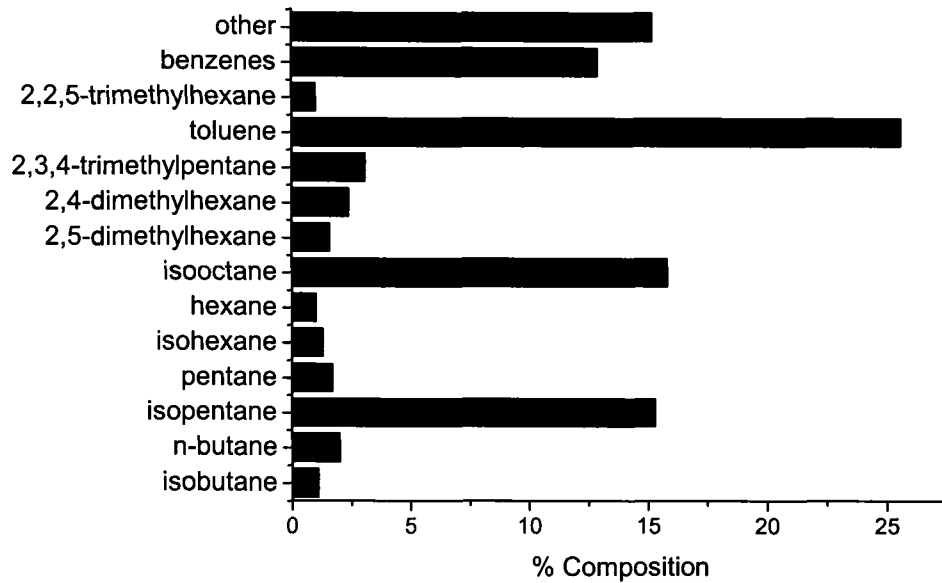


Figure 2.1: Composition of a certification fuel. Note high toluene and isooctane fractions and low butane fractions.

der similar conditions also noted high butane and pentane fractions in the vapour phase.⁴

The partial pressure of fuel vapour at saturation is a function of the temperature and species present and is a measure of the total volatility of the fuel. The Reid Vapour Pressure (RVP) test measures the vapour pressure of a substance at 38°C.⁵ RVP values can be used to compare volatilities of various fuel mixtures. Saturated vapour pressures at other temperatures can be calculated from the RVP with the following relationship, where the RVP is in kPa and the temperature T is in °C.⁶

$$P_{sat} = 10^{\frac{6.08 - 310.8[6.08 - \log(RVP)]}{T + 273}} \quad (2.5)$$

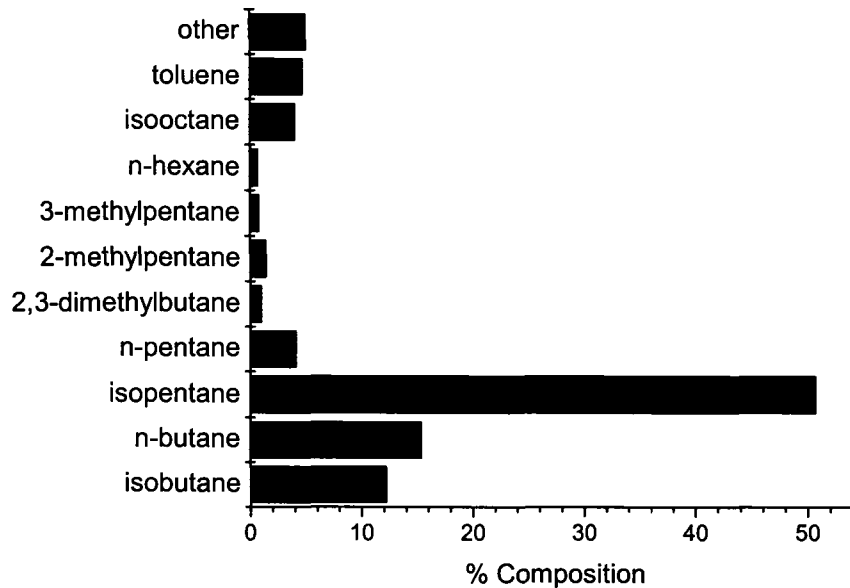


Figure 2.2: Composition of saturated vapour above the previous certification fuel. Toluene and isooctane fractions are much lower and butane is now a major component.

2.3 A History of Gasoline RVP Requirements

Traditionally, gasoline has been blended for high volatility to allow easy engine starting while preventing any fires or explosions in the fuel system by creating a rich fuel condition above the upper flammable limit. The disadvantage of high volatility is increased evaporative emissions, which have been shown to be strongly influenced by gasoline RVP.⁷ In 1989, the EPA introduced Phase I volatility regulations to reduce evaporative emissions during the summer months.⁸ At this time, RVP was required to be as low as 62 kPa (9.0 psi) depending on location and season. Phase II regulations in effect since 1992 require RVP to be less than 54 kPa (7.8 psi) in some states,⁹ but the EPA recommended guideline is as low as 48 kPa (7.0 psi) in regions such as Phoenix, Arizona.¹⁰

Since the more volatile hydrocarbons in gasoline evaporate more readily

than their low volatility counterparts, continued evaporation will change the composition of the liquid fuel. This is known as "weathering". A study in 1989 found that 48 kPa (7.0 psi) RVP gasoline can experience an RVP loss of 3.5 kPa (0.5 psi) during a drive-down from a full tank to empty.¹¹ The decrease in RVP was more pronounced for higher RVP gasoline because of the increased evaporation rate.

In 1990, research was conducted to determine possible flammability hazards under normal driving conditions with EPA's proposed additional Phase II volatility reductions.¹ The primary focus was flammability hazards under normal driving conditions at low temperatures. The vapour pressure curves as a function of temperature for four common gasoline blends can be seen in figure 2.3. The objective was to determine the temperature that low RVP gasoline creates flammable saturated vapours, with the effects of weathering during driving cycles taken into consideration.

Vapour from gasoline with a RVP of 48 kPa (7.0 psi) was found to reach the upper flammable limit at 13° F (-10° C), while 62 kPa (9.0 psi) RVP gasoline produced flammable vapours at 4.6° F (-15° C). This report concluded that flammable mixtures would be more prevalent under the Phase II requirements when low RVP gasoline was combined with low ambient temperatures, but that the associated risk of fires or explosions would remain low. Since the Phase II requirements were enacted in 1992, the additional risk was apparently within acceptable limits.

2.4 Evaporative Emissions System Overview

Evaporative emissions systems were introduced in the 1970s to reduce fuel evaporative emissions losses from vehicles.¹² Typical automotive fuel systems have a rigid fuel tank that stores a volume of liquid gasoline that decreases as the fuel is consumed during operation. The balance of the total contained volume of the fuel system is filled with a gasoline vapour and air mixture. It is not generally feasible to design the fuel system to withstand large differential pressures, so it is usually maintained at or near at-

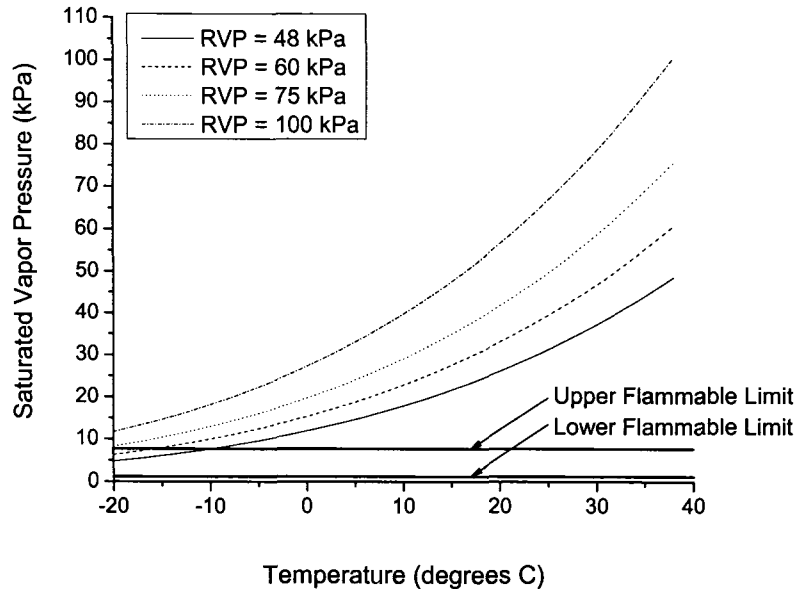


Figure 2.3: Vapour pressure of gasoline blends as a function of temperature. Upper and lower flammable limits based on saturated gasoline vapour/air mixture at 1 atm total pressure.

mospheric pressure. A vent is required to maintain this condition as the liquid volume and system temperature change. Evaporative emissions systems use an activated charcoal canister to capture fuel vapour and allow air to vent from the system. While the vehicle is running, intake manifold vacuum is used to "purge" the fuel vapour from the canister into the engine where it is burned.¹³ The minimum required components for an evaporative emissions system are shown in figure 2.4 (a).

Air quality regulations in many jurisdictions require on-road vehicles to meet standards for evaporative emissions. Although a vehicle may meet the standard when new, the effectiveness of the evaporative emissions system diminishes if a leak develops in the vapour containment envelope of the system. Leaks become more common as vehicles age and experience wear and tear. A pressure or vacuum decay test is typically employed to determine the total leakage rate from the evap system and can be conducted either

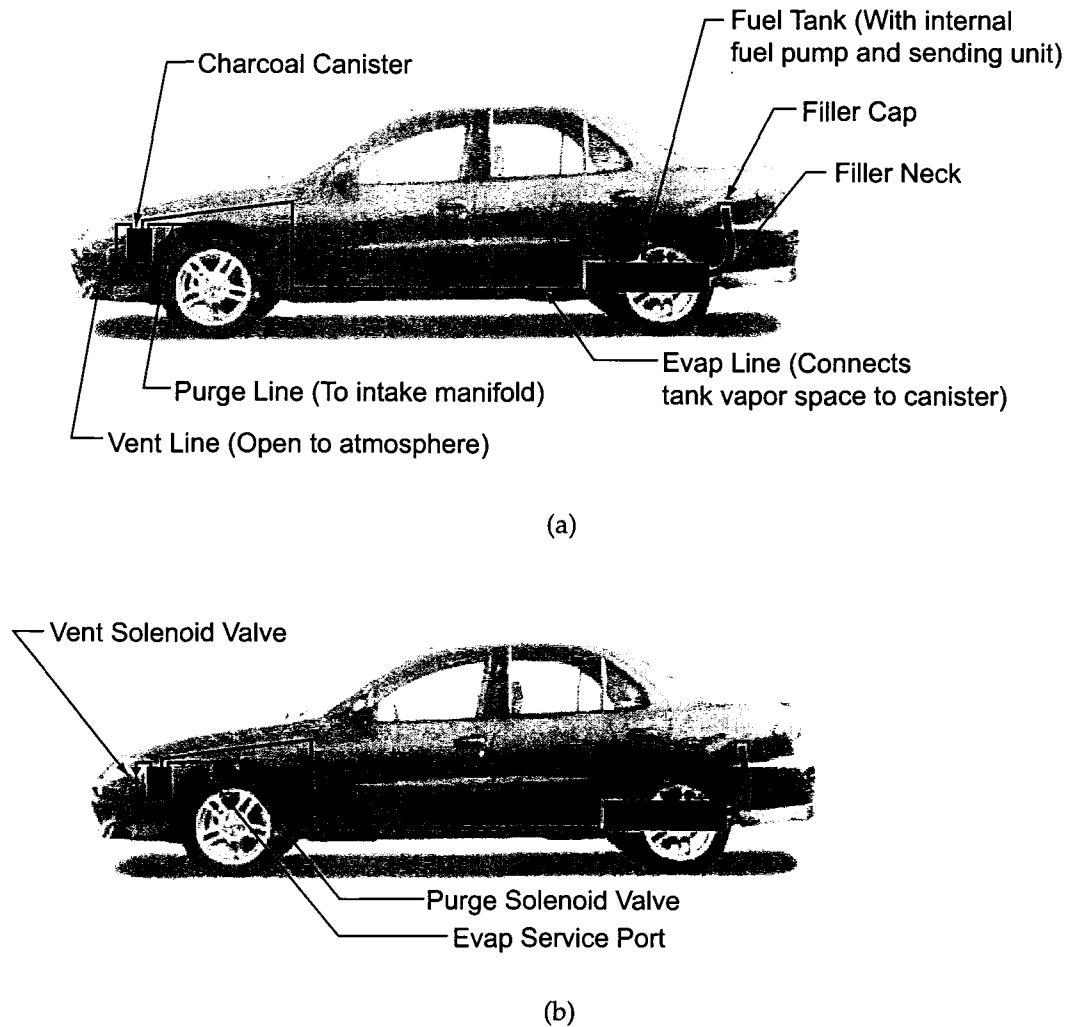


Figure 2.4: (a) Minimum required evaporative emissions system components. (b) Additional components required for OBD-II diagnostics testing. Placement of components may vary from vehicle to vehicle.

autonomously by the vehicle or manually by a service technician. Vehicles produced since 1996 include a standardized on-board diagnostics protocol (OBD-II) that provides on-board system leak detection capability.

2.5 Leak Testing Procedures

The OBD-II standard requires vehicles to have the capability to diagnose the pressure integrity of the evaporative emissions system. This is accomplished by using solenoid valves to close the purge connection to the engine intake manifold and the vent connection to the atmosphere. The status of the system is determined by placing the system under a differential pressure with both valves in the closed position. Either positive or negative (vacuum) pressure relative to atmospheric can be used for the test depending on the manufacturer and model of the vehicle.¹⁴ Two tests are generally performed to find large leaks and small leaks, respectively. The first test determines if the maximum pressure differential can be reached. If not, a gross leak code is set in the vehicle computer and the malfunction indicator light (MIL) is illuminated on the dashboard. If the maximum pressure differential is reached, the second test commences where the rate of pressure differential decay is measured. The decay rate is compared to a threshold value that corresponds to a specific orifice leak. For OBD-II vehicles produced between 1996-1999, the threshold leak rate is an equivalent leak through a 0.040" (1 mm) orifice. Vehicles produced after 2000 use a 0.020" (0.5 mm) orifice as the reference decay rate. OBD-II vehicles also have an evap service port feature. The service port consists of a schrader tee fitting on the canister purge line seen in figure 2.4 (b), designed for conveniently connecting leak detection equipment to the evap system under the hood, rather than using a gas cap adapter.

Vehicles produced prior to 1996 require testing by a technician to determine system leakage rate. Most vehicles produced before 1996 did not include an evap service port, so leak detection equipment is usually connected to the vehicle through a gas cap adapter. The vent and purge connections are pinched off with a hose clamp to close the system.¹⁵ While no leak threshold standard was set for pre-1996 vehicles when they were manufactured, new standards for pre OBD-II vehicles are presently being considered.

Once the leakage rate has been determined to exceed the emission standard, the leak(s) must be located and repaired. This can be a time consuming process because leaks can occur anywhere in the evap system. The typical procedure involves introducing a visible fog to the system which produces a visible plume at the leak point. The fog is produced by condensing oil droplets in compressed air or other gas such as nitrogen. As the fog enters the system, it combines with the existing gasoline vapour/air mixture to form a new mixture. The availability of compressed air at the majority of repair and maintenance facilities makes it the usual carrier gas of choice for the fog. A high rate of flow, typically 7 to 15 LPM,¹⁶ is introduced at the beginning of the test to completely fill the vapour space with fog. For instance, one manufacturer recommends removing the gas cap (from an OBD-II vehicle) and allowing the vapour to flow for 5 minutes.¹⁷

2.6 Potential Leak Locations

Previous research examining emissions from in-use vehicles has catalogued leak location data.^{18,19} Figure 2.5 shows the relative distribution of leaks in the evap systems of vehicles that did not meet emission requirements in one study. A large number of leaks were located in the vicinity of the tank, which is to be expected since the majority of the components (fuel pump, sending unit, filler neck, and filler cap) are in this region. While figure 2.5 shows component locations for the specific case of a 1997 Chevrolet Cavalier, the location of individual components is dependent on specific vehicle configuration. Generally, leaks may be found near any component of the system, and located anywhere in the vehicle from the engine compartment to the rear of the vehicle.

2.7 Potential Ignition Sources

In order to create a fire or explosion, an ignition source is required. Potential ignition sources fall into two categories: those within the system, and those

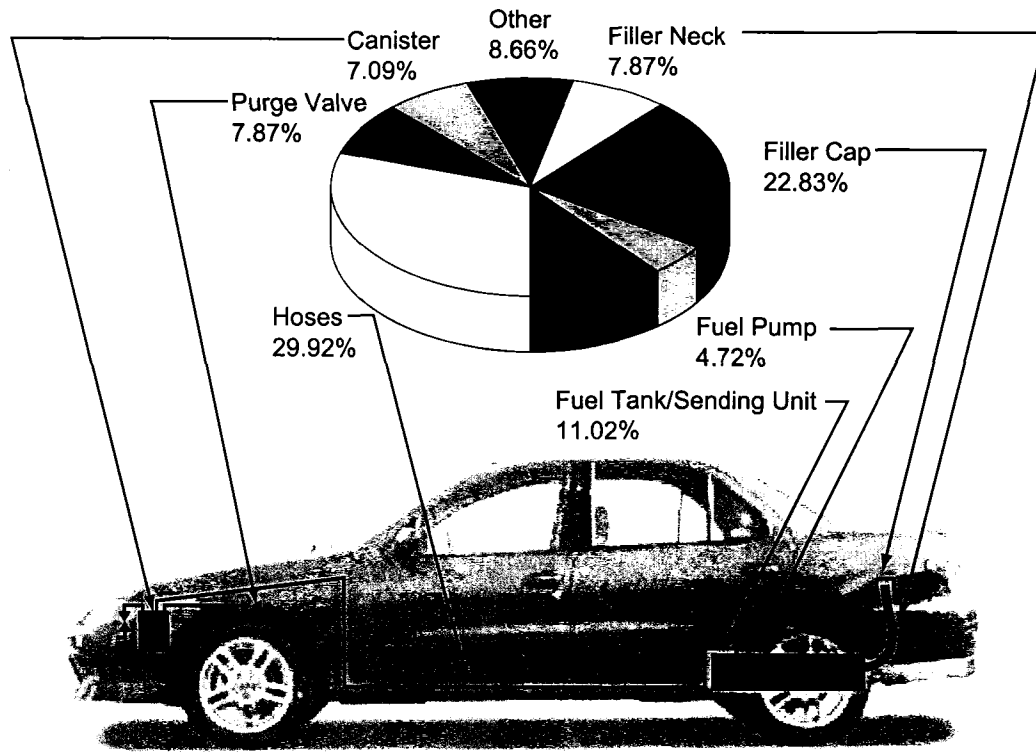


Figure 2.5: Distribution of evaporative emissions system leak locations found in a previous study of 151 automobiles. Approximately half are located in the vicinity of the fuel tank.

outside connected to the fuel system vapour space by a path of flammable mixture.

2.7.1 Internal Ignition Sources

The use of in-tank fuel pumps create a potential ignition source in the tank. Typical in-tank fuel pumps are driven by unsealed DC electrical motors with brushes that could potentially produce a spark to ignite a flammable mixture.¹ Also, the electrical connections for the pump inside the tank have been shown to fail, melting the wire insulation and creating black, sooty

deposits.²⁰ Level sending unit wiring is unlikely to produce sparks with enough energy to ignite gasoline vapours. Static discharges from improperly grounded plastic connections might possibly create an ignition source. Under normal vehicle operating conditions, the concentration within the fuel tank is by design above the UFL, so little effort has been made to eliminate ignition sources in the tank.

2.7.2 External Ignition Sources

Ignition sources that could exist outside the tank are much more varied than internal sources. Ignition of a flammable mixture within the fuel tank from an external source requires a flammable pathway that will allow a flame to propagate into the tank. Assuming a flammable pathway exists, two conditions will prevent a flame from propagating back into the tank: if the pathway is small enough to quench the flame, and if the mixture is moving fast enough away from the tank so that the mixture velocity exceeds the burning velocity.

Quenching dimensions are well documented for various hydrocarbons.²¹ Data for typical components of gasoline are shown in figure 2.6. Any path with a restriction below 1.75 mm will not allow a flame to propagate through, at standard temperature and pressure.

Flame propagation is also limited by the flame velocity of the mixture. Figure 2.7 shows the flame velocity for iso-octane, which burns slightly slower than gasoline vapour.²² A typical maximum burning velocity for gasoline vapour is 35 cm/sec, at stoichiometric proportions. The critical diameter above which a flame will travel opposite the direction of flow for tubing or hose containing a flammable gasoline vapour/air mixture is shown in figure 2.8.

Many incidents of static discharge causing ignition during refueling events have been documented.^{23,24} The majority of these incidents take place near the fuel tank filler neck. Since the filler neck is commonly used for either venting the purge flow during leak testing or as the entry point for the leak test fluid, a static discharge in this area could initiate a flame that could

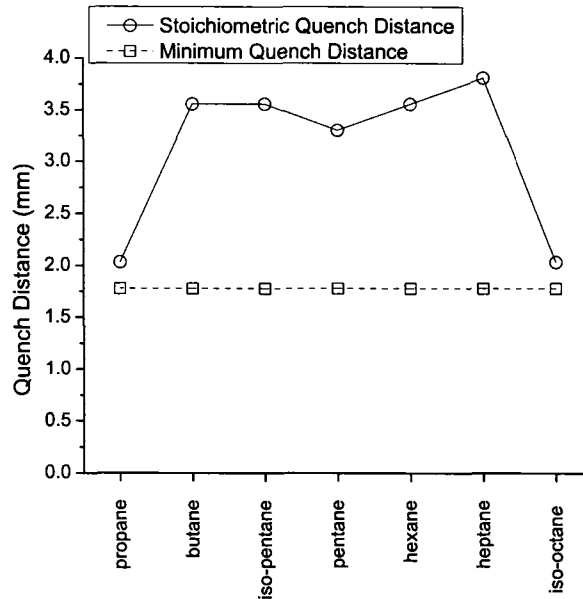


Figure 2.6: Quench distances for typical gasoline vapour components at atmospheric conditions. While the quench distance varies depending on mixture composition, the minimum distance for most hydrocarbons in this range is 1.75 mm.

propagate back into the fuel tank.

2.8 Previous Fuel System Flammability Research

Work on flammable mixtures formed above liquid fuels in enclosed tanks is limited. A study has been done on flammable mixtures formed above a liquid hydrocarbon fuel in an enclosed container when it is exposed to an air atmosphere. Flammable mixtures formed in an enclosed container initially containing saturated vapour with no liquid fuel and vented to an air atmosphere are also examined.²⁵ Neither of these cases is applicable under leak testing circumstances, where the initial condition in the vapour space is saturated, but liquid is usually present, and air is actively introduced to the system rather than vented.

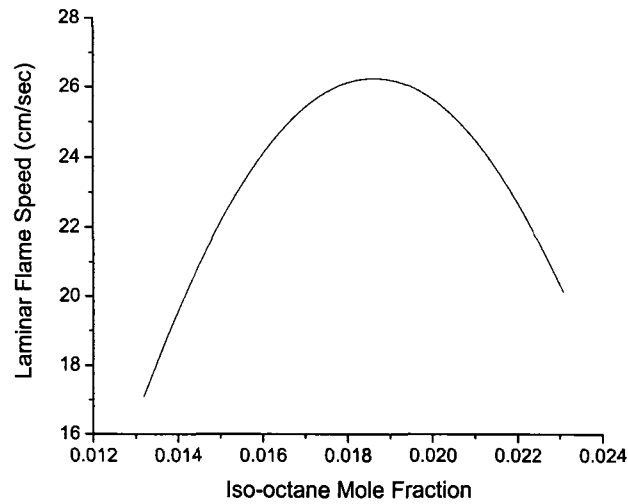


Figure 2.7: Iso-octane laminar flame speed at ambient conditions ($T = 298$ K, $P = 1$ atm).

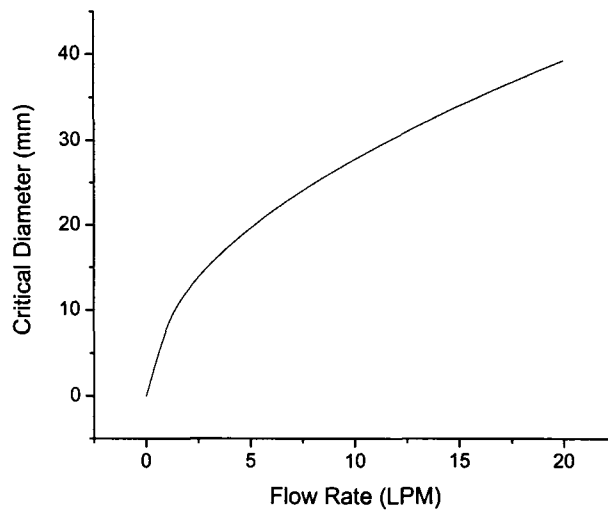


Figure 2.8: Critical diameters for a flame to travel opposite the direction of flow in a tube containing flammable gasoline vapours. Maximum gasoline burning velocity of 35 cm/sec at ambient conditions ($T = 298$ K, $P = 1$ atm).

2.8.1 Aviation Fuel Tank Research

The bulk of research on flammable mixtures in fuel tanks has been done by the aerospace industry, particularly after the TWA 800 incident in 1996 where a Boeing 747-100 center wing tank exploded.²⁶ The approach that aerospace has taken to prevent the ignition of flammable vapours in fuel tanks is considerably different than that of the automotive industry.

First, aviation fuel has significantly different volatility characteristics than automotive gasoline. The flash point, or temperature at which equilibrium fuel vapours reach the lower flammable limit for Jet A fuel is 38°C, compared to -51°C for gasoline.²⁷ As long as the fuel temperature in an aircraft is below the flash point (38°C for Jet A), the vapour mixture produced will be too lean to burn. This approach is much more suitable for aircraft because of low ambient temperatures²⁸ at typical cruising²⁹ altitude that would create a flammable mixture with typical automotive gasoline volatility.

Second, while aviation fuel is unlikely to enter the flammable region during airplane operation, the Federal Aviation Administration (FAA) in the United States has assumed that fuel tank mixtures are always flammable for the purposes of certification.³⁰ Hence, they have attempted to eliminate any possible ignition sources within the fuel tank itself, by specifying that any in-tank electrical equipment be designed to prevent energy discharges above 0.2 mJ, the typical minimum ignition energy (MIE) for fuel vapour.³¹

Indeed, conditions where both approaches were not sufficient were present in the TWA 800 incident,³⁰ and likely in other less documented incidents.³² The TWA 800 incident has led to a substantial effort to implement other methods of preventing fuel tank explosions, such as inerting with nitrogen enriched air.^{33,34}

2.8.2 Automotive Research

Additional research, applicable directly to automotive fuel systems, has concentrated on flammable mixtures formed during the refueling process.

EPA mandated maximum vapour emission levels during refueling have required the implementation of vapour recovery systems.³⁵ Two approaches have been taken to reduce refueling emissions: vehicle onboard recovery systems (ORVR) and EPA Stage II gasoline dispensing facility vapour recovery systems.³⁶ Onboard recovery systems use charcoal canisters to store the vapour generated by refueling. The extra vapour generated requires a larger canister than that used for standard evaporative emissions systems.³⁷ The vapour handling characteristics of these systems has led to debate over potential fire hazards.

The primary concern within the confines of the fuel system has been the combined use of ORVR and Stage II vapour recovery.³⁸ A CARB study cited in this report showed 80% of refueling events resulted in a flammable mixture, but the extent of the mixture was not sufficient to warrant additional safety measures.

2.9 Summary and Conclusions

Current environmental regulations have brought about a requirement for leak testing evaporative emissions systems. Finding the leaks in the system creates an unavoidable fuel vapour release to the environment and changes the properties of the vapour mixture in the fuel system.

Previous research has shown flammable mixtures formed in fuel tanks under certain conditions, such as nearly empty, vented fuel tanks, aviation fuel tanks at high temperatures, and flammable mixtures formed in automotive filler necks during refueling. No research is available on the effects of typical leak testing flows on gasoline vapour concentrations in automotive fuel tanks. The extent of the leak testing effects on the vapour mixture in fuel tanks is discussed in further chapters.

REFERENCES

- [1] W. F. Marshall and G. A. Schoonveld. "Vapor space flammability of automobile tanks containing low RVP gasolines". *SAE Paper No. 902096*, 1990.
- [2] Yunus A Cengel and Michael A Boles. *Thermodynamics: An Engineering Approach*. McGraw Hill, Inc., 3rd edition, 1998.
- [3] W. O. Siegl, M. T. Guenther, and T. Henney. "Identifying sources of evaporative emissions - using hydrocarbon profiles to identify emission sources". *SAE Paper No. 2000-01-1139*, 2000.
- [4] M. L. Greenfield and Giuseppe Rossi. "Vapor and liquid composition differences resulting from fuel evaporation". *SAE Paper No. 1999-01-0377*, 1999.
- [5] Anonymous. D323-99A, Standard test method for vapor pressure of petroleum products (Reid method). ASTM.
- [6] H. Itakura, T. Kato, and K. Naoya. "Analysis of the HC behavior in the air intake system while vehicle is parked". *SAE Paper No. 2004-01-0141*, 2004.
- [7] K. Koseki, T. Matsumoto, K. Morita, M. Hirose, and S. Sembokuya. "RVP dependence of evaporative emissions for japanese current and older vehicles and U.S. vehicles using typical japanese gasoline". *SAE Paper No. 2000-01-1170*, 2000.

- [8] Anonymous. "Regulation of fuels and fuel additives: Volatility regulations for gasoline and alcohol blends sold in calendar years 1989 and beyond, final rule". *Federal Register*, 54(54), 1989. 40 CFR Part 80.
- [9] Code of Federal Regulations. "Protection of environment: Regulations of fuels and fuel additives". 40 CFR 80.27, 2006.
- [10] Anonymous. Guide on federal and state summer R.V.P. standards for conventional gasoline only. Technical report, U. S. Environmental Protection Agency 420-B-05-012, 2005.
- [11] A. D. Brownlow, J. K. Brunner, and J. S. Welstand. "Changes in Reid vapor pressure of gasoline in vehicle tanks as the gasoline is used". *SAE Paper No. 892090*, 1989.
- [12] J. A. Gunderson and D. K. Lawrence. "Control of refueling emissions with an activated carbon canister on the vehicle". *SAE Paper No. 750905*, 1975.
- [13] A. Pittel and A. Weimer. "High vacuum purge and vapor canister performance". *SAE Paper No. 2004-01-1435*, 2004.
- [14] J. Gordon. "Evap code blues". *Motorage*, pages 16–22, January 2005.
- [15] Anonymous. "IM240 and evap technical guidelines", 2000. U. S. Environmental Protection Agency 420-R-00-007.
- [16] Anonymous. "Competitive product comparison. Retrieved June 15, 2006, from <http://www.redlinedetection.com/DOCS - Competitive Product Comparison.pdf>.
- [17] R. L. Banyard. Personal communication, Apr 10, 2006. Star Envirotech Inc. Technical Director.
- [18] H. M. Haskew and T. F. Liberty. "Diurnal emissions from in-use vehicles". *SAE Paper No. 1999-01-1463*, 1999.

- [19] "H. M. Haskew, K. D. Eng, T. F. Liberty, and R. M. Reuter". "Running loss emissions from in-use vehicles". *SAE Paper No. 1999-01-1464*, 1999.
- [20] Anonymous. "Fuel tech solution 1". Carter Fuel Delivery Systems, 2004. Form CA041004.
- [21] H. C. Barnett and R. R. Hibbard. "NACA report 1300". Technical report, National Advisory Committee for Aeronautics, 1957.
- [22] John B. Heywood. *Internal Combustion Engine Fundamentals*. McGraw Hill, Inc, 1988.
- [23] Anonymous. "Report on the risk of static ignition during vehicle refueling: A study of the available relevant research". Technical report, The Institute of Petroleum, 2001.
- [24] R. N. Renkes. "Fires at refueling sites that appear to be static related. Technical report, Petroleum Equipment Institute, 2006.
- [25] R. Bunama. *Numerical Simulation of the Formation of Flammable Atmospheres Within Enclosures Due to the Convective Diffusion of Mass and Heat*. PhD thesis, University of Calgary, December 1998.
- [26] J. A. Malley. "Aircraft systems design: Lessons learned from SFAR 88". *SAE Paper No. 2003-01-2991*, 2003.
- [27] F. A. Wyczalek and C. M. Suh. "Fuel tank combustible mixtures: New lessons learned". *IECEC-97 Proc.*, 1:664–669, 1997.
- [28] E. A. Avallone and T. Baumeister III. *Mark's Standard Handbook for Mechanical Engineers*. McGraw Hill, Inc, 10th edition, 1996.
- [29] Anonymous. "727 specifications". Retrieved June 13, 2006, from <http://www.boeing.com/commercial/727family/product.html>.
- [30] Anonymous. "Aircraft accident report: In-flight breakup over the atlantic ocean trans world airlines flight 800". Technical Report NTSB/AAR-00/03, National Transportation Safety Board.

- [31] M. Birky, J. Kolly, J. E. Shepherd, and et. al. "Summary and conclusions of explosion research team". Retrieved June 13, 2006, from http://www.galcit.caltech.edu/EDL/projects/JetA/reports/explosion_team_summary_aug1.pdf.
- [32] D. W. Naegeli and K. H. Childress. "Lower explosion limits and compositions of middle distillate fuel vapors". *SAE Paper No. 982485*, 1998.
- [33] W. M. Cavage and O. Kils. "Inerting a boeing 747SP center wing tank scale model with nitrogen-enriched air. Technical report, United States Department of Transportation, 2002.
- [34] R. Phillips, B. Tom, O. Vandroux, and N. Schmutz. "Inerting aircraft fuel tanks - reducing the hazard". *SAE Paper No. 2000-01-2267*, 2000.
- [35] Anonymous. "Control of air pollution from new motor vehicles and new motor vehicle engines: Refueling emission regulations for light-duty vehicles and light-duty trucks". *59 FR 16262*, 1994.
- [36] T. C. Austin and G. S. Rubenstein. "A comparison of refueling emissions control with onboard and stage II systems". *SAE Paper No. 851204*, 1985.
- [37] M. C. Lockhart. "Predicting tank vapor mass for on-board refueling vapor recovery". *SAE Paper No. 970308*, 1997.
- [38] W. H. Koch. "ORVR/Stage II: Certification and safety issues". *Petroleum Equipment and Technology*, March 1998.

CHAPTER 3

FUEL TANK VAPOUR FRACTION UNDER IMPOSED FLOW CONDITIONS

Evaporative emissions system leak testing procedures dilute equilibrium gasoline vapour/air mixtures within fuel tank vapour spaces, which are initially above the flammable limit. If air is used as the leak test fluid, flammable mixtures can potentially be formed within the tank during testing. An experimental setup for measuring gasoline vapour concentrations in an automotive fuel tank during leak testing flow is presented. Results for a range of typical non-oxygenated gasoline volatilities and leak test conditions show that flammable conditions are possible under conditions of low initial gasoline vapour concentration and sufficient leak testing flow rate and duration.

3.1 Introduction

AUTOMOTIVE fuel systems contain a mixture of gasoline vapour and air in the vapour space above the liquid gasoline in the fuel tank. The volatility of gasoline is specified such that the mole fraction of gasoline vapour in the system is well above the upper flammable limit under normal operating conditions. However, recent developments in regulations requiring the evaporative emissions system to meet a maximum leak threshold have introduced a new set of conditions present in the fuel system. Testing procedures used to find leaks introduce flow to the system, diluting the gasoline vapour in the tank. If air is used as a component of the leak testing

fluid, the mixture in the tank could potentially become flammable.

The mixture composition in the tank will depend on a number of factors, including the initial condition in the tank and the flow rates used during leak testing. The flow and mixing characteristics in the tank are complex. Density differences between the test fluid and the gasoline vapour/air mixture cause buoyancy effects. The gasoline vapour diffuses into the fresh air mixture entering the tank, and the fresh air diffuses into the lower air concentration in the gasoline vapour mixture. Bulk convective mixing occurs as the test fluid enters the system. As the concentration of the gasoline vapour is reduced below equilibrium, additional gasoline begins to evaporate at the liquid-vapour interface. The evaporation process requires energy which is extracted through heat transfer in the liquid and vapour phase. The imposed flow creates a time-dependent gasoline distribution as it reduces the gasoline concentration below equilibrium.

This chapter details an experimental method for determining the gasoline vapour distribution in a typical automotive fuel tank under leak test conditions. The effects of inlet flow parameters and initial conditions on the vapour fractions in a small passenger car fuel tank are presented. The experimental work completed in this chapter will be used to provide confirmation of the model presented in the next chapter.

3.2 Methodology

The fuel tank contains the majority of the vapour space in the evaporative emissions system. A low fuel level in the tank provides the greatest vapour space, with the majority of the vapour space volume in the fuel tank. The source of gasoline vapour in the system is the liquid-vapour interface in the tank, from which vapour will evaporate until the concentration above the interface reaches saturation. The saturation concentration depends on the pressure, temperature, and gasoline composition in the fuel system. Normally, the vapour space mixture will be essentially uniformly saturated prior to leak testing. Some deviations can occur if the vehicle has recently

been driven, causing fuel temperature variations, or if components of the fuel system have been disassembled.

The introduction of flow to a fuel tank vapour space during a leak testing procedure results in a time-varying gasoline vapour fraction. The primary challenge of these experiments was to capture the time-dependent gasoline vapour distribution within the tank while maintaining the flow characteristics of a fuel tank under leak testing conditions. Studies of open tanks have used sliding ignitors to determine the location of flammable vapours within,¹ but this method was not suitable in the closed automotive fuel tank examined here.

Another method for obtaining gasoline vapour samples from automotive fuel tanks has involved collecting samples in evacuated Tedlar bags for gas chromatograph analysis.² This method is suitable for uniform fuel vapour at equilibrium in a fuel tank but is not ideal for a transient condition in the tank. Extracting samples from the tank constitutes a flow disturbance, altering the gasoline vapour distribution within the tank. The transient response is not adequately reflected in this type of measurement either because the number of samples that can be obtained is time limited.

Oxygen sensors provide a measurement of the partial pressure of oxygen present at the sensor location. Because the mixture in the tank is a binary mixture of two components, gasoline vapour and air, the gasoline fraction can be computed from the oxygen partial pressure. If the total pressure, P_T is known then the oxygen fraction can be calculated as:

$$\chi_{O_2} = \frac{P_{O_2}}{P_T} \quad (3.1)$$

where P_{O_2} is the oxygen partial pressure and P_T is the total pressure. Since the vapour space contains a binary mixture of air (21% oxygen) and gasoline vapour (0% oxygen):

$$\chi_{gasoline} = 1 - \chi_{O_2}/.21 \quad (3.2)$$

A similar method has been used for a previous study where the gasoline

vapour concentration was measured by sucking gasoline vapour through a hose connected to an oxygen analyzer.³ This method only provided measurement at one point and would cause a significant affect on the flow within the tank for this case.

The oxygen sensors continuously monitored the oxygen partial pressure, capturing the time response characteristic of the gasoline vapour distribution. The sensors were inserted on the outside periphery of the tank, minimizing the effects on the flow within the tank.

To calibrate and verify the oxygen sensor output, gas chromatograph sample points were placed near the sensor locations. A full description of the gas chromatograph sample procedure can be found in Appendix B. The GC sample volume was limited to 4 mL to minimize flow effects within the vapour space.

Oxygen sensor output for equilibrium mixtures could also be calibrated by measuring the equilibrium vapour pressure. The full procedure for measuring vapour pressure is described in Appendix A.

3.3 Experimental Setup

3.3.1 Equipment

A fuel tank from a compact passenger car (1997 Chevrolet Cavalier) was chosen as the test vessel. The fuel tank capacity of 57 L and welded seam construction are representative of typical front wheel drive passenger car fuel tank characteristics. A similar tank from a 1999 Cavalier was selected in a study of fuel tank fire resistance to represent "thin profile" tanks commonly seen in these cars.⁴ The fuel pump and sending unit for these tanks are installed on a plastic hanger assembly as shown in figure 3.1. A plastic "bowl" surrounds the sending unit and fuel pump, and is open at the top of the tank. A small hole at the bottom allows for liquid transfer.

The fuel tank was set up for two possible testing scenarios, where the leak detection equipment was either connected to the filler neck with a modified filler cap or connected to the service port in the engine compartment.

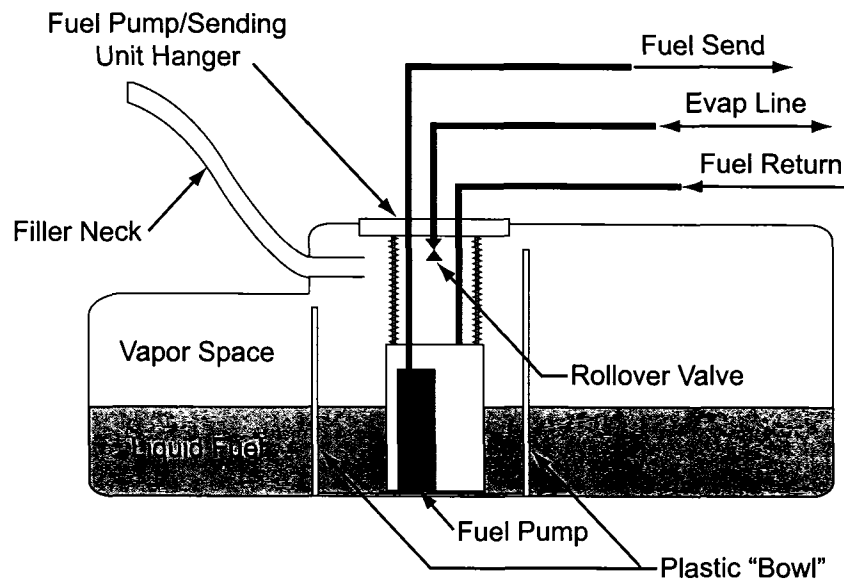


Figure 3.1: The configuration of the fuel tank components in a typical "thin profile" tank, common among front wheel drive passenger cars (side view).⁵ Connections for liquid fuel send and return and a vapor line to the evaporative emissions canister are mounted on the sending unit hanger. A rollover valve is installed where the evaporative emission line enters the gas tank to prevent fuel leakage in a vehicle rollover. The sending unit is surrounded by a plastic "bowl", which has a small hole at the bottom to allow liquid transfer and a small gap at the top to allow vapor transfer. The filler neck termination is located in the "bowl" area of the tank as well.

Leak testing can occur in either manner depending on specific vehicle configuration, noted in chapter 2. The first step in the leak detection process is usually to purge the vapour space with test fluid. If the leak detection equipment is connected to the filler cap flow is allowed to exit from the tank through the canister, and if the equipment is connected to the service port, the filler cap is removed and flow is allowed to exit through the filler neck.

Ambient temperature was monitored with a Omega HH11 thermometer, and ranged from 23°C to 25°C. Because the oxygen sensors used for this experiment measure oxygen partial pressure, an OMEGA PX303-015G5V pressure transducer was connected to the filler cap to monitor the total pres-

Sensor No.	Height (mm)	Location
1	150	Front Left Corner
2	50	Front Left Corner
3	180	Rear Left Corner
4	65	Rear Left Corner
5	40	Rear Left Corner
6	25	Rear
7	210	Rear

Table 3.1: Oxygen sensor locations, see figure 3.2.

sure in the system. The pressure drop in the tank and in the filler neck was assumed to be negligible compared to the pressure drop in the smaller hose and fittings. As such, the pressure in the gas tank was assumed to be uniform at the measured value. Fittings for the EnviteC[®] Oxiplus A oxygen sensors were installed in the tank to monitor oxygen partial pressure. Each oxygen sensor fitting was paired with a septum fitting for extracting gas chromatograph samples. The fitting locations can be seen in figure 3.2, with sensor height from the bottom of the fuel tank listed in table 3.1. The fitting locations were chosen to determine the approximate gasoline vapour vertical fraction gradient at the two points farthest from the air inlet. The vapour distribution in the tank was assumed to be roughly symmetrical from side to side, regardless of slight tank geometry asymmetries.

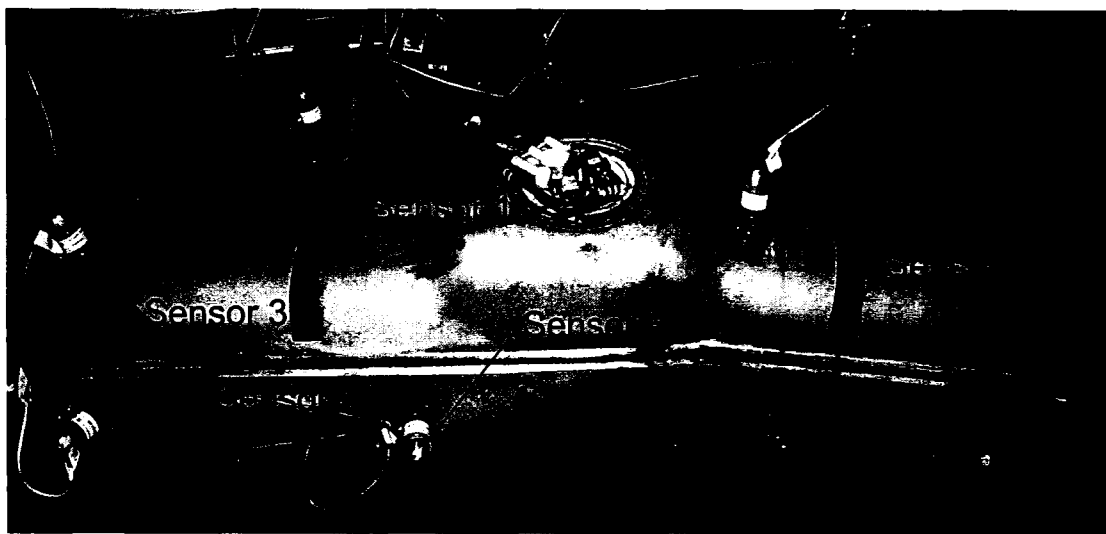
3.3.2 Gasoline Samples

Gasoline samples used for testing were obtained from a Shell service station and the Imperial Oil Strathcona Refinery. Imperial Oil provided 6, 4 L gasoline samples within the typical volatility range blended for Canadian conditions.⁶ The vapour pressures of the gasolines used for testing are listed in table 3.2.

Additional tests were performed on the Shell gasoline to reduce the volatility by removing lighter hydrocarbons through weathering. An extended 20 minute flow with 4 L liquid gasoline volume substantially weath-



Side View



Rear View

Figure 3.2: Oxygen sensor locations on the fuel tank, see table 3.1. The oxygen sensors were paired with gas chromatograph sample points for calibration.

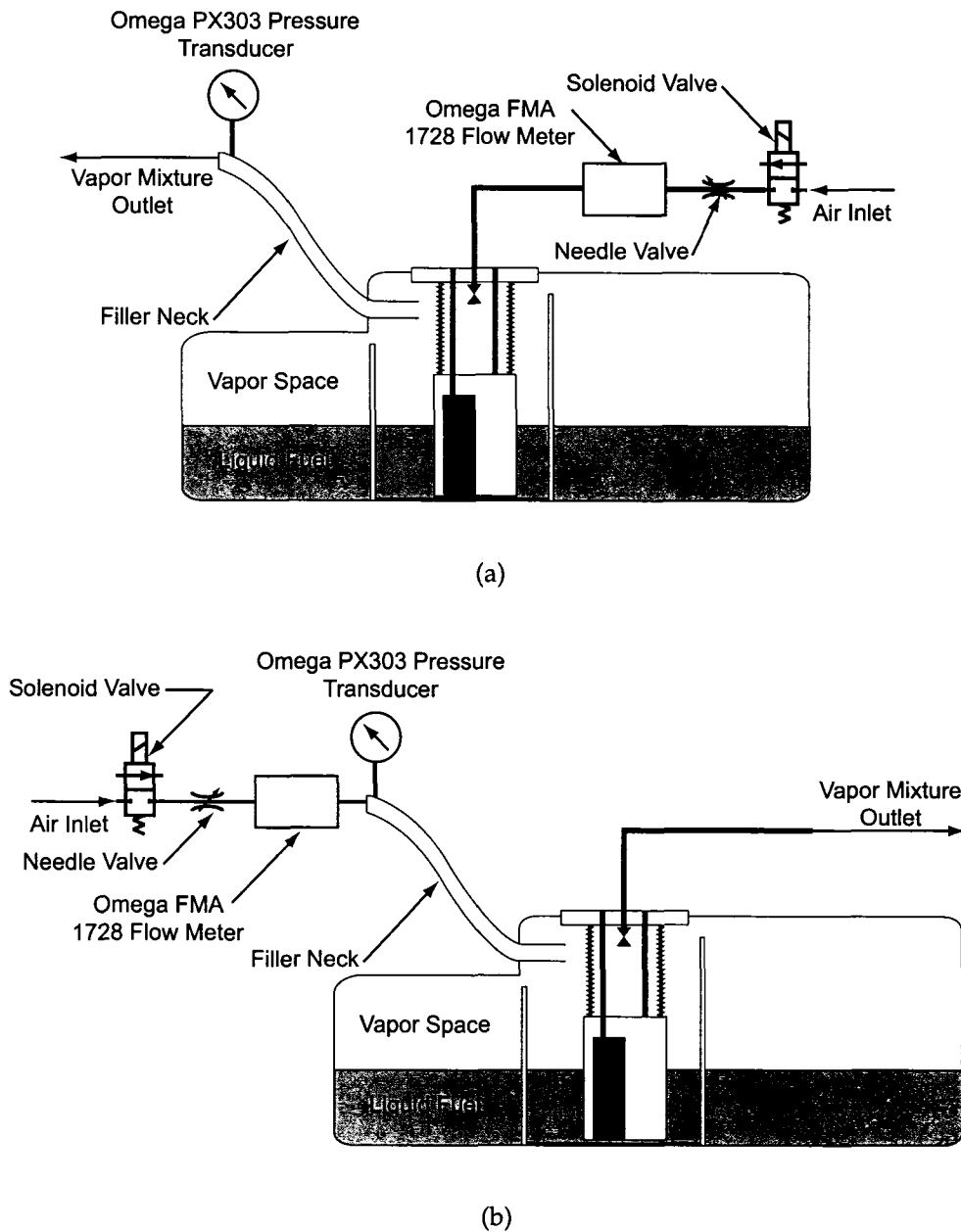


Figure 3.3: Flow diagram of experimental setup. The flow rate was set with a needle valve, while pressure and flow were monitored and recorded. A solenoid valve controlled the flow duration automatically. Figure (a) represents a leak test configuration where the service port is used for the air inlet, and (b) represents a test where a filler cap adapter is used for the air inlet.

Description	Designation	RVP (kPa)
Shell	S. 90	90
Imperial Oil 1	I. O. 96	96
Imperial Oil 2	I. O. 71	71
Imperial Oil 3	I. O. 60	60

Table 3.2: Tested gasoline volatilities.

Description	Designation	Sat. Gasoline Vapour Frac.	Evaporated Liquid (L)
Shell Weathered 1	S. W. 1	0.42	0.12
Shell Weathered 2	S. W. 2	0.37	0.10
Shell Weathered 3	S. W. 3	0.31	0.08
Shell Weathered 4	S. W. 4	0.26	0.08
Shell Weathered 5	S. W. 5	0.22	0.07
Shell Weathered 6	S. W. 6	0.15	0.13

Table 3.3: Weathered gasoline vapour fractions at test conditions ($T_{amb} = 23^{\circ}\text{C}$ and $P_{atm} = 93 \text{ kPa}$). The estimated liquid volume that was evaporated during each cycle is given.

ered the fuel, dropping the equilibrium concentration to 42% at test conditions. Subsequent tests were performed to continue weathering the fuel. The designations for the weathered Shell gas are listed in table 3.3.

3.3.3 Oxygen Sensor Calibration Procedures

The general operating principles for the Oxiplus A transducer are listed in detail in appendix C. Figure 3.4 demonstrates that the sensor sensitivity was significantly altered by the presence of gasoline vapour. The likely cause of the sensitivity change was heavier hydrocarbons (C5 and greater) either condensing on the oxygen permeable membrane of the sensor altering the oxygen diffusion characteristics of the membrane, or condensing in the sensor's electrolyte, changing the ion diffusion characteristics. The hydrocar-

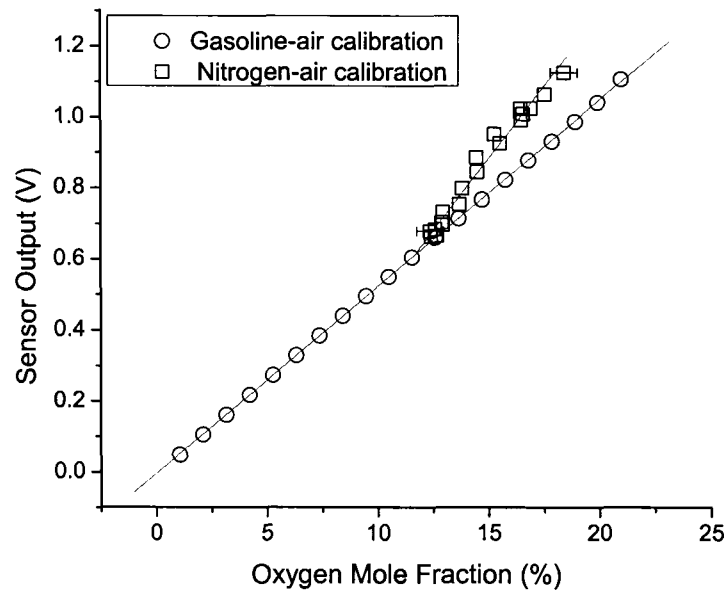


Figure 3.4: Gasoline vapour calibration of sensor 1. The sensitivity was significantly altered by the presence of gasoline vapour. Gasoline calibration error bars ± 2 S. D., due to gas chromatograph sampling procedure. See appendix B for details.

bons might also have a catalytic effect on the sensor performance. However, a calibration with butane shown in figure 3.5 had very similar output to a nitrogen calibration, so this is not likely. The sensors were linear down to 3.0% hydrocarbon, or 19.5% oxygen.

3.3.4 Test Procedures

Before testing was initiated the oxygen sensors were installed in the fuel tank. A pressure test was conducted on the entire experimental setup prior to testing to ensure that no unknown leaks would disrupt the flow pattern within the fuel tank. A minimum of 7 kPa gauge pressure was used for the pressure test, which was not exceeded during testing.

To start each test, the gasoline vapour concentration was allowed to

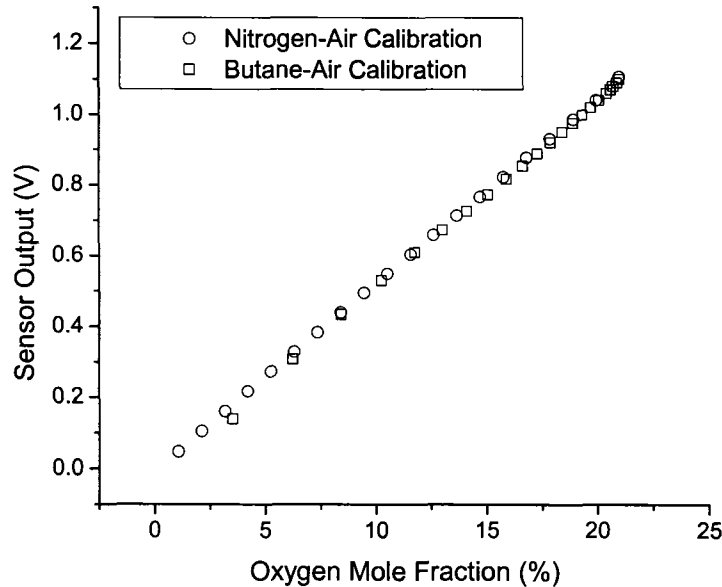


Figure 3.5: Butane calibration of sensor 1. Butane did not alter the response significantly when compared with nitrogen.

reach equilibrium while the tank was open to the atmosphere, as it would in a relatively constant temperature environment such as an automotive repair shop. This could be verified by observing the oxygen sensor output rate of change decrease to zero and by comparing the oxygen sensor outputs to the expected value at the equilibrium vapour pressure. Once the vapour concentration reached equilibrium, the solenoid valve shown in figure 3.3 was opened, allowing flow through the tank. Leak detection machines are commonly designed to run in 5 minute cycles,⁷ so tests were run to 10 minutes simulating 2 complete purge cycles. Longer cycles were used to accelerate fuel weathering. An extended test timeline for fuel weathering is shown in figure 3.6, with sensor output. Once the specified flow time was reached, the solenoid valve was closed and the gasoline vapour was allowed to return to equilibrium. The oxygen sensors were removed after each test and replaced with rubber stoppers to prevent excessive evaporative losses to the

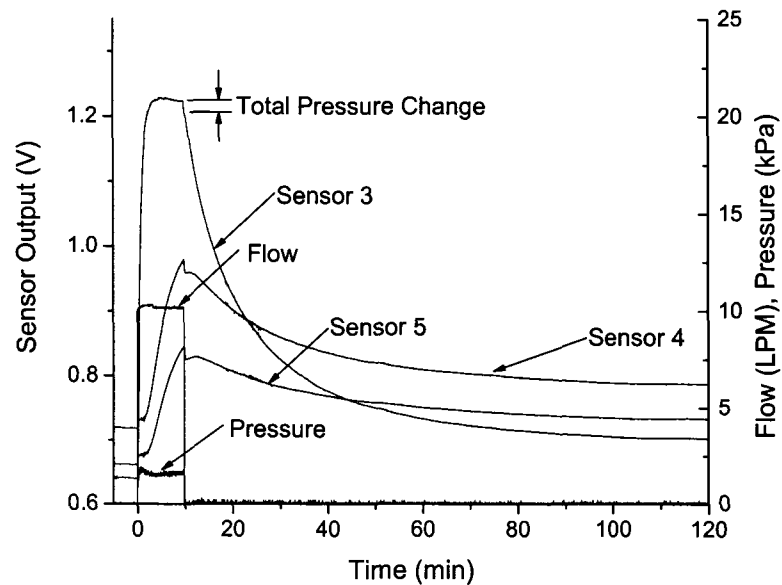


Figure 3.6: Typical test timeline. Once the gasoline vapour has reached equilibrium in the tank, the solenoid valve is opened and flow begins. After a set time (in this case 60 minutes), the flow is shut off and the gasoline vapour concentration is allowed to return to equilibrium. Raw sensor output is shown for sensors 3, 4, and 5 only for clarity. Ambient conditions were $T_{amb} = 23^{\circ}\text{C}$ and $P_{atm} = 93 \text{ kPa}$. The gasoline tested was S. 90, see table 3.2 for gasoline designations.

environment.

After the test was complete, the gasoline vapour concentration was calculated from the measured total pressure and oxygen sensor output, following the method shown in Appendix C. The gasoline vapour concentrations calculated for sensors 3, 4 and 5 from the previously shown test are shown in figure 3.7.

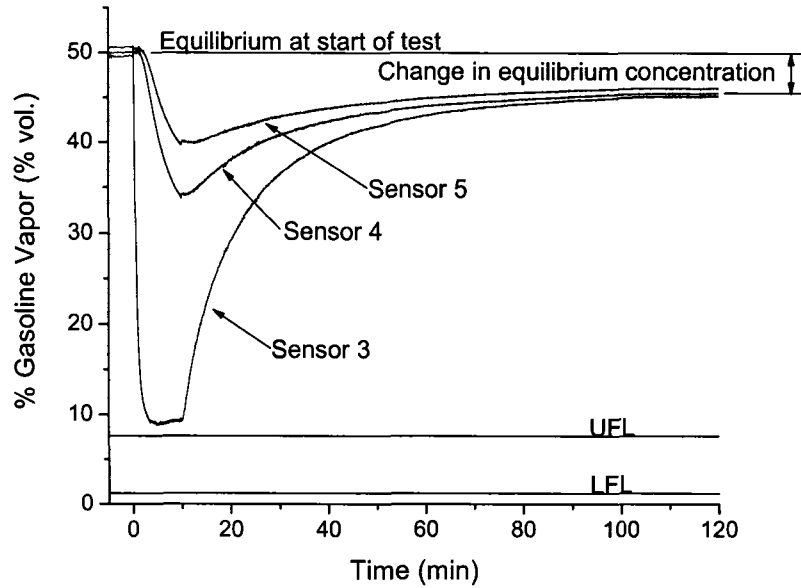


Figure 3.7: Typical gasoline vapour fraction profiles during test sequence. Note the decrease in equilibrium fraction due to lighter hydrocarbon components evaporating faster than heavy components, or weathering. Gasoline vapour fractions shown at sensors 3, 4, and 5 only for clarity. Ambient conditions were $T_{amb} = 23^{\circ}\text{C}$ and $P_{atm} = 93 \text{ kPa}$. The gasoline tested was S. 90, see table 3.2 for gasoline designations.

3.4 Results

3.4.1 Inlet Condition Effects

The gas mixture in the fuel tank is affected by the connection point of the leak detection equipment. If air flows into the system from the service port, it enters at the top of the tank high velocity because the area of the hose is small. The mixture exits the filler neck, situated lower in the tank. If the flow enters at the filler neck, it enters at low velocity in a horizontal direction. Figure 3.8 shows the mole fraction profile at the edge of the tank for each inlet condition with an inlet flow of 10 and an initial mole fraction of 50% gasoline vapour. The profile is shown at 2.5, 5, and 10 minutes flow

duration. Using the service port as the connection point for the leak detection equipment causes a greater decrease in the gasoline vapour concentration in the tank. The higher velocity jet entering the tank promotes greater mixing than the low velocity entering at the filler neck. The vertical concentration gradient creates a higher gasoline vapour concentration at the filler neck than at the service port connection. When the filler neck is the exit point, more gasoline vapour leaves the tank than if the service port is the exit point. Under the conditions of this experiment, no flammable mixture was formed after 10 minutes of flow when the filler neck was used as the inlet.

3.4.2 Inlet Flow Rate Effects

The volume of air added to the fuel tank and inlet velocity are proportional to the inlet flow rate. Leak detection equipment is typically regulated at 15 inH₂O for testing evaporative emissions systems. For most cases, this pressure difference creates a flow of 7 LPM to 15 LPM in the fuel system.^{8,9} The effect of varying the flow rate from approximately half this rate (5 LPM) to double (20 LPM) was measured and shown in figures 3.9 and 3.10. While the gasoline used for each test was the same, ambient temperature and barometric pressure variations caused the initial gasoline concentration to vary by approximately 5%. As expected, increasing the flow rate caused the mole fraction to decrease at a faster rate. At all flow rates, the filler neck inlet flow did not affect the mole fraction as much as the service port inlet flow. However, flammable mixture was eventually formed at 15 and 20 LPM flow with the filler neck inlet flow.

The service port inlet is located higher than the filler neck. Lighter mixtures containing a higher air fraction are buoyed to the top and removed at the service port, hence less fuel is removed when the service port is the exit point. The large filler neck diameter also reduces the entrance velocity for an equivalent flow rate.

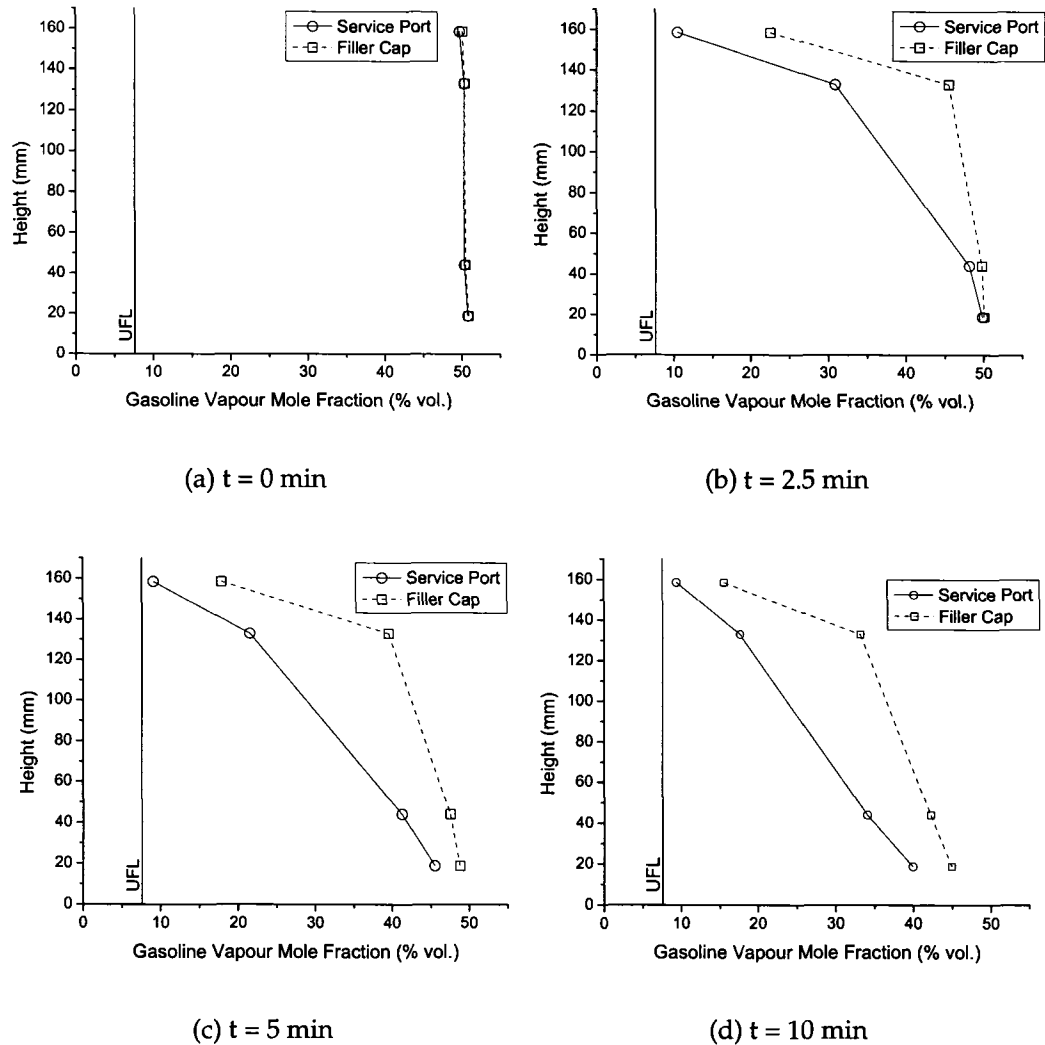


Figure 3.8: Gasoline vapor fraction profile comparison for 10 LPM flow from the service port and filler cap, as measured from the bottom of the fuel tank. Ambient conditions were $T_{amb} = 23^{\circ}\text{C}$ and $P_{atm} = 93 \text{ kPa}$. The gasoline tested was S. 90, see table 3.2 for gasoline designations.

3.4.3 Initial Volatility Effects

The results examined in previous sections used Central Alberta spring gasoline. Many regions with hotter climates are supplied with much lower

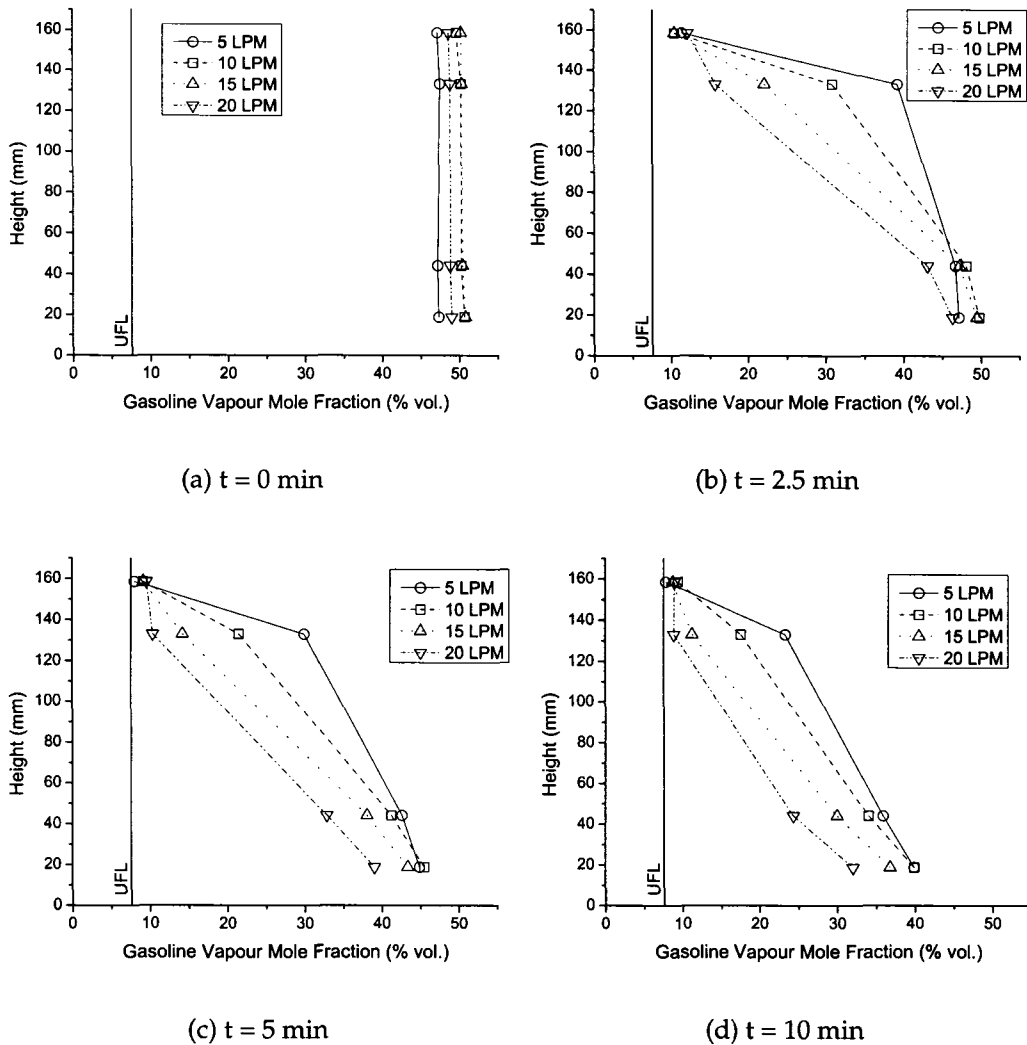


Figure 3.9: Gasoline vapour mole fraction profile for 4 service port inlet flow rates; 5, 10, 15, and 20 LPM. Ambient conditions were $T_{amb} = 23^{\circ}\text{C}$ and $P_{atm} = 93$ kPa. The gasoline tested was S. 90, see table 3.2 for gasoline designations.

volatility gasoline, significantly reducing the initial saturated gasoline vapour concentration in the fuel system. Figure 3.11 shows the mole fraction profile formed for 4 gasoline volatilities, the lowest being blended for the Fraser Valley in British Columbia.⁶ As the initial gasoline vapour mole fraction

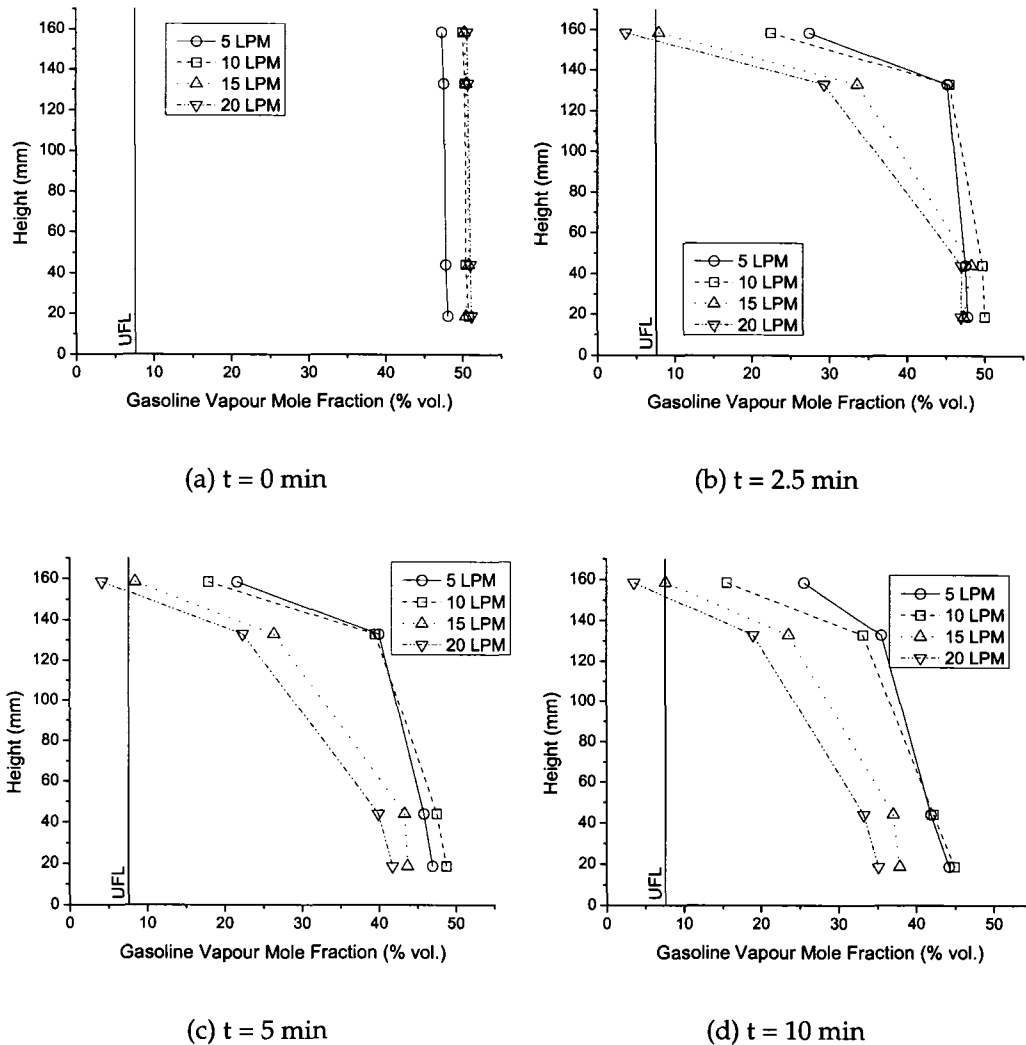


Figure 3.10: Gasoline vapor mole fraction profile for 4 filler cap flow rates; 5, 10, 15, and 20 LPM. Ambient conditions were $T_{amb} = 23^{\circ}\text{C}$ and $P_{atm} = 93$ kPa. The gasoline tested was S. 90, see table 3.2 for gasoline designations.

was reduced, the flammable volume in the tank increased. After a flow duration of 10 minutes, the gasoline vapour was allowed to return to equilibrium, while the tank was vented to atmosphere. The lower volatility gasoline took longer to return to equilibrium as shown in figure 3.12. The higher

volatility gasoline mixtures returned above the UFL almost immediately. The 59.9 kPa gasoline vapour mixture was still flammable at the top of the tank 5 minutes after the flow was turned off. After 20 minutes, all mixtures had essentially returned to equilibrium.

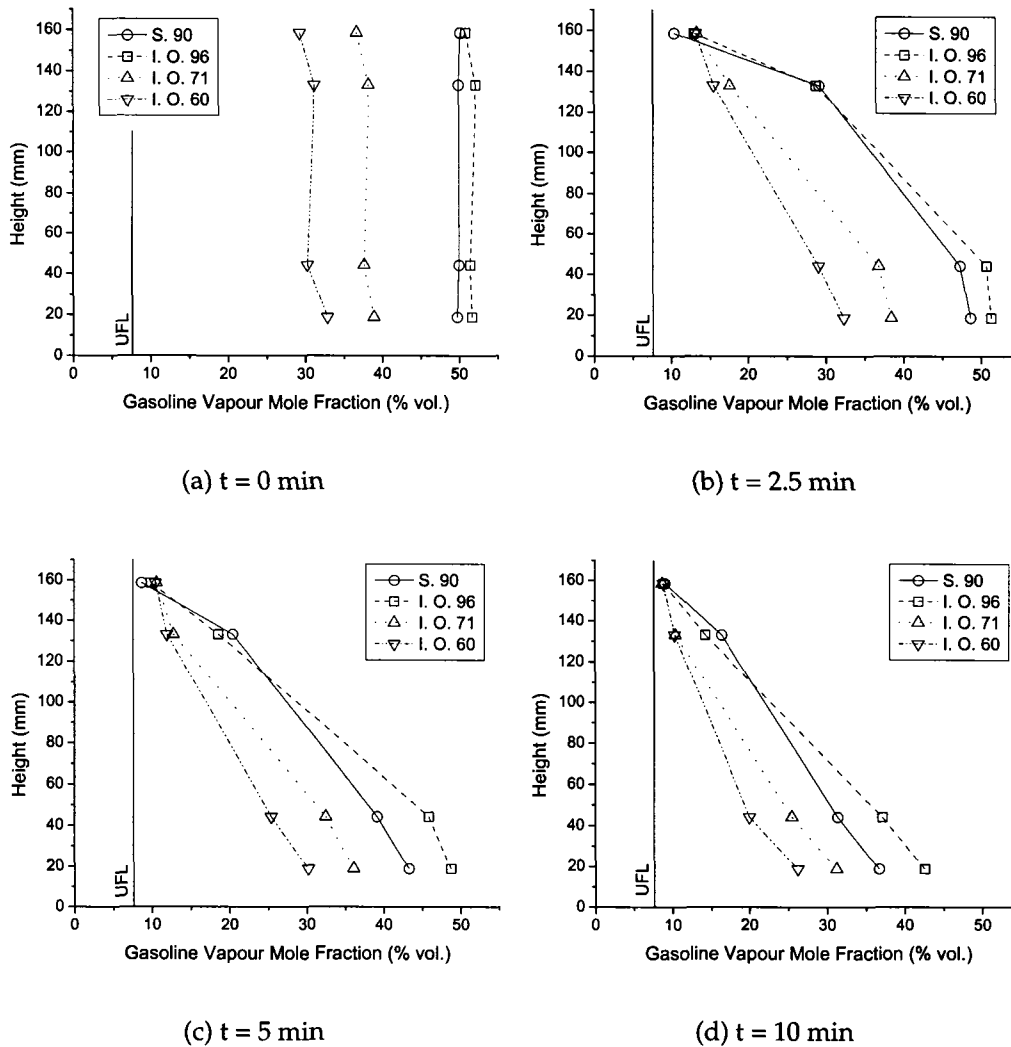


Figure 3.11: Gasoline vapor mole fraction profile for gasoline with varying volatility. The flow rate for these tests was 10 LPM from the service port. Ambient conditions were $T_{amb} = 23^{\circ}\text{C}$ and $P_{atm} = 93$ kPa. See table 3.2 for gasoline designations.

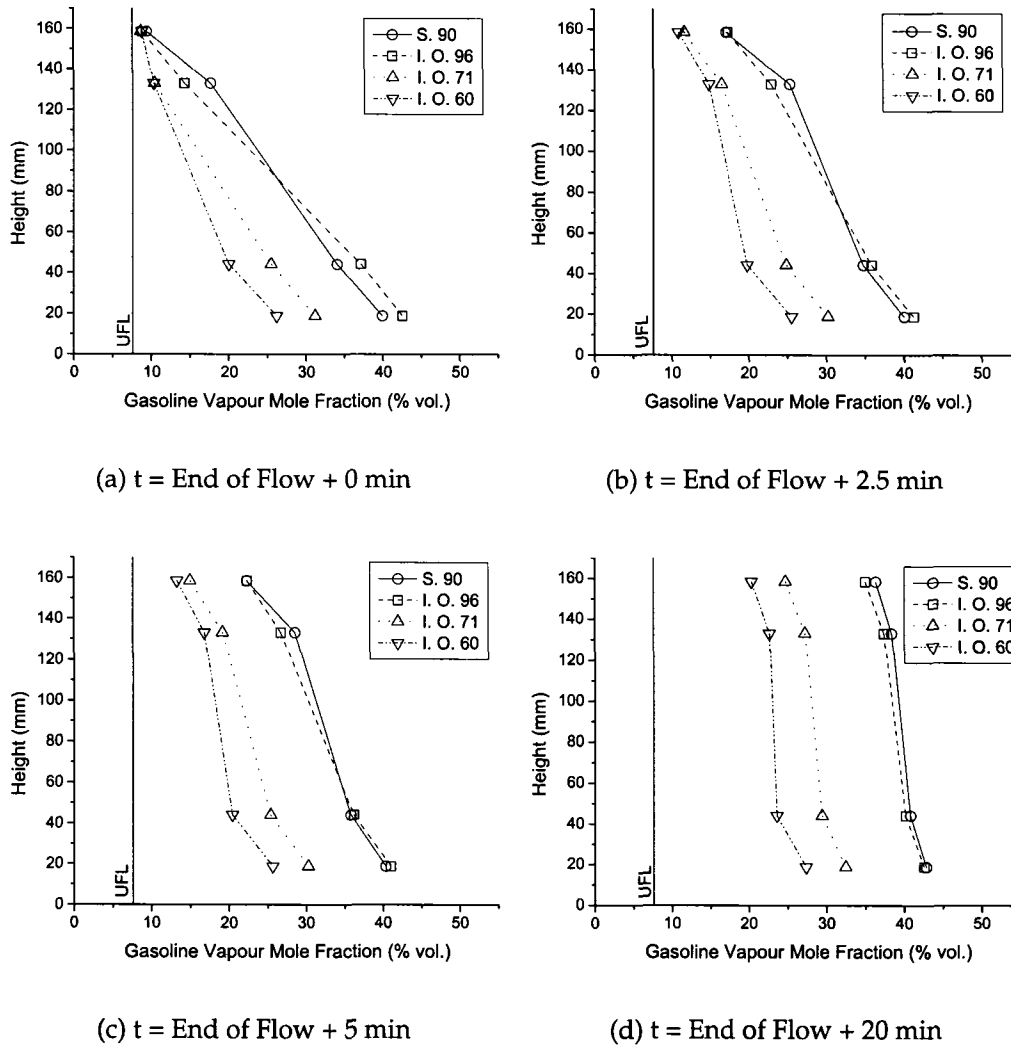


Figure 3.12: After the flow is shut off at 10 minutes, the mixture returns to equilibrium. The lower volatility gasoline takes longer to return to equilibrium. Ambient conditions were $T_{amb} = 23^{\circ}\text{C}$ and $P_{atm} = 93 \text{ kPa}$. See table 3.2 for gasoline designations.

3.4.4 Weathering Effects

As gasoline is exposed and evaporates, the equilibrium vapour pressure is reduced as the higher volatility components evaporate faster than their low

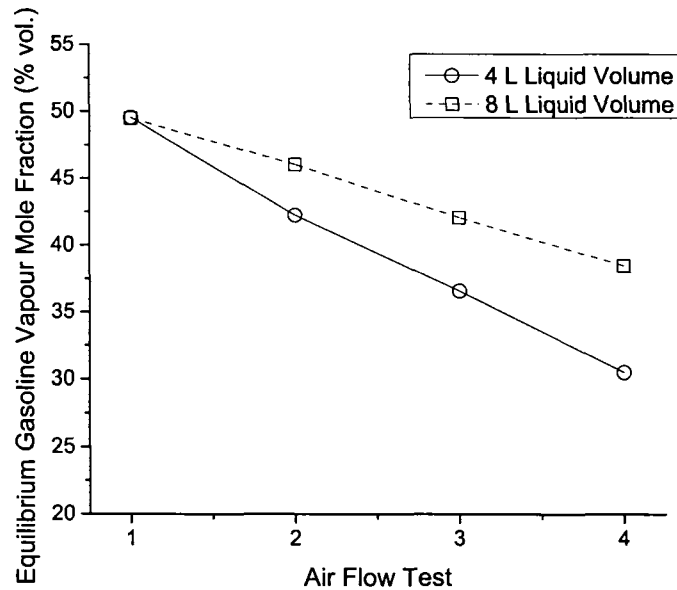


Figure 3.13: Reduction in gasoline vapour equilibrium mole fraction from air flow. 20 minute flow tests at 10 LPM were conducted with liquid gasoline volumes of 4 L and 8 L. The gasoline vapour was allowed to reach equilibrium after the test, while being vented to the atmosphere. Ambient conditions were $T_{amb} = 23^{\circ}\text{C}$ and $P_{atm} = 93 \text{ kPa}$.

volatility counterparts. The weathering effect is dependent on the liquid volume, as shown in figure 3.13. The flow introduced to a gas tank during leak testing causes accelerated evaporation and therefore accelerated weathering. A series of flow tests were conducted on a volume of 4 L of gasoline in the tank to incrementally weather the gasoline over time. Figure 3.14 shows the mixtures formed under service port inlet flow at 10 LPM. The volume of flammable mixture formed in the tank is strongly dependent on the initial gasoline concentration in the tank. With an initial mole fraction in the tank of 16%, still over double the rich flammable limit of gasoline, 75% of the fuel tank volume was flammable after 10 minutes of 10 LPM flow.

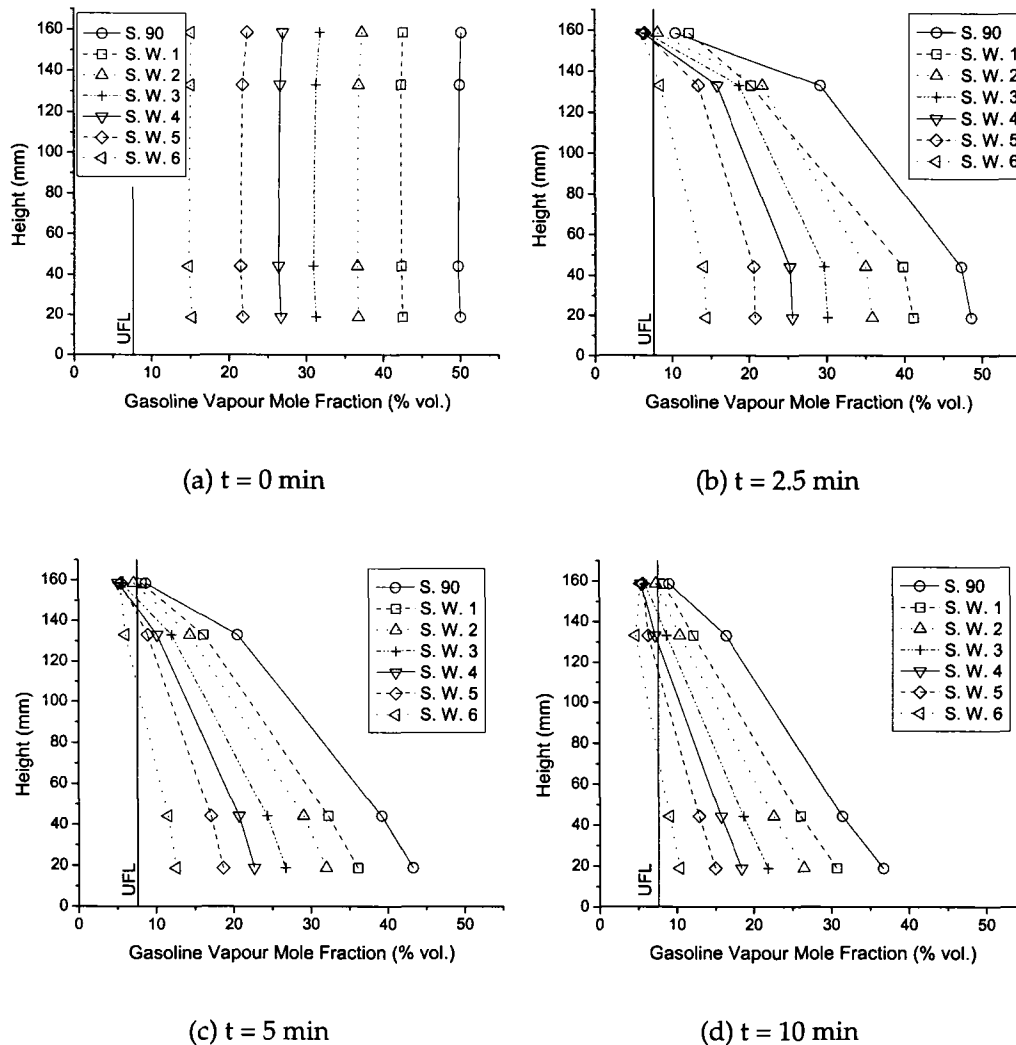


Figure 3.14: Gasoline vapor mole fraction profile for weathered gasoline, with 10 LPM flow from the service port inlet. Ambient conditions were $T_{amb} = 23^{\circ}\text{C}$ and $P_{atm} = 93$ kPa. See tables 3.2 and 3.3 for gasoline designations.

3.4.5 Weathering and Volatility Comparison

The composition of a weathered gasoline is different than a gasoline blended for low volatility. The effects of composition were compared by compar-

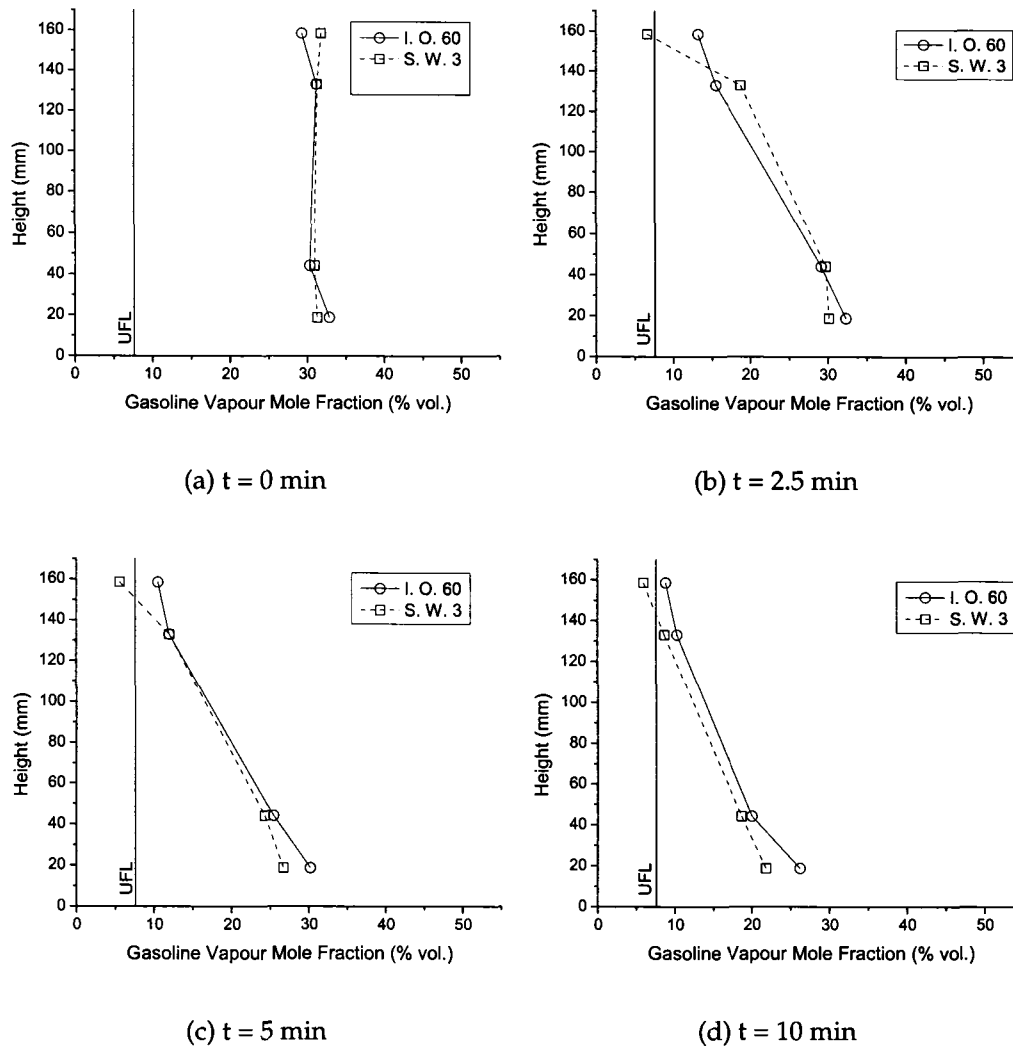


Figure 3.15: A comparison of low volatility gasoline and weathered gasoline. Test conditions were 10 LPM flow from the service port. Ambient conditions were $T_{amb} = 23^{\circ}\text{C}$ and $P_{atm} = 93 \text{ kPa}$. See tables 3.2 and 3.3 for gasoline designations.

ing a weathered gasoline and a low volatility gasoline with similar saturated gasoline vapour mole fractions. The mole fraction gradient within the tank was slightly different for the two cases. Although the initial mole fractions were similar, the difference in composition likely altered the diffu-

sion, density, and evaporation rate properties. However, the same volume of flammable mixture was formed after 5 minutes. Slightly more flammable mixture was formed after 10 minutes with weathered gasoline.

3.4.6 Fuel Tank Flammable Mixture Ignition

The presence of a flammable gasoline vapour/air mixture in the fuel tank was verified by performing an ignition test in the field. Full details are given in appendix E. Ignition was successful and a significant amount of damage to the tank and related components was noted.

3.5 Conclusion

An experimental setup was used to determine the gasoline vapour mole fraction profile in a "thin profile" fuel tank under typical leak test conditions. Electrochemical oxygen sensors provided real time indication of fuel mole fraction during the transient flow regime of leak testing. Gas chromatography and fuel vapour pressure measurements were used to calibrate and verify output from the oxygen sensors. Significant decreases in fuel mole fractions were noted by introducing air flow to the tank under conditions similar to evaporative emission leak testing. The density of the fuel-air mixture in combination with evaporation from the liquid-vapour interface and diffusion produced a fuel vapour fraction gradient under flow conditions that was affected by the inlet flow condition, leak testing flow rate, and initial gasoline vapour mole fraction.

Leak detection equipment is usually either connected at the filler neck or the service port, with the alternate open to allow the leak test fluid to completely fill the vapour space. Flow from the filler neck and out the service port connection was shown to be safer, creating less flammable mixture within the tank. Because a vertical concentration gradient is established in the tank, the higher exit point vents less gasoline vapour, keeping the gasoline vapour mole fraction higher in the tank. Also, the lower inlet velocity reduces mixing.

The flow rate into the system had an effect on the concentrations in the tank as expected. Higher volumes of air entering the tank diluted the gasoline vapour/air mixture at a greater rate.

Lower volatility gasoline reduced the initial gasoline vapour mole fraction within the tank. Low volatility was either a result of the specific blend of the gasoline or weathering effects, but either way, more flammable mixture was created when the initial mole fraction was lower. Hence, gasoline produced for use in hot climates is more likely to create a hazard.

The presence of flammable mixtures within the tank under leak testing conditions was verified by ignition. Under the conditions tested, substantial damage to the tank was sustained.

The experimental work done in this chapter provides a basis to confirm the model results presented in the next chapter.

REFERENCES

- [1] R. Bunama and G. A. Karim. "The flammability of atmospheres within nearly-empty liquid fuel tanks". *SAE Paper No. 2001-01-1966*, 2001.
- [2] W. F. Marshall and G. A. Schoonveld. "Vapor space flammability of automobile tanks containing low RVP gasolines". *SAE Paper No. 902096*, 1990.
- [3] U. von Pidoll, H. Kramer, and H. Bothe. "Avoidance of electrostatic hazards during refuelling of motorcars". *Journal of Electrostatics*, 40:523–528, 1997.
- [4] J. R. Griffith Jr, C. R. Machado, and B. B. Bendele. "Comparative evaluation of automotive fuel tanks in general accordance with ECE R34.01, annex 5 section 5.0 'resistance to fire'". *SAE Paper No. 2005-01-1561*, 2005.
- [5] F. J. Thiessen and D. N. Dales. *Automotive Principles and Service*. Prentice Hall, 1980.
- [6] R. L. Gagnon. Personal communication, May 8, 2006. Imperial Oil Fuels Area Specialist, Strathcona Refinery QA Lab.
- [7] Anonymous. "*Operator's Quick Reference Manual*". Redline Detection LLC, 2512 Fender Ave. Unit A, Fullerton, CA 92831, 01-0002c edition.
- [8] R. L. Banyard. Personal communication, Apr 10, 2006. Star Envirotech Inc. Technical Director.

-
- [9] Anonymous. "Competitive product comparison. Retrieved June 15, 2006, from <http://www.redlinedetection.com/DOCS - Competitive Product Comparison.pdf>.

CHAPTER 4

NUMERICAL SIMULATION OF VAPOUR COMPOSITION IN NEARLY-EMPTY FUEL TANKS UNDER IMPOSED FLOW CONDITIONS

Fuel tank leak testing flows can reduce the concentration of fuel vapour within the vapour space of the tank. A model for predicting gasoline vapour concentration in a fuel tank is developed and applied to typical automotive fuel tank geometry and conditions. Model results are compared to previously obtained experimental results and show similar trends in gasoline vapour concentrations. A significant volume of flammable vapour is predicted under leak testing conditions with a high air flow rate and low initial gasoline vapour concentration.

4.1 Introduction

INTRODUCING flow to the vapour space of a tank containing a volatile liquid fuel will impact the concentration of the fuel vapour within the tank, as has been shown experimentally in Chapter 3. However, experimental methods can only reveal what is happening at the boundary of the tank without significantly affecting the flow within. Numerical modeling techniques can be applied to predict the vapour concentration distribution throughout the entire tank volume.

A numerical model representing a "thin profile" automotive fuel tank was used to simulate leak testing conditions, identifying possible situations

where flammable mixtures could be formed. The initial gasoline vapour concentration and inlet air flow rate effects on total flammable volume in the tank are investigated in this chapter to evaluate the risks involved with typical leak testing procedures.

4.2 Physical Description

4.2.1 Geometry

The fuel tank geometry under consideration is shown in figure 4.1 and was chosen to represent the vapour space of a "thin profile" tank geometry with an in tank fuel pump, similar to the one used for experimental work in chapter 3. The plastic "bowl" and fuel pump enclosure were included in the model because they represent significant obstructions to the vapour flow inside the tank. The service port connection was centered above the fuel pump enclosure. While most tanks do not form perfect symmetry, the model geometry was considered to be symmetrical to keep computational requirements reasonable.

4.2.2 Fuel Tank Contents

Fuel tanks will usually have two discrete phases with liquid fuel filling the bottom of the tank and a mixture of fuel vapour and air in the balance of the tank volume. Under normal evaporative emission leak testing procedures, flow will only occur in the gaseous phase in the tank. However, the liquid will contribute fuel vapour through evaporation if the vapour concentration is below equilibrium. For the purposes of the model, the walls and top of the vapour space were assumed dry, so the liquid-vapour interface at the bottom of the vapour space was the only source of gasoline vapour.

4.2.3 Initial Conditions

Unless the vehicle has recently been driven or fuel system components have been removed, the gasoline vapour in the tank will be at equilibrium ini-

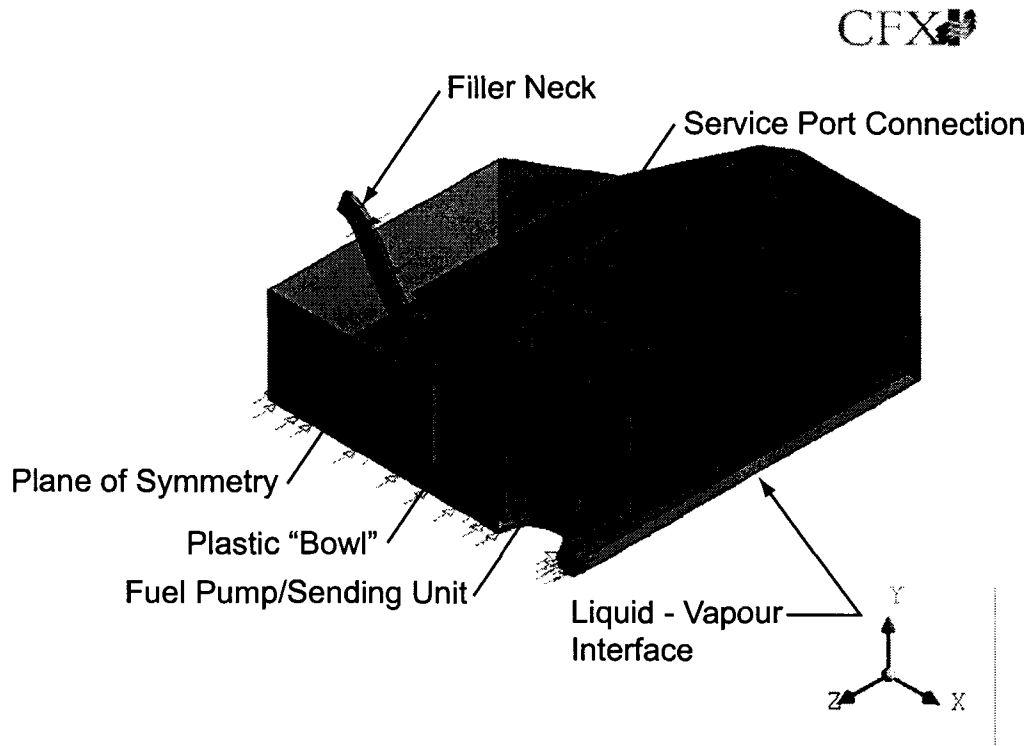


Figure 4.1: Fuel tank model geometry. Similar to geometry of the "thin profile" tank used for experimental work.

tially:

$$P_{gasoline} = P_{gasoline,sat}@T_{amb} \quad (4.1)$$

The total pressure in the tank is either at or very close to atmospheric pressure, so the gasoline vapour mole fraction can be calculated.

$$\chi_{gasoline} = \frac{P_{gasoline,sat}}{P_{atm}} \quad (4.2)$$

The balance of the vapour space in the tank is initially air. The gasoline vapour mole fraction is most useful for determining if the gasoline vapour is within the flammable range. The mass fraction, useful for diffusion purposes, can also be calculated as follows:

$\chi_{gasoline,sat}$	Fuel RVP (kPa)	T_{amb} (°C)	P_{atm} (kPa)
.50	90	23	93
.31	60	23	93
.21	45	18	101

Table 4.1: Initial conditions considered for the model.

$$Y_{gasoline} = \frac{\chi_{gasoline} M_{gasoline}}{\chi_{gasoline} M_{gasoline} + (1 - \chi_{gasoline}) M_{air}} \quad (4.3)$$

The equilibrium vapour pressure of a fuel is a factor of fuel volatility and ambient temperature as described previously in chapter 2. Initial, equilibrium mixtures during leak testing can vary widely. Table 4.1 summarizes the initial conditions considered in the model. A high and low volatility fuel at ambient conditions simulating the experimental test conditions were included. A third condition was included to simulate a slightly weathered California summer gasoline¹ tested on a cool day at sea level.

4.2.4 Leak Testing Flow Regimes

The two leak testing flow patterns as described in chapter 2 were both considered. The purging flow either enters from the service port connection and exits at the filler neck or vice versa. Typical purge flow rates are on the order of 11 LPM. A range of 5 to 20 LPM from service port connection was considered for this model. An oil "fog" carried by air or nitrogen is generally used as the test fluid. The time of flow was 10 minutes, representing two complete purge flow cycles for typical leak detection machines.²

4.3 Model Characteristics

CFX® computational fluid dynamics software was used to create and solve the numerical model of the fuel tank. A number of assumptions were made in the creation of the model. The following sections describe the theory used in the model³, the boundary conditions applied, and the assumptions made

in the construction of the model.

4.3.1 Model Theory

The numerical model included a number of assumptions to reduce computational requirements to a manageable level. The behaviour of the system was assumed to follow the ideal gas equation of state. The volume of liquid was assumed to remain constant as evaporation proceeded. Pure gasoline vapour will, depending on exact conditions and composition, occupy approximately 250 times the volume of liquid gasoline. Therefore it takes a very small amount of liquid gasoline to produce a large amount of vapour.

Heat transfer within the system was neglected as the system was considered isothermal. While heat transfer has been shown to be significant in some cases, these cases were either looking at steady state evaporation⁴ or the case where a liquid is exposed to an atmosphere containing none of its vapour⁵. The vapour space above the liquid is initially entirely saturated in this case so the evaporation rate is not as great. A study on fuel system components during refueling⁶ has shown good agreement with experimental results with the isothermal assumption.

Because the system is assumed isothermal, diffusion due to temperature gradients is neglected accordingly. Regardless, this assumption has been shown to be valid for evaporation systems where the liquid vapour has higher density than the gaseous mixture.⁷

The model solves the governing equations of mass conservation and momentum for the fluid properties. Single velocity and pressure fields were calculated for both components of the fluid. A general representation of the continuity and momentum equations respectively can be given as below (see Nomenclature for an explanation of the symbols used).

$$\frac{\partial \rho}{\partial t} + \nabla \cdot (\rho \mathbf{U}) = 0 \quad (4.4)$$

$$\frac{\partial \rho \mathbf{U}}{\partial t} + \nabla \cdot (\rho \mathbf{U} \otimes \mathbf{U}) = \nabla \cdot (-p\delta + \mu(\nabla \mathbf{U} + (\nabla \mathbf{U})^T)) + S_M \quad (4.5)$$

The flow in this model is both unsteady and has variable density, so no further simplifications can be made. Because the fluid has two components, the transport of each component by diffusion is solved with a binary diffusion equation.⁸

$$\frac{\partial \rho_A}{\partial t} + \nabla \cdot (\rho_A \mathbf{U}) = (\nabla \cdot \rho D_{AB} \nabla Y_A) \quad (4.6)$$

Thus, convection and diffusion of the components are considered by the momentum and diffusion equations respectively. The density, ρ_A , is equivalent to:

$$\rho_A = Y_A \rho \quad (4.7)$$

4.3.2 Reynolds Averaged Governing Equations

Unfortunately, solving the above equations directly would require a mesh of minute proportions to correctly model turbulence within the flow. Instead, quantities within the flow are split into an time averaged and time varying component in a process known as Reynolds Averaging.

$$\mathbf{U} = \bar{\mathbf{U}} + \mathbf{u} \quad (4.8)$$

While the total continuity equation remains unchanged and can be written identically to above with time averaged quantities, the momentum equation becomes:

$$\frac{\partial \rho \bar{\mathbf{U}}}{\partial t} + \nabla \cdot (\rho \bar{\mathbf{U}} \otimes \bar{\mathbf{U}}) = \nabla \cdot (-\bar{p}\delta + (\mu + \mu_t)(\nabla \bar{\mathbf{U}} + (\nabla \bar{\mathbf{U}})^T)) \quad (4.9)$$

A new turbulent viscosity (μ_t) is introduced, which represents the Reynolds stresses due to turbulence within the flow. The transport equation for each

component also requires modification to reflect turbulent eddy dissipation.

$$\frac{\partial \rho_A}{\partial t} + \nabla \cdot (\rho_A \bar{\mathbf{U}}) = (\nabla \cdot \Gamma_{A_{eff}} \nabla Y_A) \quad (4.10)$$

In this case:

$$\Gamma_{A_{eff}} = \rho D_{AB} + \frac{\mu_t}{Sc_t} \quad (4.11)$$

where Sc_t is the turbulent Schmidt number.

4.3.3 Turbulence Model

The turbulent eddy dissipation model requires additional equations to solve for the turbulent viscosity μ_t . The two equation $k-\epsilon$ model was used for this work. The term k represents turbulent kinetic energy and ϵ represents the turbulent eddy dissipation rate. A more detailed description can be found in literature.⁹ This model was compared to other two equation models such as the $k-\omega$ and RNG $k-\epsilon$ models but was more robust. The other models considered did not meet the minimum residual convergence criteria of 1E-4.

4.3.4 Fluid Properties

The fluid entering the fuel tank from the leak detection equipment was modelled as air only. The gasoline vapour was simulated by a single component fuel vapour. As mentioned in chapter 2 gasoline vapour composition can vary widely, but the primary components are generally pentane and butane isomers, with some heavier components forming the balance of the mixture.

The transport properties used for the fuel vapour were equivalent to pentane. The binary diffusivity for pentane-air mixtures was calculated with the method of Reid.¹⁰ Full details can be found in Appendix D.

4.3.5 Density Considerations

The density of a gasoline vapour/air mixture is:

$$\rho_{mix} = \frac{P(\chi_{gasoline}M_{gasoline} + (1 - \chi_{gasoline})M_{air})}{\bar{R}T} \quad (4.12)$$

Gasoline has a higher molecular weight than air, so gasoline vapour/air mixtures are heavier than air. Initially, assuming a uniform, equilibrium gasoline vapour/air mixture within the tank, the density is constant throughout the vapour space. Adding air to the tank creates density differences before the gasoline vapour has an opportunity to diffuse uniformly into the added air. This density difference creates a buoyant force on any part of the mixture with lower gasoline vapour concentrations.

To model buoyancy properly, the CFX® full buoyancy model was used. This adds a source term to the momentum equation:

$$S_{M,buoy} = (\rho - \rho_{ref})g \quad (4.13)$$

which acts in the y direction. The reference density was arbitrarily set to 1.18 kg/m^3 , approximately air density at standard atmospheric conditions. For the full buoyancy model, the density is calculated everywhere in the mesh based on the composition at each point.

4.3.6 Boundary Conditions

A constant normal velocity was specified at the inlet to the tank based on the required air flow rate. The outlet was modeled as an opening at atmospheric pressure to allow inflow and outflow. Any inflow at the outlet was considered to be 100% air. All dry surfaces within the tank, including the walls and top, were modeled as a no slip wall boundary.

At the liquid-vapour interface, the fuel mass fraction was assumed to remain at equilibrium. The velocity at the liquid-vapour interface was solved by considering the mass flux of air at the interface. The liquid fuel was assumed to remain saturated with dissolved air throughout the duration of flow. As such, the net air flux normal to the liquid interface was zero.⁸ Fick's law for the flux of gasoline vapour can be written as:

$$\dot{m}''_{gasoline} = Y_{gasoline}(\dot{m}''_{gasoline} + \dot{m}''_{air}) - \rho D_{AB} \nabla Y_{gasoline} \quad (4.14)$$

Assuming that a concentration gradient exists only in the vertical y direction:

$$\dot{m}''_{gasoline} = Y_{gasoline}(\dot{m}''_{gasoline} + \dot{m}''_{air}) - \rho D_{AB} \frac{\partial Y_{gasoline}}{\partial y} \quad (4.15)$$

Setting the air mass flux to zero and solving for the gasoline vapour mass flux:

$$\dot{m}''_{gasoline} = -\frac{\rho D_{AB}}{(1 - Y_{gasoline})} \frac{\partial Y_{gasoline}}{\partial y} \quad (4.16)$$

Thus, the mass flux and concentration at the liquid-vapour interface are specified. A symmetry boundary condition was also specified at the mid-plane of the tank, reducing computational time by half.

4.4 Solution Strategy

The initial condition for the model run was set by a steady state run with a wall located at the flow inlet and the outlet remaining as an opening. This approach provided CFX with a initial solution with no flow into the model. A subsequent transient run of 4800 time steps of 0.125 seconds, and a maximum of 9 loops for each time step provided the transient flow response within the fuel tank model over a typical leak test flow duration. Solution convergence was determined by meeting a maximum residual requirement of 1E-5. A solution converged to a residual of 1E-4 was essentially identical to that converged to 1E-5. A model was also run on a finer mesh, with similar results. Details on the mesh sensitivity study are given in appendix D.

4.5 Results

4.5.1 Air Flow Characteristics

The air velocity profile at the center plane filler neck and service port inlet to the fuel tank can be seen in figure 4.2. The fuel pump enclosure beneath the service port inlet tended to reflect the flow of air jetting downward into the tank back to the top of the tank. This upward air velocity assisted the buoyant force from the dense fuel vapour-air mixture on the relatively light air entering the tank. As a result, the majority of the air travels along the top of the tank, and mixing primarily becomes dependent on the diffusion characteristics of the mixture.

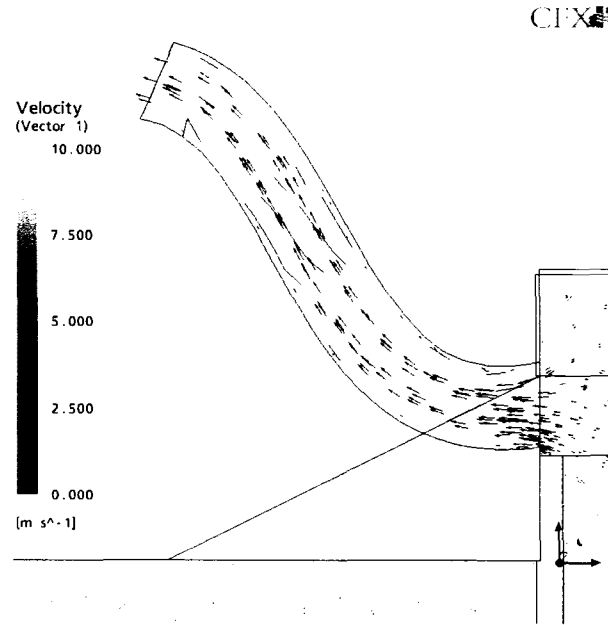
4.5.2 Comparison to Experimental Results

A comparison of the model and experimental results obtained in chapter 3 was done by looking at the concentration profile at the rear corner of the tank for three different initial concentrations. The model showed the best agreement with the low initial concentration typical of slightly weathered, low volatility fuel, shown in figure 4.3. Figure 4.5 compares the model concentration profile to the three sensors at this location (sensors 3, 4, and 5). The model showed excellent agreement after 2.5 minutes of flow. As the flow continued to 5 and 10 minutes, the model began to deviate from the experimental results.

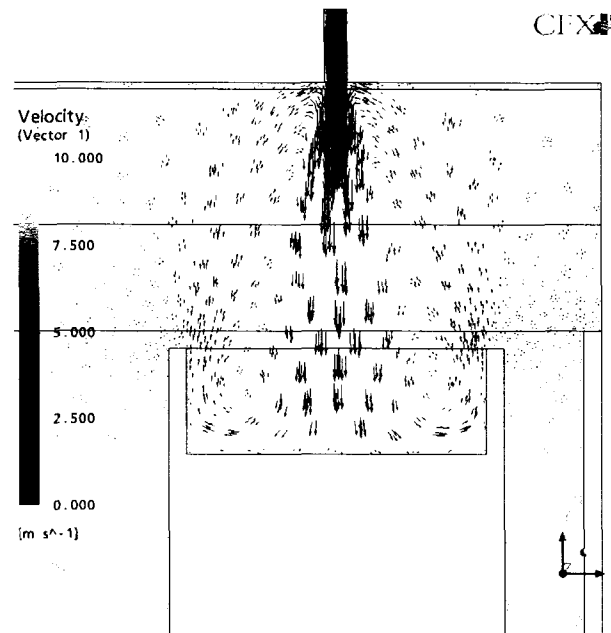
The deviation is likely caused by some mixing process that is present in the experimental tank but is not seen in the model. The experimental air flow entering the tank may have a swirl component from a 90 degree elbow in the fuel sending unit, just before it enters the tank. Also, the experimental inlet was not located in the direct center of the sending unit as modelled.

4.5.3 Flammable Mixtures

The goal of this chapter is to evaluate the flammable mixtures formed during leak testing procedures when air is used as the test fluid in a typical au-



(a) Filler neck velocity profile



(b) Service port inlet velocity profile

Figure 4.2: Velocity vector diagrams at the mid plane of the fuel tank for a flow of 10 LPM from the service port. The filler neck is shown in (a) and the service port inlet is shown in (b).

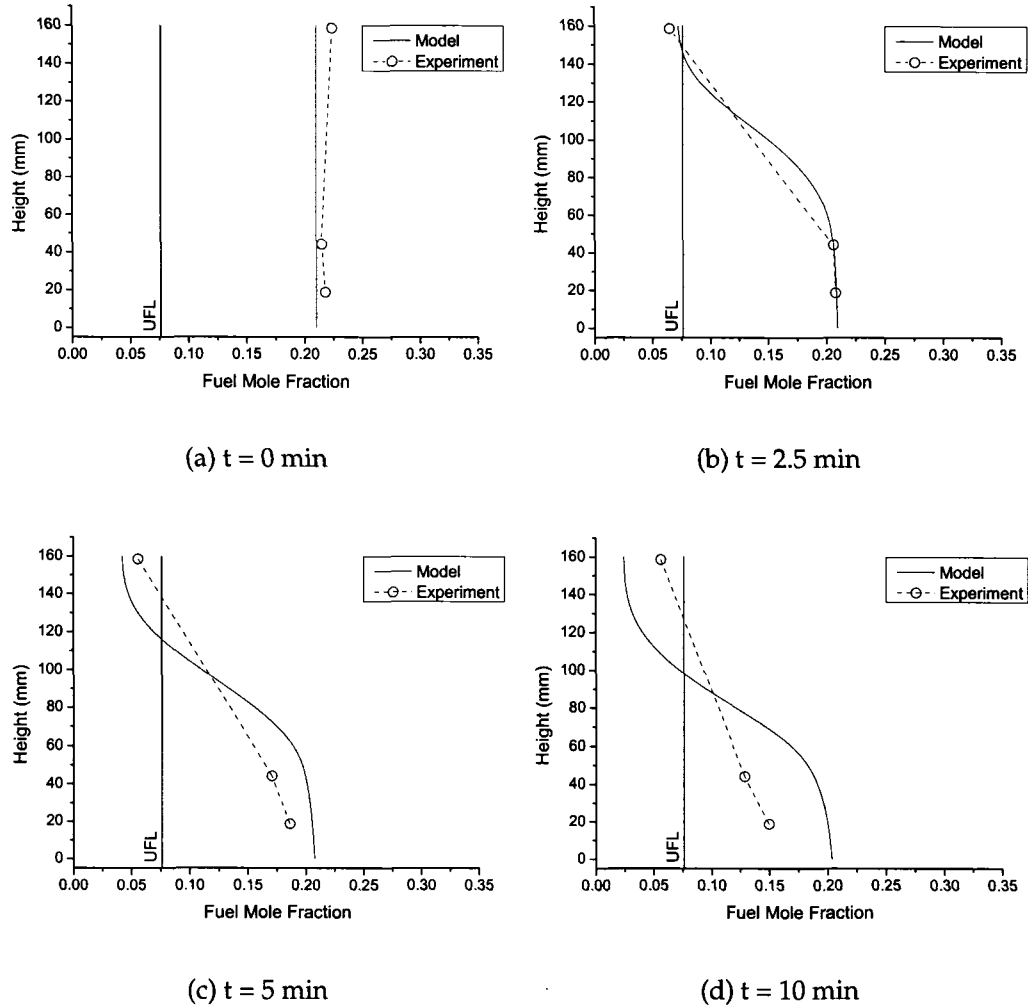


Figure 4.3: Comparison of model and experimental gasoline vapour mole fraction for weathered gasoline S. W. 5 with an initial gasoline vapour mole fraction of 21% at a flow rate of 10 LPM.

tomotive fuel tank. A wide range of conditions can be experienced during leak testing, and the effects of the two primary conditions, air flow rate and initial fuel concentration, are discussed here. Figure 4.6 shows the relative effect of the initial fuel vapour fraction on the flammable volume formed in the tank for a 10 LPM air flow from the service port. At higher initial

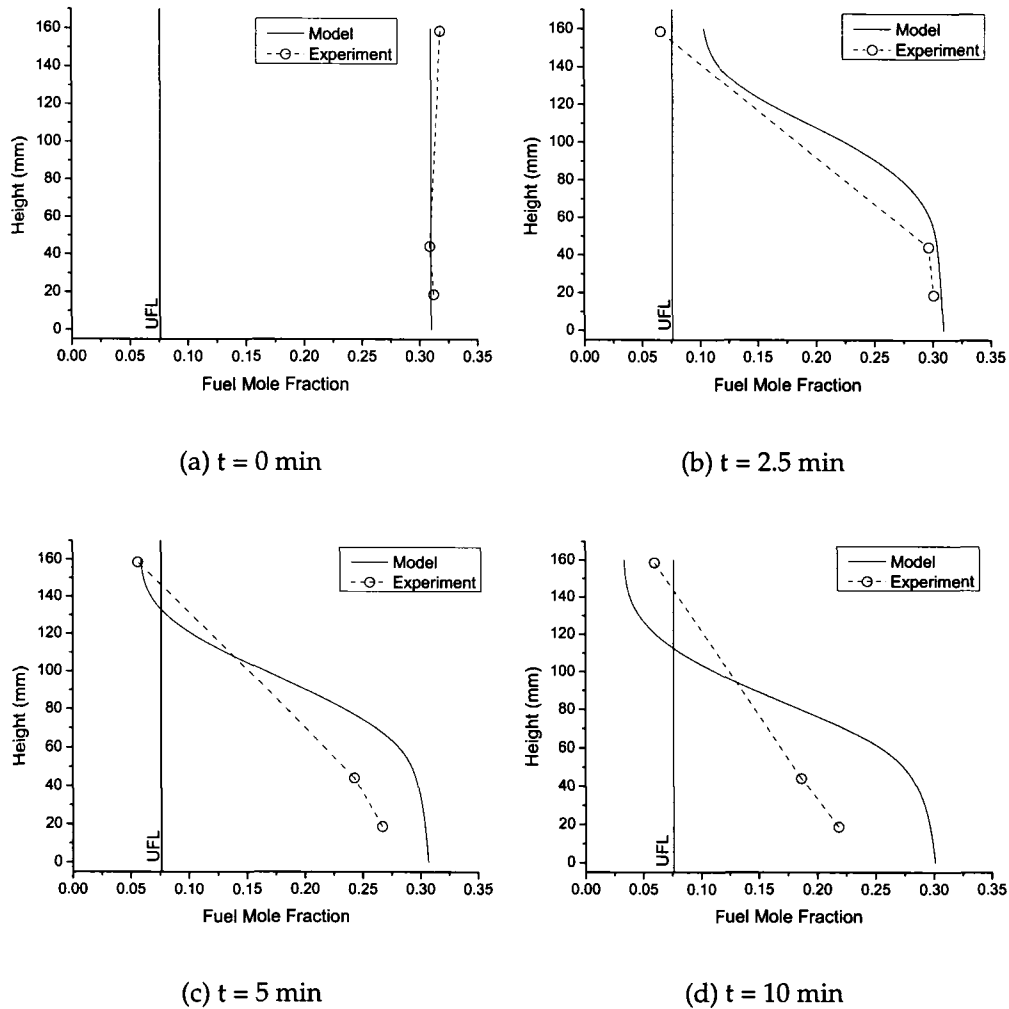


Figure 4.4: Comparison of model and experimental gasoline vapour mole fraction for low volatility gasoline.

concentrations, the time for the initial dilution to the flammable region is increased. With 90 kPa gasoline, very little flammable mixture is formed until 4.5 minutes has elapsed. Therefore, one method of keeping leak testing safe is to use high volatility gasoline while limiting the test duration to approximately 5 minutes, at a flow rate of 10 LPM.

The inlet flow rate also has a significant affect on the flammable mixture

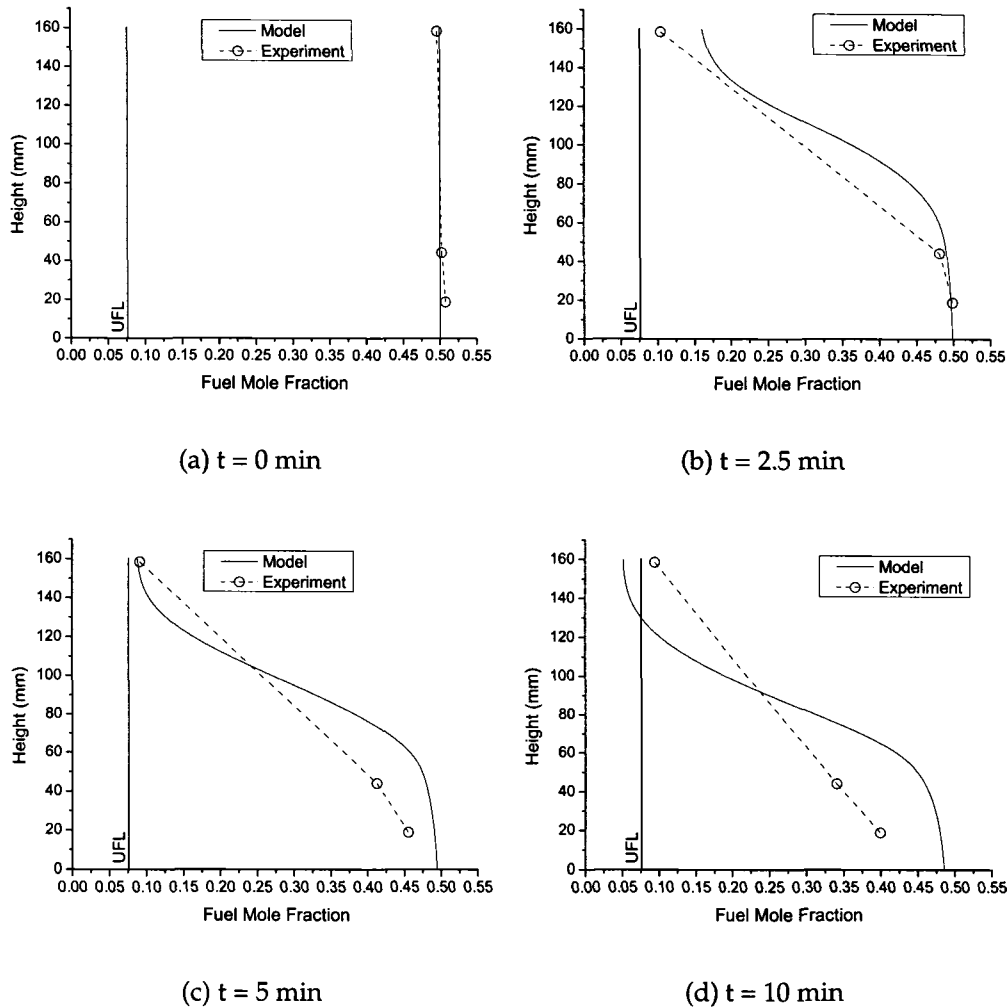


Figure 4.5: Comparison of model and experimental gasoline vapour mole fraction for S. 90 with an initial gasoline vapour mole fraction of 50% at a flow rate of 10 LPM.

formed in the tank. Figure 4.7 compares the flammable volume formed over a range of flow from 5 LPM to 20 LPM with an initial fuel vapour fraction of 21%. Limiting the flow to 5 LPM creates very little flammable volume until nearly 4 minutes has elapsed, even with the low initial gasoline vapour fraction. The combination of limiting the flow rate with a limited flow duration

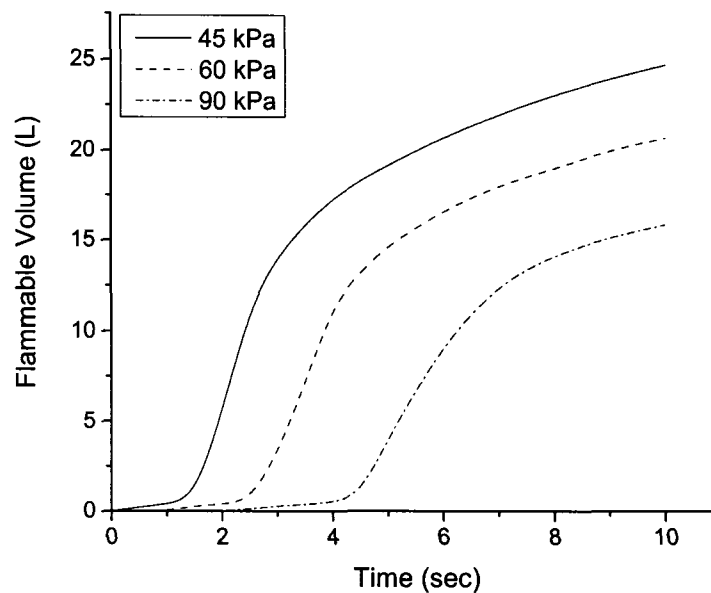


Figure 4.6: Effect of initial composition on flammable volume formed within the fuel tank. Flow rate 10 LPM.

will also reduce the flammable volume formed during leak testing.

The greatest hazard is encountered when low volatility gasoline is combined with a high air flow rate and a long test duration. Figure 4.8 shows the buildup of flammable mixture in the fuel tank for an initial gasoline vapour fraction of 21% and a flow rate of 10 LPM. The flammable region initiates at the air inlet as expected and gradually fills the tank from the top down, because of the density difference between the air entering the tank and the rich gasoline vapour/air mixture in the tank, as well as the gasoline evaporating from the liquid interface at the bottom of the tank. Ignition sources near the top of the tank are much more likely to ignite any flammable vapours in the tank because of the top-down nature of the flammable volume.

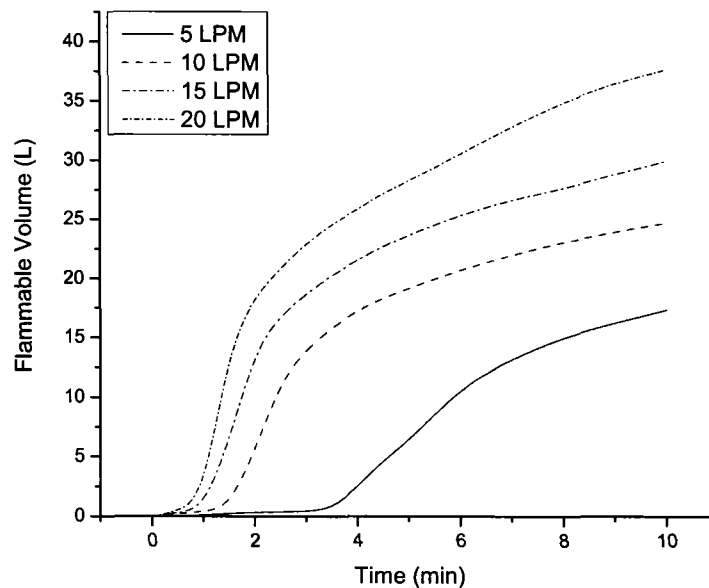


Figure 4.7: Effect of flow rate on flammable volume formed within the fuel tank. Initial fuel vapour fraction in the tank is 21%.

4.6 Summary And Conclusions

Typical leak detection flows can significantly decrease fuel vapour concentrations in fuel tanks under test. Numerical methods can be used to gain insight to vapour concentration distribution in a fuel tank that is not possible with experimentation. A numerical model has been created to predict the vapor composition effects of air flow into a fuel tank vapor space for evaporative emission testing. The flammable volume formed in a fuel tank during leak testing can be limited by maintaining a high initial gasoline vapour fraction in the tank with high volatility fuel above 20°C and limiting the air flow rate into the tank. At an initial gasoline vapour fraction of 50% a 10 LPM flow of air into a fuel tank is likely to be safe for up to 4 minutes. Likewise, a 5 LPM flow into a tank containing 21% gasoline vapour will likely be safe up to 4 minutes. If the gasoline volatility is unknown, a different approach is likely required to maintain a safe mixture in the fuel

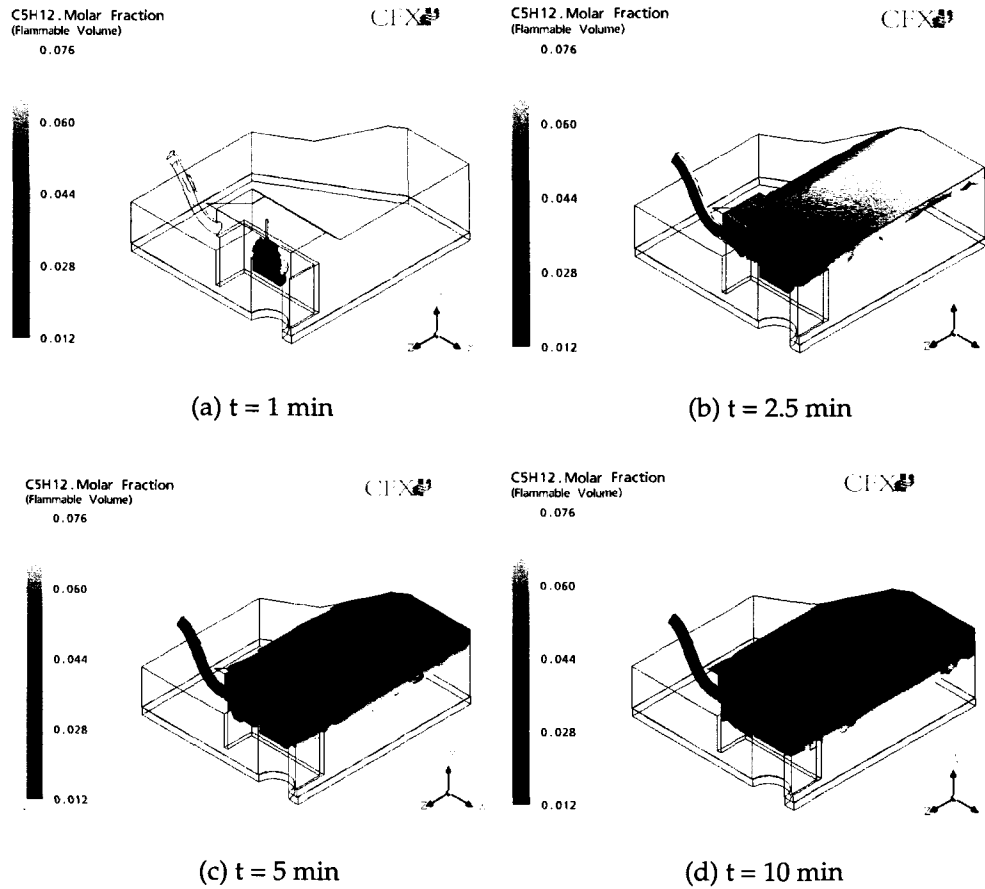


Figure 4.8: Flammable vapours predicted for an initial mole fraction of 0.21 and a flow rate of 10 LPM.

tank during leak testing. Chapter 5 discusses the use of inert gas to prevent flammable mixtures in automotive fuel tanks during leak testing.

REFERENCES

- [1] A. D. Brownlow, J. K. Brunner, and J. S. Welstand. Changes in Reid vapor pressure of gasoline in vehicle tanks as the gasoline is used. *SAE Paper No. 892090*, 1989.
- [2] Anonymous. *Operator's Quick Reference Manual*. Redline Detection LLC, 2512 Fender Ave. Unit A, Fullerton, CA 92831, 01-0002c edition.
- [3] Anonymous. "*Basic Solver Capability Theory, CFX-5 Solver Theory*". ANSYS, 2004.
- [4] A. T. Prata and E. M. Sparrow. "diffusion driven non-isothermal evaporation". *ASME J. Heat Transfer*, 107:239–242, 1985.
- [5] R. Bunama. *Numerical Simulation of the Formation of Flammable Atmospheres Within Enclosures Due to the Convective Diffusion of Mass and Heat*. PhD thesis, University of Calgary, December 1998.
- [6] R. Banerjee and et. al. "CFD simulations of critical components in fuel filling systems". *SAE Paper No. 2002-01-0573*, 2002.
- [7] W. J. Minkowycz, E. M. Sparrow, and R. G. Eckert. "diffusion-thermo effects in stagnation-point flow of air with injection of gases of various molecular weights into the boundary layer". *AIAA Journal*, 2:652–659, 1964.
- [8] R. B. Bird, W. E. Stewart, and E. N. Lightfoot. *Transport Phenomena*. John Wiley & Sons, 1960.

-
- [9] Anonymous. *"Turbulence Theory, CFX-5 Solver Theory"*. ANSYS, 2004.
- [10] S. R. Turns. *An Introduction to Combustion: Concepts and Applications*. McGraw Hill, Inc, 2nd edition, 2000.

CHAPTER 5

CONCLUSIONS AND RECOMMENDATIONS

The flammable volume present in a fuel tank vapour space from a leak testing procedure can be minimized or prevented by several methods: maintaining high gasoline volatility, limiting the leak test flow rate, limiting the leak test flow duration, and using an inert gas as the driving component of the test fluid. This chapter evaluates each method for suitability in evaporative emissions system leak testing. The work completed in this thesis is summarized and the major conclusions are presented.

5.1 Hazard Reduction Analysis

A number of approaches can be taken to reduce or eliminate flammable mixtures formed within fuel tanks during leak testing procedures. Filling the tank with gasoline before testing the system will minimize the total vapour space within the tank and reduce the weathering effect on the fuel. This may not be ideal because the indicating fluid will not be able to exit the leak if it is located below the liquid interface in the tank, and a liquid gasoline leak might not be as easily found.

The gasoline vapour concentration present in the tank before testing should be maintained as high as possible. High volatility gasoline blends will increase the initial concentration; however, most jurisdictions concerned with evaporative emissions will have regulations requiring low volatility gasoline. Vehicles will usually come to the shop with pre-existing gasoline in the tank and most repair facilities do not have the capability to measure

gasoline volatility. Emptying and refilling the fuel tank will also take valuable shop time so this is not the most desirable approach to ensure safety.

The initial gasoline vapour concentration can also be increased by increasing the temperature of the fuel system prior to testing. Liquid fuel temperatures typically rise approximately 0.14°C per minute during the first hour of operation, with the exact rate depending on the vehicle configuration.¹ Therefore, from the perspective of the fuel tank contents, testing a hot vehicle that has recently been operating is safer than testing a vehicle that has been sitting for a long period. The other option is to maintain a high ambient temperature in the test environment; however, some unheated shops may not have the option of controlling the ambient temperature during leak testing. It should be noted that purging the vapour contents of a fuel tank containing a high initial gasoline concentration will result in more gasoline vapour released in the environment surrounding the evaporative emissions system. If ignited, this vapour could produce a flash fire outside the system.

Reducing the flow rate of air during leak testing will also reduce the volume of flammable vapour formed during testing. A flow rate of 5 LPM resulted in 6 L of flammable mixture after 5 min with an initial gasoline vapour concentration of 21%, compared with 19 L of flammable mixture for a 10 LPM flow rate. This was approximately a three-fold reduction.

Limiting the leak testing flow duration reduces the amount of air entering the system and of fuel vapour exiting the system. Some leak detection machines include automatic flow shutoff after a 5 min flow duration.² However, nothing prevents service personnel from running multiple consecutive cycles.

If the use of air is unavoidable for leak testing, every effort should be made to eliminate any ignition sources around the tank for at least 20 minutes after the test cycle has been completed. Proper grounding will prevent static discharges, and the vehicle ignition key should remain off for this period to prevent any sparks generated by the fuel pump electrical circuit.

Another option for preventing flammable mixture formation in fuel tanks is to use an inert gas such as nitrogen or carbon dioxide as the driving com-

ponent of the test fluid. This approach has been used in the aircraft industry, as noted in chapter 2. The flammable range is decreased by adding inert gas to the mixture.³ Figure 5.1 demonstrates the difference between using nitrogen and air.⁴ Adding 100% nitrogen to a typical fuel tank equilibrium vapour mixture will completely prevent flammable mixtures from forming within the tank, as long as the initial mixture is above the flammable range. A 50% nitrogen/50% air (90% nitrogen/10% oxygen) mixture will prevent flammable mixtures from forming when the gasoline vapour is initially above 20%.

5.2 Summary and Conclusions

The recent developments in evaporative emissions regulations have created a need for finding leaks in automotive fuel systems, specifically the equipment used to control evaporative emissions. Automobile fires in public service stations have shown an upward trend since the introduction of automotive evaporative emissions control equipment. While statistics that specifically pinpoint the cause of these fires are limited because of the difficulty of determining the fire origin, concerns have been raised regarding the potential fire or explosion hazards during a typical fuel system leak detection procedure. A fire or explosion in an automotive fuel system requires a fuel vapour-air mixture within the flammable range and an ignition source. The many possible scenarios for ignition make ignition source elimination impractical. Controlling the properties of the mixture within the evaporative emissions system is a more realistic method of controlling the hazards. The goal of this work was to identify leak testing situations where flammable mixtures can be formed within a fuel tank.

Flammable mixtures can be formed both within and outside the fuel system. Any time rich fuel vapour is leaking from the fuel system to the atmosphere, a fire can potentially be started, because the air in the atmosphere will dilute the gasoline vapour to the flammable region. Such a fire could potentially spread to other vehicle components, possibly consuming the en-

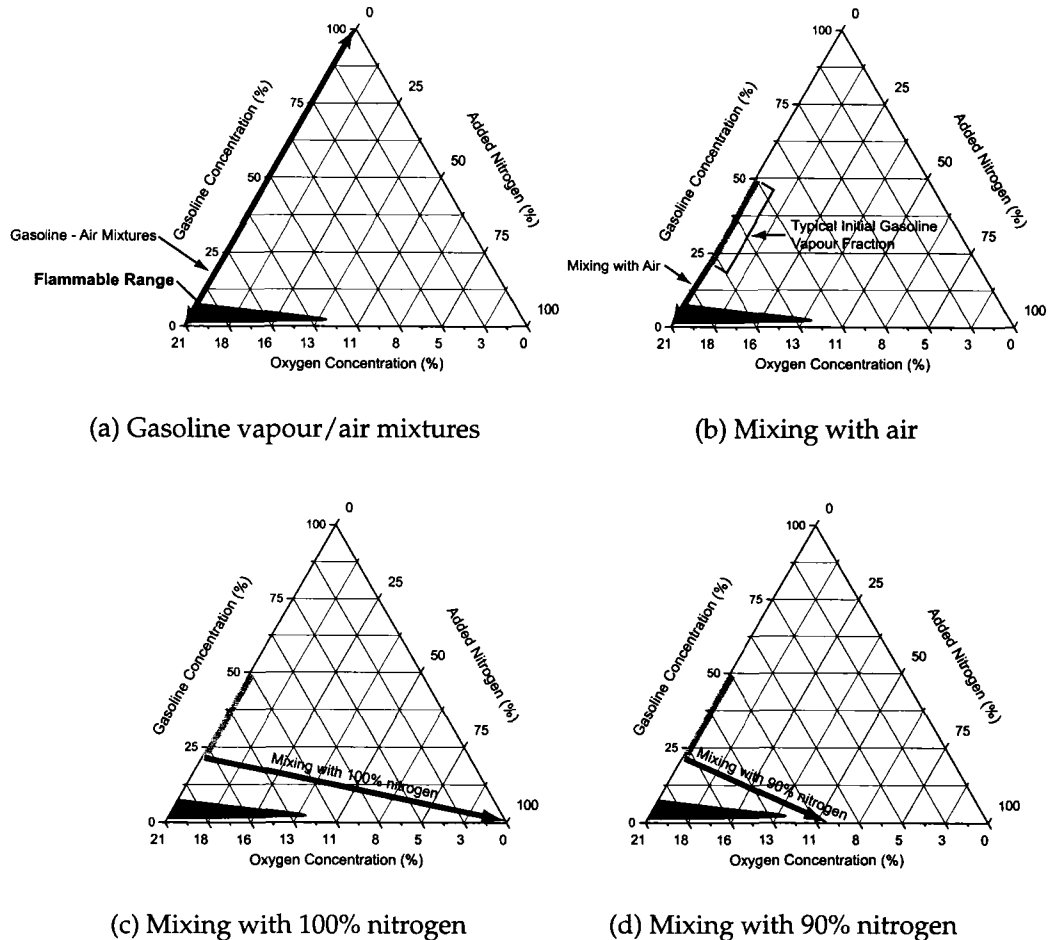


Figure 5.1: Ternary diagrams showing the difference between using nitrogen and air as the driving component of the test fluid. Gasoline vapour/air mixtures are represented by the left hand axis (a). The typical range of initial gasoline vapour mole fraction is between 21% and 50% (b). The mixture passes through the flammable range when mixed with air (78% nitrogen). By mixing with 100% nitrogen, the mixture does not approach the flammable range (c). As low as 90% nitrogen (balance oxygen, nominally a 50% nitrogen/50% air mixture) can be used to dilute the initial gasoline vapour mixture without passing through the flammable range (d).

tire vehicle. Flammable mixtures formed within the system can create a significant pressure rise if ignited, leading to fuel system component failure. At a minimum, any failed components will require replacement. If liquid gasoline is spilled, an escalating pool fire can continue to burn and spread. This dissertation focused on evaluating and predicting gasoline vapour/air mixtures in the fuel tank with low liquid levels present, the case where the fuel system has nearly maximum vapour volume. Experimentation and numerical modelling were used to determine the extent of flammable mixtures formed during leak test procedures.

An experimental test rig was developed based on a common passenger car fuel tank/filler neck configuration. Oxygen sensors mounted directly on the fuel tank provided real time monitoring of the oxygen concentration without compromising flow characteristics within the fuel tank. The calibration of the sensors was verified with vapor pressure measurements and gas chromatography. With the oxygen concentration known, the gasoline vapor concentration could be calculated.

A numerical model was created to predict fuel vapor concentrations in fuel tanks during evaporative emissions testing. Typical leak detection scenarios where flow entered the tank from the service port were modeled. The total flammable volume was calculated for a range of flow rates and initial gasoline vapour concentrations.

The numerical model showed similar trends in the distribution of gasoline vapour concentration in the tank to the experimental results, particularly within the first 5 minutes of flow. As time increased, the model increasingly deviated from the experimental results, indicating that some large scale mixing phenomenon was not being modeled ideally. However, the model provided a good indication of the flammable mixture volume formed in the tank under the conditions tested.

The initial gasoline vapour concentration in the tank was the primary factor affecting flammable mixture formation. Initial concentrations typical of low volatility gasoline at cool ambient temperatures created the greatest hazard.

The volume of flammable mixture formed was also dependent on leak test flow rate. Flammable quantities of up to 25 L were noted at a leak test flow of 10 LPM.

The flammable mixture volume within the fuel tank increased up to the maximum flow duration of 10 minutes. At least 20 minutes were required after flow testing for the tank to return to near equilibrium.

A field test was conducted to see the extent of damage when a fuel tank containing flammable mixture from a leak test procedure was ignited, as described in Appendix E. The fuel tank sending unit was propelled out of the tank and the tank experienced significant deformation.

5.3 Recommendations

Ideally, an inert gas such as nitrogen should be used for all leak testing procedures. Nitrogen concentrations over 90% are effective at eliminating flammable volumes within the fuel tank. In the event that there is no inert gas available, air can be used with caution. The liquid level in the fuel tank should be kept as high as possible to reduce the total vapour space and the effects of weathering. Preferentially, the tank should be filled with high volatility gasoline. The air flow rate should be limited below 10 LPM and the flow duration should be limited to 5 minutes. Ignition sources should be limited as much as possible during and for a minimum of 20 minutes after a leak test where air is used.

5.4 Future Work

This work demonstrates that significant quantities of flammable mixture can be formed within fuel tank vapor space during leak testing. The fuel tank considered in this work was representative of "thin profile" tanks commonly found in front wheel drive passenger cars. Flammable mixtures may form differently in other fuel tank geometries.

Alcohol blended fuels can have lower initial vapour concentrations and

a wider flammable range than gasoline.⁵ Also, the weathering characteristics of such a mixture could be exacerbated. The combination of these factors will likely cause greater volumes of flammable mixtures when leak testing is performed on a vehicle containing an alcohol blended fuel than similar circumstances with a non-oxygenated fuel. Additional work could identify the extended conditions where leak testing is a hazard with alcohol containing fuels.

Ignition and flame propagation from an external source will be dependent on the dispersion characteristics of the gasoline vapour as it is expelled from the fuel system. A study on vapour behaviour outside the fuel tank could shed some light on the possibility of ignition from external sources.

REFERENCES

- [1] H. M. Haskew and T. F. Liberty. "Diurnal emissions from in-use vehicles". *SAE Paper No. 1999-01-1463*, 1999.
- [2] R. L. Banyard. Personal communication, Apr 10, 2006. Star Envirotech Inc. Technical Director.
- [3] M. G. Zabetakis. "Flammability characteristics of combustible gases and vapors". *U.S. Bureau of Mines Bulletin 627*, 1965.
- [4] Anonymous. "Standard on explosion prevention systems". National Fire Protection Association, 2002.
- [5] R. H. Vaivads, M. F. Bardon, and V. K. Rao. "Flammability tests of alcohol/gasoline vapours. *SAE Paper No. 950401*.

APPENDIX A

EQUILIBRIUM VAPOR PRESSURE MEASUREMENTS

A.1 Introduction

The flammability of a gasoline vapour mixture can only be determined if the relative quantity of gasoline vapour is known. As noted in chapter 2, gasoline is a volatile liquid at room temperature and will produce vapour at a liquid-gas interface up to an equilibrium vapour pressure. The concentration of a gasoline vapour/air mixture at equilibrium can be calculated if the gasoline vapour pressure and the total pressure are known. This appendix describes the method used for equilibrium gasoline vapour pressure measurement.

A.2 Vapour Pressure Measurement Standards

Volatility is one of the most critical properties for gasoline performance in engines¹ and standards have been developed by ASTM to accurately and repeatably measure the equilibrium vapour pressure. The most common method used for measuring Reid Vapour Pressure is standardized in ASTM D 323.² A filled liquid sample container is connected to a vapour chamber containing air at 37.8°C and atmospheric pressure. Once the pressure in the vessel immersed in a 37.8°C water bath has reached a stable value for 2 minutes the gauge pressure relative to atmospheric pressure is recorded as the vapour pressure of the fuel. This method requires a purge of the

vapour volume with warm water between tests to remove any remaining volatile components. An alternative procedure, described in D 4953,³ is a dry procedure and does not require a warm water purge.

A method which measures Dry Vapour Pressure Equivalent (DVPE) is covered by ASTM D 5191,⁴ and is also used by Health Canada for determining vapour pressure of petroleum products.⁵ The method is essentially identical to that listed above in ASTM D 4953, but the liquid sample is injected to an initially evacuated chamber. The vapour pressure is calculated by adding correction factors to the total pressure achieved in the test vessel. Using an evacuated vapour chamber has the advantage that it does not need to be maintained at the test temperature prior to adding the liquid sample. The vapour pressure can then be measured at various temperatures. For the testing done for this thesis, the vapour pressure at ambient conditions can be converted into the equilibrium vapour concentration in the fuel tank, so a procedure was developed that used an evacuated vapour chamber.

A.3 Test Equipment and Procedure

A test bomb was constructed as shown in figure A.1. Liquid and vapour chambers were separated by a ball valve. The liquid/vapour volume ratio was 1:4.2, within the range prescribed by ASTM D 4953. A Marsh Instruments combination pressure/vacuum gauge was used to measure pressure within the bomb. Before each test, the bomb was evacuated with a Leybold vacuum pump. The vacuum was monitored for 5 minutes to identify any leaks and to ensure removal of any volatile components from the previous test. A water bath and an Omega HH11 thermometer were used to maintain and measure the test bomb temperature.

The test procedure followed the steps shown in figure A.2. The liquid sample was pulled from the gas tank and added to the test bomb immediately to minimize evaporative losses. The ball valve separating the liquid and vapour chambers was closed, and excess liquid was drained from the vapour volume. The vapour chamber was then evacuated and sealed with a

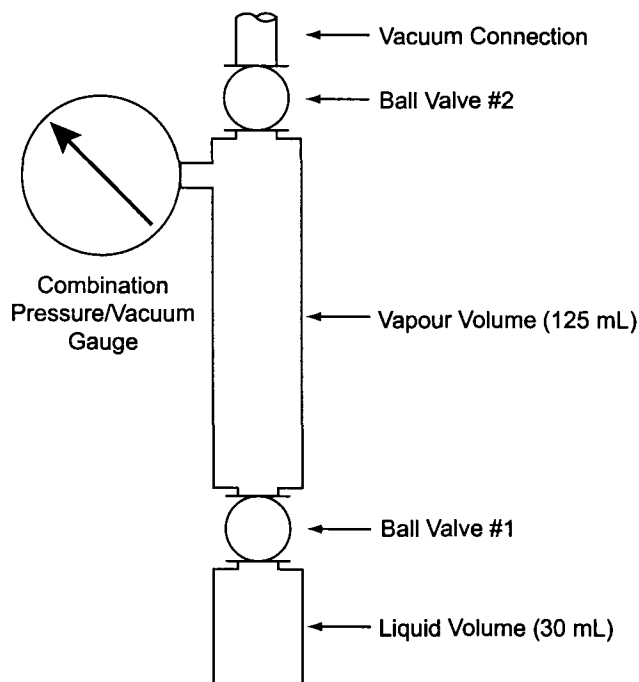


Figure A.1: Diagram of vapour pressure test bomb construction. The bomb was separated by a ball valve into liquid and vapour chambers with a liquid/vapour volume ratio of 1:4.2. The vapour pressure was measured by a combination pressure/vacuum gauge.

ball valve. The vacuum pressure in the vapour chamber was monitored for 5 minutes to determine if any leaks or volatile liquid residue were present. At this point, the ball valve separating the liquid and vapour chambers was opened and the apparatus was shaken for 1 to 2 minutes to obtain equilibrium. After 15 minutes or until the pressure indication stabilized the vapour pressure was recorded at ambient temperature. The bomb was then inserted into the water bath and the pressure allowed to stabilize at a temperature of 38°C.

The total pressure within the vessel was calculated with the measured gauge pressure and atmospheric pressure obtained from a mercury barometer.

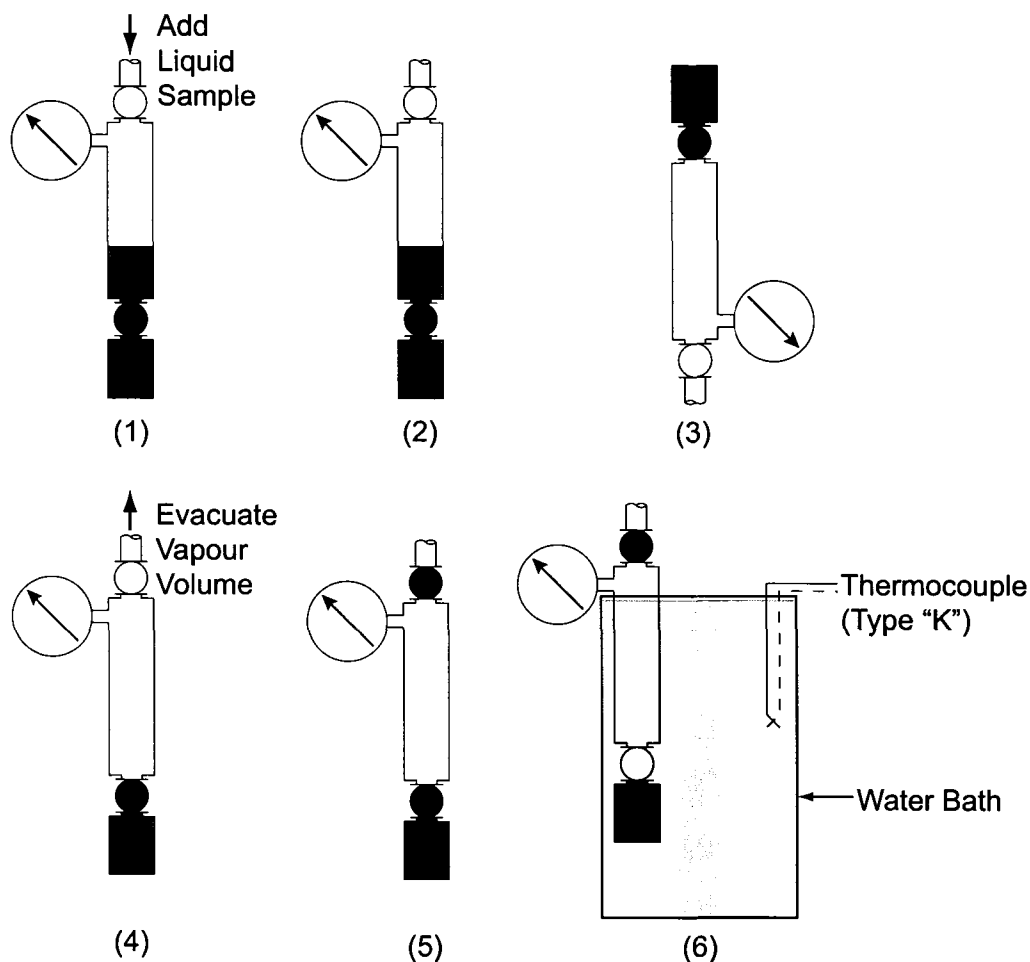


Figure A.2: Diagram of vapour pressure test procedure. By filling the bomb above the lower ball valve (1), closing the valve (2), and emptying the remaining contents of the bomb (3), a 4.2:1 vapour to liquid ratio was obtained. After evacuating (4) and sealing the upper portion of the bomb (5), the lower ball valve was opened and the vessel was rapidly agitated to reach equilibrium. A vapour pressure measurement was taken at ambient temperature and at 38°C in a water bath (6). The vapour pressure was measured by a Marsh Instruments combination pressure/vacuum gauge.

A.4 Vapour Pressure Measurement Uncertainty

The uncertainty in the vapour pressure measurement procedure was obtained by taking measurements with a pure substance of known vapour

pressure (n-pentane), comparing measurements with independently obtained measurements for 3 different gasoline volatility blends, and by taking repeatability measurements.

A.4.1 Pentane Vapour Pressure Measurement

Multicomponent mixtures such as gasoline are difficult to sample accurately for vapour pressure measurement, because high volatility components will evaporate relatively faster and the overall volatility of the remaining liquid will decrease. Pure substances are less sensitive to sampling procedures, so n-pentane was chosen to verify the accuracy of the test bomb itself. Also, the vapour pressure of n-pentane is well documented in literature, and can be calculated from the following relationship:⁶

$$P_{sat} = \frac{e^{78.741 - \frac{5420.3}{T} - 8.8253 \ln(T) + 9.6171 \cdot 10^{-6} (T)^2}}{1000} \quad (\text{A.1})$$

Figure A.3 shows a comparison of pentane vapour pressure from literature with the measured values. The measured values showed excellent agreement with the above relationship, with a maximum error of 2%.

A.4.2 Gasoline Vapour Pressure Measurement

The Imperial Oil Strathcona Refinery provided gasoline samples that had been RVP tested at their laboratory. High volatility (RVP = 96 kPa) and low volatility (RVP = 60 kPa) gasoline blends were tested with the vapour pressure test procedure. The measured values were compared to theoretical values calculated with equation 2.5(A.2) over a range of temperatures, shown in figure A.4.

$$P_{sat} = 10^{\frac{6.08 - 310.8[6.08 - \log(RVP)]}{T + 273}} \quad (\text{A.2})$$

The measured values reasonably matched the theoretical vapour pressure over a temperature range from 16°C to 38°C, covering typical ambient shop temperatures up to the RVP measurement temperature. The maxi-

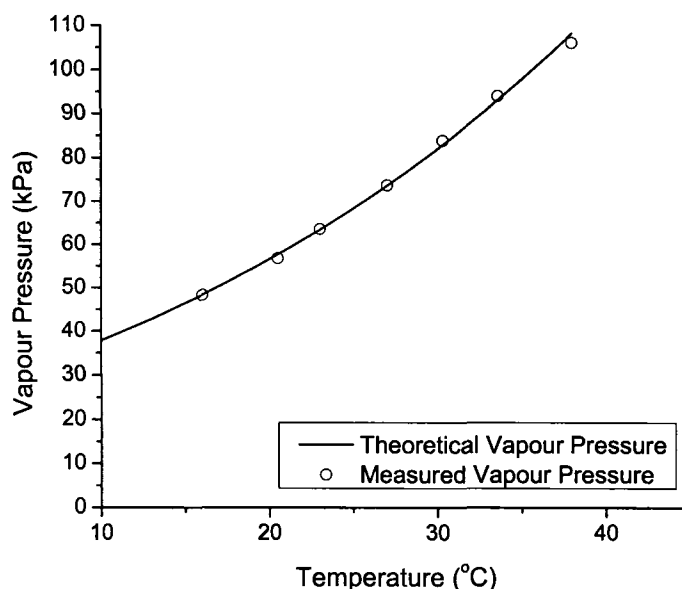
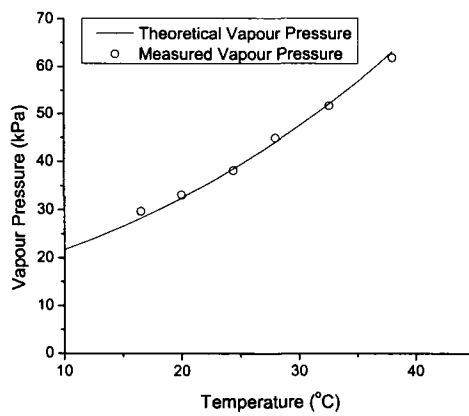


Figure A.3: Comparison of measured and theoretical vapour pressure for n-pentane.

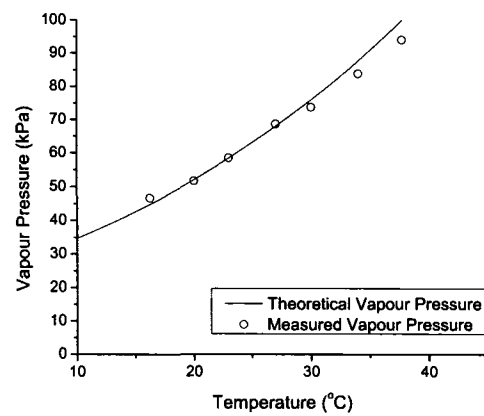
imum error between the measured and theoretical vapour pressure was 5%. The vapour pressure measured was lower than expected at high temperatures for the high volatility gasoline. This was likely because the entire bomb was not submersed in the water bath by design. Near the test temperature of 23°C, the vapour pressure error was within 2%.

A.4.3 Repeatability

A series of three measurements were taken on two separate gasoline blends to determine repeatability of the vapour pressure measurement procedure. In each case, the measurements agreed within 2%.



(a) I. O. 60



(b) I. O. 96

Figure A.4: Vapour pressure measurement for two gasoline blends. The theoretical curve is based on equation 2.5 and the independently measured Reid Vapour Pressure of 59.9 kPa (a) and 95.9 kPa (b). Gasoline designations are listed in table 3.2.

REFERENCES

- [1] John B. Heywood. *Internal Combustion Engine Fundamentals*. McGraw Hill, Inc, 1988.
- [2] Anonymous. D323-99A, Standard test method for vapor pressure of petroleum products (Reid method). ASTM.
- [3] Anonymous. D4953-99a, Standard test method for vapor pressure of gasoline and gasoline-oxygenate blends (dry method). ASTM, 1999.
- [4] Anonymous. D5191-04a, Standard test method for vapor pressure of petroleum products. ASTM, 2004.
- [5] Anonymous. "*Product Safety Reference Manual Book 5 - Laboratory Policies and Procedures*". Health Canada, 2004.
- [6] R. H. Perry and D. W. Green. *Perry's Chemical Engineers' Handbook*. McGraw Hill, Inc, 7th edition, 1997.

APPENDIX B

GAS CHROMATOGRAPH MEASUREMENTS

B.1 Introduction

The oxygen sensors used for the work in this project showed different response characteristics to gasoline-air mixtures than to nitrogen-air or butane-air mixtures. Vapour pressure measurements were convenient for calibrating the sensor response at different equilibrium concentrations, created by varying the composition of the fuel. However, vapour pressure measurements could not be used to verify the transient response of the oxygen sensors when the composition remained essentially the same. A procedure was developed to pull gas samples from the fuel tank and analyze them with a gas chromatograph (GC).

B.2 GC Measurement Procedure

A SGE 10 mL gas tight syringe was used to pull samples from the gas tank. The syringe was initially purged with air by stroking the plunger 2 times before sampling, ensuring a common starting point for all samples. The needle was inserted into silicone septums in fittings at 8 locations on the gas tank and a 4 mL sample was pulled. This sample was immediately expelled into a Vacutainer® 3 mL draw sample tube, which initially contained air under partial vacuum. The 4 mL sample size was chosen to maintain a positive pressure in the 3 mL sample tube.

The initial air contents of the sample tubes diluted the injected samples to some degree. The dilution reduced the gasoline vapour concentration in the sample tube. This was important so a moderate temperature decrease would not result in gasoline vapour components condensing in the sample tube when saturated samples were taken. The GC used was a Hewlett Packard 5890 II with an Agilent thermal conductivity detector. A 250 μL sample was injected in a Alltech CTR I column.¹

To calculate the fuel concentration in the fuel tank at the point of sample, the GC results had to be corrected for the initial sample tube contents and any air that introduced due to the sampling process. A 5 L tedlar bag was filled with pure nitrogen and sampled with the same method as used for the fuel tank samples. Figure B.1 shows the GC output for a pure nitrogen sample. The air content was calculated by subtracting the oxygen, carbon dioxide peaks, and calculating the nitrogen contribution of the air from a lab air sample, shown in figure B.2.

Once the extra air in the sampling process was accounted for, the gasoline vapour fraction could be calculated. The GC output for a typical gasoline vapour/air sample from the fuel tank is shown in figure B.3. The fuel concentration was determined by subtracting the initial air contents and the air added in the sampling process, and subtracting the air from the total remaining.

B.3 Uncertainty in GC Measurements

Gas chromatography measurements have many sources of error. The GC itself may introduce error if any leaks are present in the column or associated equipment, or if the carrier gas is off specification. For the measurements taken using the above method, the sampling process likely introduces the greatest error. The sample tubes, while under vacuum, do contain some gases and the composition may vary between tubes. The volume extracted from the tank with the syringe is diluted with this gas in the tube. The volume of the sealed portion of the syringe has some uncertainty and the

Sample Size	10
Mean	91.8%
Standard Deviation	0.5%

Table B.1: Nitrogen sample statistics.

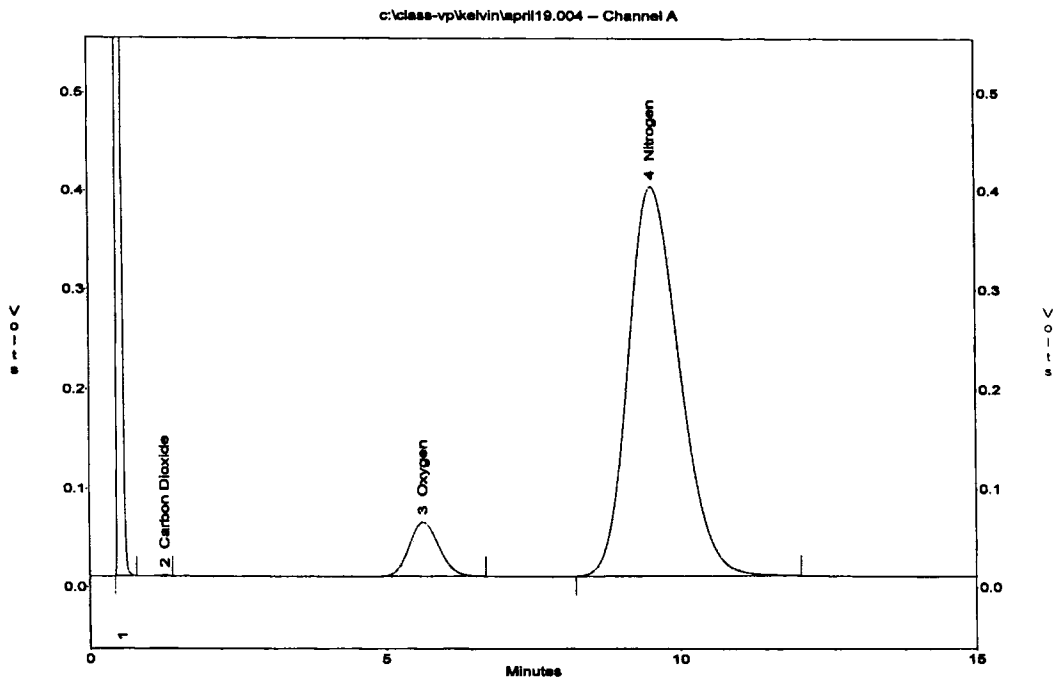
contents of the needle portion that does not get sealed are unknown, as air can diffuse into the needle as the sample is transferred from the tank to the sample tube.

To estimate the uncertainty in the GC measurements, ten samples of pure nitrogen were pulled and measured in the GC. Sample tubes were randomly selected from the entire population. Summary statistics for the gas chromatograph measured nitrogen concentration are shown in table B.1.

The nitrogen sampling and GC measurement procedure was repeatable within 1% percent, to two standard deviations.

The uncertainty in measuring gasoline vapour fraction with the GC procedure was measured by extracting four samples from the gas tank at sample points 3, 5, 6, and 7 when the vapour in the tank was at equilibrium. The GC measurement was then compared with the vapour pressure measurement at ambient temperature. The repeatability among the four sample points was 0.6%, to two standard deviations. The GC measured value of 50.2% agreed well with the predicted 50.8% gasoline fraction based on the vapour pressure measurement.

File : c:\class-vp\kelvin\april19.004
 Method : c:\class-vp\kelvin\oxypure.met
 Sample ID : t1
 Acquired : Apr 19, 2006 14:12:25



Channel A Results

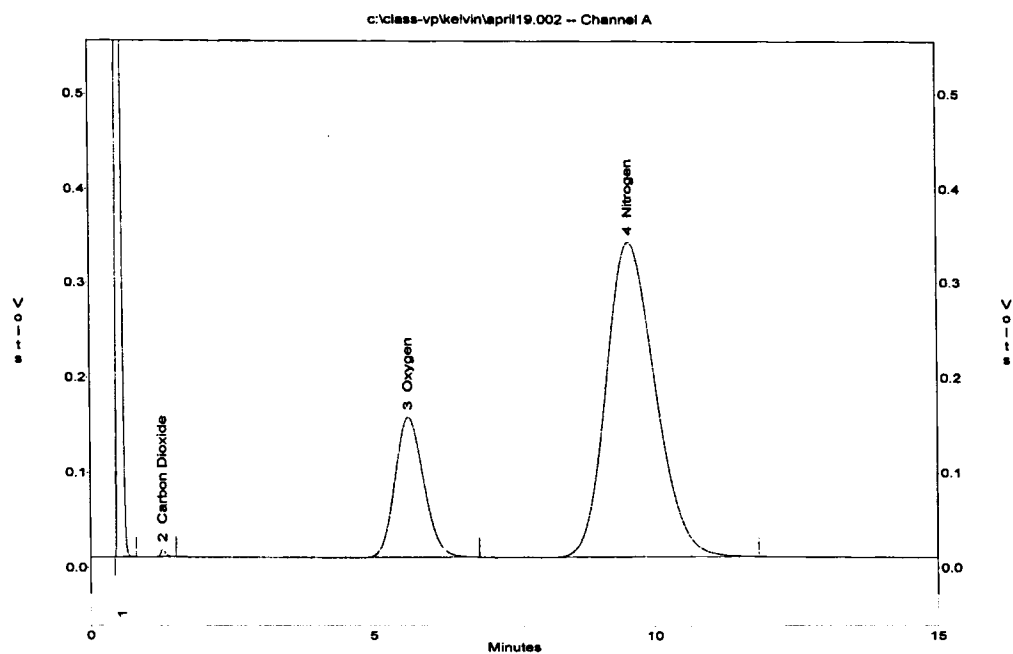
Pk No	RT	Area	Conc (%)	PEAK NAME
1	0.55	7139892	0.00	
2	1.28	5251	0.00	Carbon Dioxide
3	5.64	1927962	8.07	Oxygen
4	9.53	23716354	92.36	Nitrogen

Totals :
 32789460

Figure B.1: Pure nitrogen sample taken in Vacutainer®. Oxygen present from residue in container.

File : c:\class-vp\kelvin\april19.002
Method : c:\class-vp\kelvin\oxypure.met
Sample ID : lab air
Acquired : Apr 19, 2006 13:36:50

Page 1 of 1 (2)



Channel A Results

PK No	RT	Area	Conc (%)	PEAK NAME
1	0.56	7455676	0.00	
2	1.28	44131	0.00	Carbon Dioxide
3	5.63	5216089	21.82	Oxygen
4	9.55	19994804	77.86	Nitrogen

Totals :
32710700

Figure B.2: Laboratory air GC sample.

File : c:\class-vp\kelvin\april19.018
 Method : c:\class-vp\kelvin\oxypure.met
 Sample ID : 1
 Acquired : Apr 20, 2006 11:51:39

Page 1 of 1 (18)

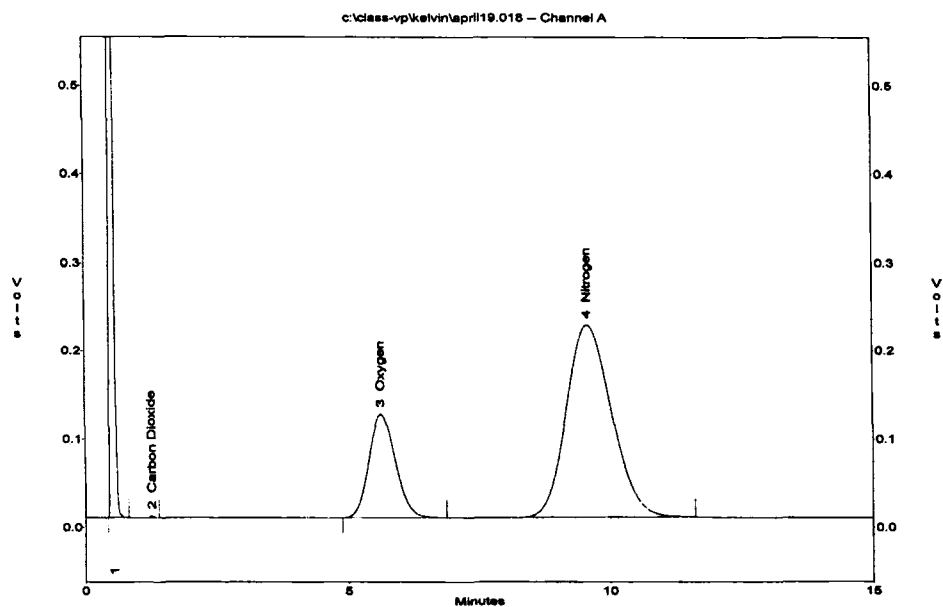


Figure B.3: Fuel tank contents sample taken in Vacutainer®. Fuel vapour concentration calculated from oxygen and nitrogen contents.

REFERENCES

- [1] K. Lien. Personal communication, June 15, 2006. Laboratory Technician, University of Alberta.

APPENDIX C

ENVITEC® O₂ SENSOR CALIBRATION

C.1 Introduction

To obtain experimental data on the gasoline vapour fractions in an automotive gasoline tank under flow conditions, a method for measuring the concentrations in the tank during testing without affecting the flow is required. Oxygen sensors can measure the oxygen fraction at a point in real time, and if the mixture at the sensor is known to be entirely composed of air and gasoline vapour, the complementary gasoline vapour fraction can be calculated.

C.2 Sensor Description and Theory

EnviteC® Oxiplus A O₂ sensors were used for experimental testing. Specifications for these sensors are given in Table C.1. The sensing element in these sensors is an electrochemical cell that produces voltage from a chemical reaction with oxygen. The operating principle is similar to a fuel cell or battery, with a cathode, electrolyte, and anode. The oxygen exposed to the sensor diffuses through a teflon membrane as shown in figure C.1, where it contacts the sensing electrode. The oxygen is reduced to hydroxyl ions and subsequently oxidizes the anode material, which is usually composed of lead.¹ The voltage output of the sensor is proportional to the rate of oxygen diffusing through the membrane.

Oxiplus A Sensor Specifications	
Measurement Range	0 to 100% oxygen
Output in Ambient Air	7 to 13 mV
Zero Offset Voltage	$\leq 40\mu\text{V}$ in N ₂
Temperature Compensation	Built In NTC
Humidity Effect	$\leq 0.03\%$ per % R.H. at 25°C
Output Drift	\leq per month
Operating Temperature	0 to 50°C
Operating Humidity	0 to 99% R.H.

Table C.1: Oxiplus A Sensor Specifications

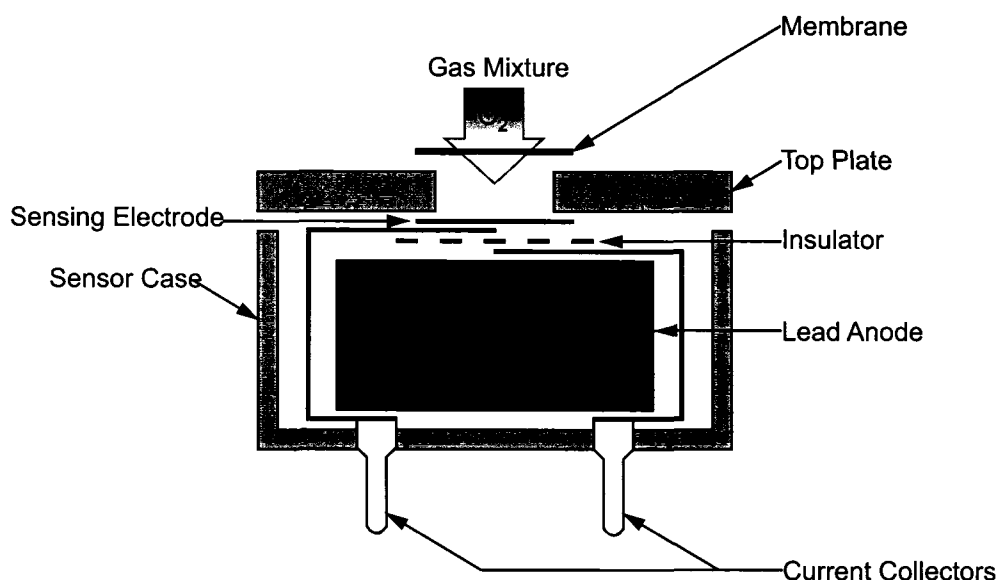


Figure C.1: Oxiplus A sensor schematic showing major components. Sensor output is dependent on rate of oxygen diffusion through a Teflon® membrane.

Oxygen diffusion through the membrane is determined by the partial pressure of oxygen present at the membrane, temperature, and the composition of the non-oxygen balance of the mixture. The Oxiplus A sensor has electronic temperature compensation to correct for any temperature deviations during testing. Carrier gas components with small molecules will allow oxygen to diffuse more readily than components with large molecules.²

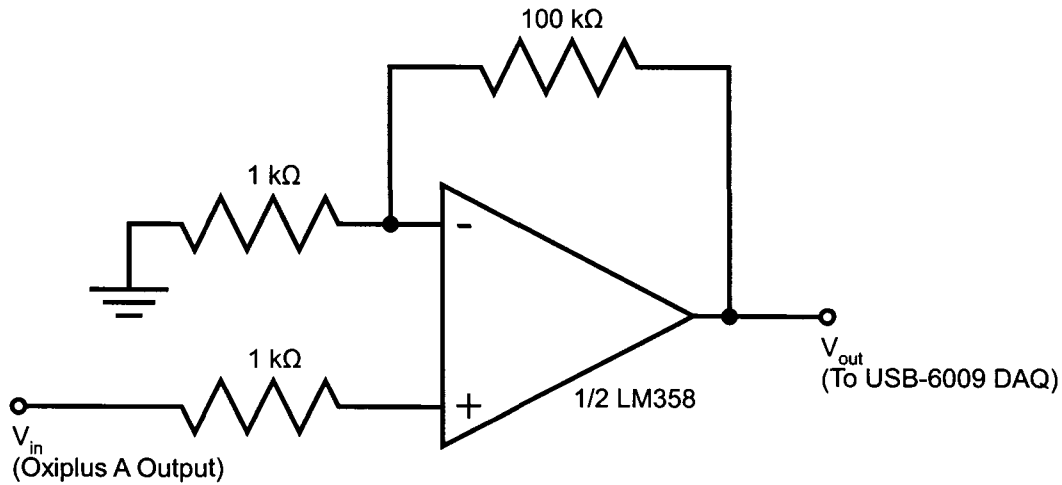


Figure C.2: A non-inverting amplifier was used to amplify the sensor output signal with a gain of 101.

A sensor calibration test sequence was required to compensate for the effect of each carrier gas used in conjunction with the sensor.

The sensitivity of the sensor is variable because of the nature of the chemical reactions within the cell. The output is dependent on the electrolyte concentration, and as the sensor ages, voltage output decreases. The effect is small over a short period of time ($\leq 1\%$ oxygen concentration drift in output per month). The sensitivity varies between sensors due to the variability of the manufacturing process, so each sensor requires individual calibration.

C.3 Signal Conditioning

Typical sensor output for the Oxiplus A sensor was approximately 7 to 11 mV for air at atmospheric pressure. Obtaining adequate resolution with the 0-10 V, 13 bit A/D converter in the National Instruments™ USB-6009 required amplification. A non-inverting amplifier with a gain of 101 as shown in figure C.2 increased ambient air output above 1 V. Resolution for this configuration was approximately 0.02 % oxygen per step for nitrogen-air mixtures with average sensor sensitivity.

The low millivolt output of the sensor introduced some noise to the acquired data. A 10 value non-weighted moving average filter implemented in the data acquisition software provided smoothing without affecting transient response significantly.

Samples were recorded at a rate of 4 Hz during the first phase of testing when air was flowing into the system. The sampling rate was decreased to 0.5 Hz after the flow was stopped and data was collected until the gasoline vapour in the system returned to equilibrium.

C.4 Sensor Calibration

The eight sensors used to monitor oxygen content at various positions in the gas tank were connected in series to a Dasibi Multi-Gas Calibrator. The Dasibi was used to produce volumetric air-nitrogen and air-butane mixtures at atmospheric pressure. Butane was chosen as one of the major components in the gasoline vapor, and because it is a gas at atmospheric conditions. The voltage output was compared between the air-butane and air-nitrogen mixtures to determine if the butane had a measurable effect on the sensor output when mixed with air. Finally, a calibration was performed with gasoline vapour.

As previously mentioned, the sensor measures oxygen partial pressure. The oxygen volumetric concentration can be calculated from the partial pressure as follows:

$$\chi_{O_2} = \frac{P_{O_2}}{P_T} \quad (C.1)$$

C.4.1 N₂-Air Calibration

An initial calibration with nitrogen was done for all 7 sensors mounted directly in the fuel tank. The calibration for sensor 1 can be seen in figure C.3. The non-inverting amplifier created a small voltage offset which was compensated for with the calibration.

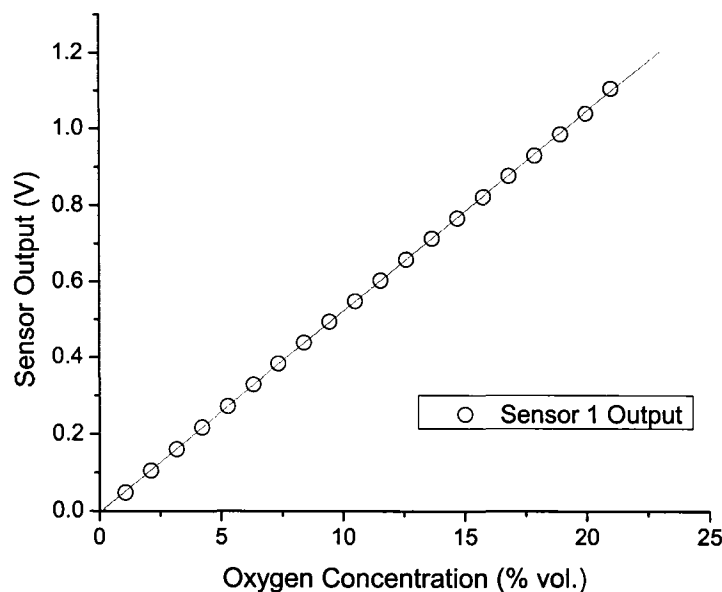


Figure C.3: Initial nitrogen-air calibration of sensor 1. The sensors exhibited excellent linearity under these conditions. Some offset from the non-inverting amplifier was evident.

C.4.2 Butane Calibration

Since the effect of significant hydrocarbon presence on sensor output was unknown, an additional calibration test was run with butane-air mixtures. Butane was chosen as the heaviest alkane that does not produce liquid at atmospheric ambient conditions, and also because it is a significant component of gasoline vapour. Butane did not produce a significant effect on sensor output compared to nitrogen-air mixtures.

C.4.3 Gasoline Vapour Calibration

Two different techniques were used for measuring gasoline vapour fraction at the oxygen sensors. Equilibrium vapour pressure measurements were taken with an evacuated test bomb. The procedure for this process is described in Appendix A. A range of equilibrium vapour pressures were ob-

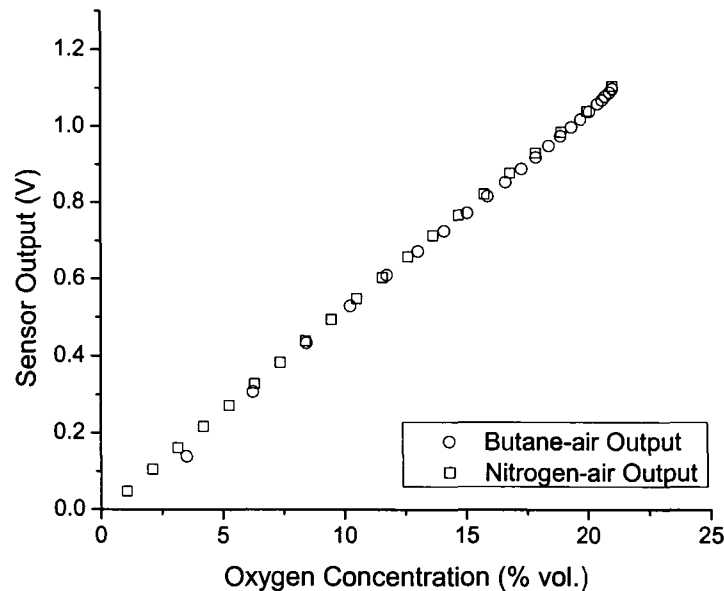


Figure C.4: Sensor 1 response to butane-air mixtures. The presence of butane did not significantly affect output compared to straight nitrogen-air mixtures.

tained by progressively weathering the gasoline with flow cycles. Gas chromatograph samples were also taken at sensor 1 during a flow cycle to verify the equilibrium vapour pressure calibration. Figure C.5 shows the comparison between calibration methods. No significant difference was noted over the concentration range seen during the flow cycle tested. Subsequently, the sensor output was not affected by the gasoline vapour composition changes due to weathering.

The electrochemical cell nature of the oxygen sensors does not provide consistent sensitivity between individual sensors. A transfer function for each sensor used to convert output voltage to gasoline vapour concentration was calculated based on the equilibrium vapour pressure calibration and is shown in figures C.6 and C.7.

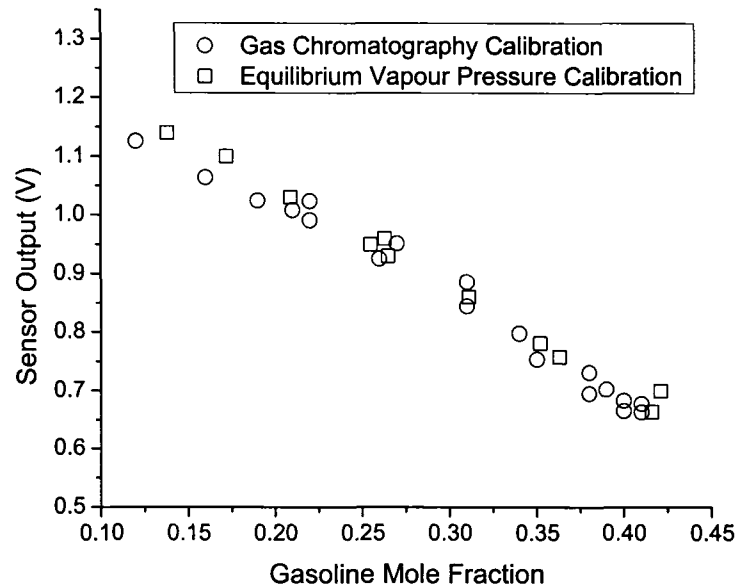


Figure C.5: Comparison of equilibrium vapour pressure calibration to transient gas chromatograph calibration. Ambient conditions were $T_{amb} = 23^{\circ}\text{C}$ and $P_{atm} = 93 \text{ kPa}$.

C.5 Sensor Transient Response

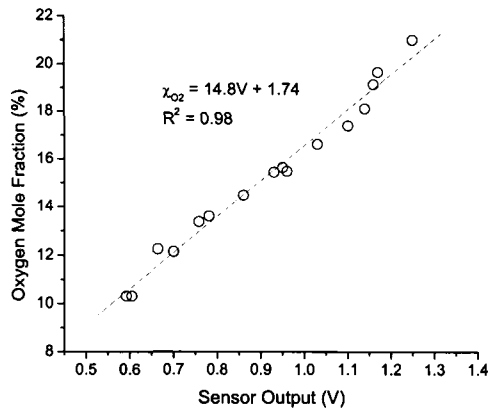
C.5.1 Oxygen Concentration Response

The time response of the oxygen sensors was important when measuring transient oxygen concentrations. Sensor response was considered to two transient parameters: oxygen concentration in a nitrogen/air mixture and total pressure of air.

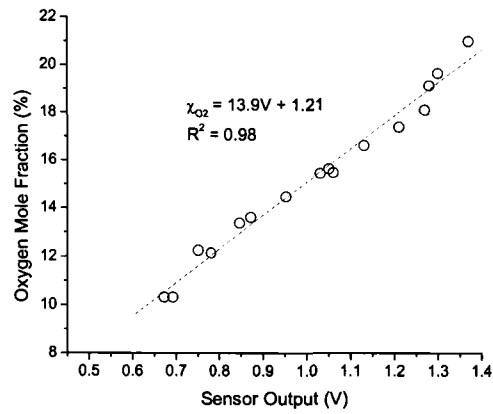
First, the sensors were exposed to a step change in oxygen concentration from 21% (pure air) to 0% (pure nitrogen). The response is shown in figure C.8. The sensor exhibited first-order response characteristics as expected.

The differential equation describing this response is³

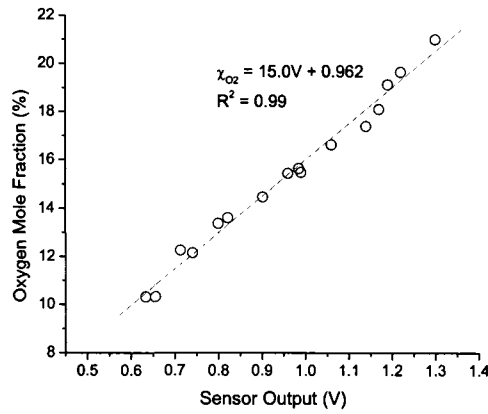
$$\tau \frac{dy}{dt} + y = Kx \quad (\text{C.2})$$



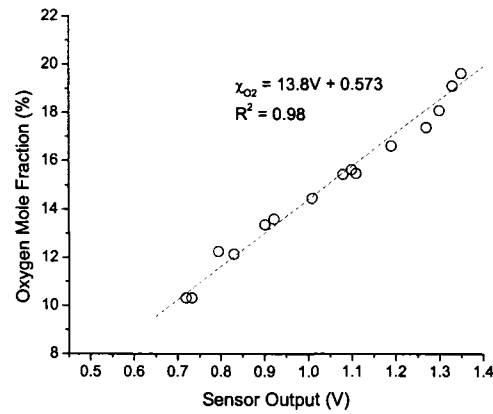
(a) Sensor 1



(b) Sensor 2



(c) Sensor 3

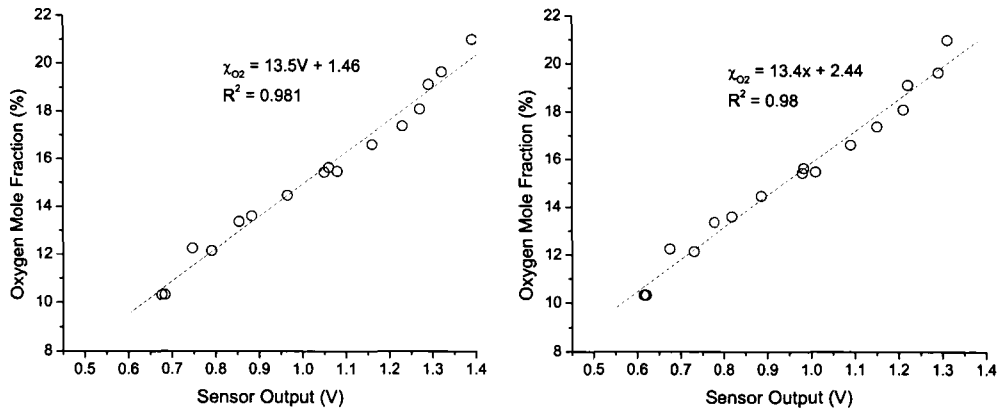


(d) Sensor 4

Figure C.6: Gasoline vapour fraction transfer functions for sensors 1 through 4 when measuring gasoline vapour/air mixtures. Ambient conditions were $T_{amb} = 23^{\circ}\text{C}$ and $P_{atm} = 93 \text{ kPa}$.

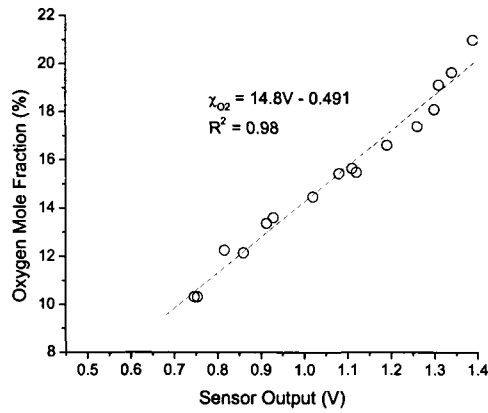
In this case, the initial condition at $t = 0$ is $y = 21\%$. At $t = 0$, the input x_o drops to 0% . The general equation for the output y is

$$y = Ce^{\frac{-t}{\tau}} + Kx_o \quad (\text{C.3})$$



(a) Sensor 5

(b) Sensor 6



(c) Sensor 7

Figure C.7: Gasoline vapour fraction transfer functions for sensors 5 through 7 when measuring gasoline vapour/air mixtures. Ambient conditions were $T_{amb} = 23^\circ\text{C}$ and $P_{atm} = 93 \text{ kPa}$.

At $t = 0$, $y = 21\%$, and $x_o = 0$, so

$$C = 21 \quad (\text{C.4})$$

Thus, the sensor response under these conditions becomes

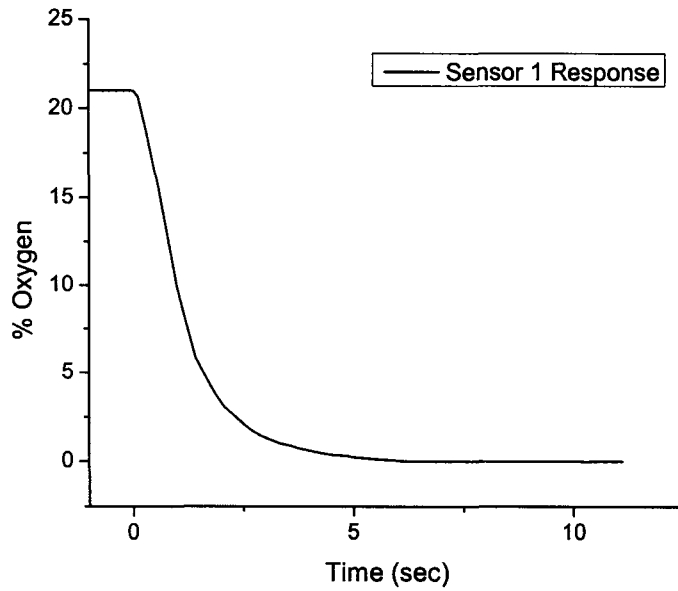


Figure C.8: Sensor 1 response to a step input from air to 100 % nitrogen. The output reached 90% of the steady state value in 2.9 seconds.

$$y = 21e^{-\frac{t}{\tau}} \quad (\text{C.5})$$

Based on the sensor response in figure C.8, the time constant $\tau = 1.1$ sec.

C.5.2 Total Pressure Response

The transient response to total pressure changes was also measured. A step pressure change from atmospheric pressure (93 kPa absolute) to 8 kPa (101 kPa absolute) with air was imposed on the sensor.

In this case, the initial condition is now a oxygen partial pressure of $y = 20.3$ kPa at $t = 0$. The step input is now $x_o = 22.2$. Under these conditions, equation C.3 becomes

$$y = 22.2 - 1.9e^{-\frac{t}{\tau}} \quad (\text{C.6})$$

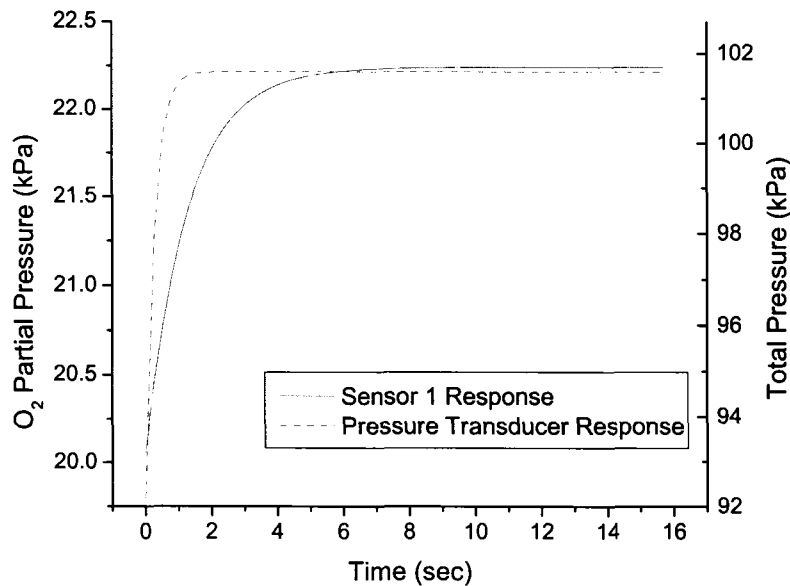


Figure C.9: Sensor 1 response to a step input from air at atmospheric pressure (93 kPa absolute) to 101 kPa absolute. The output reached 90% of the steady state value in 2.7 seconds.

Based on the measured step response, the time constant $\tau = 1.3$ sec for this case.

C.5.3 Moving Average Filter Effects on Transient Response

Electrical noise introduced in the amplification was reduced with a 10 value non-weighted moving average filter. The pressure step input was repeated with the filter active to see if the transient response was affected. The filter increased the time response by 15%, shown in figure C.10. The time constant τ was increased to 1.4 sec with the use of the filter.

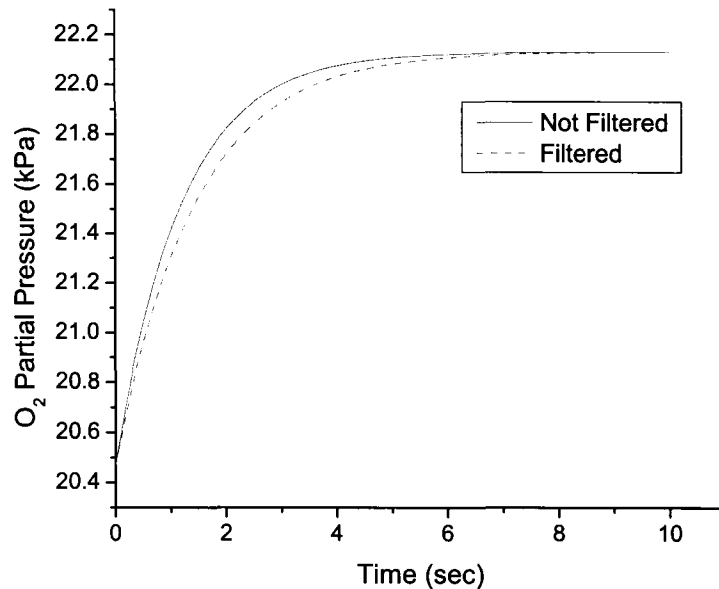


Figure C.10: Sensor 1 response to a step input from air at atmospheric pressure (93 kPa absolute) to 101 kPa absolute, with no filtering and with a 10 value non-weighted moving average filter. The output reached 90% of the steady state value in 3.4 sec, an increase of 15%.

C.6 Measurement Uncertainty

The application of the Oxiplus A sensor to measuring transient oxygen concentrations in gasoline vapour/air mixtures introduces uncertainty from the transient response characteristics of the sensor and the altered sensor sensitivity from the gasoline.

C.6.1 Transient Response Uncertainty

As previously determined in section C.5.1, the time constant for the oxygen sensors was $\tau = 1.4$ sec. The maximum rate of change of gasoline vapour fraction measured was 101% HC per minute at the sensor 7 location. Based on a time lag of τ ,

$$\epsilon_{\chi_{gas}} = \frac{\partial \chi_{gas}}{\partial t} \tau \quad (C.7)$$

The maximum error in gasoline vapour fraction due to the transient sensor response was 2% HC.

C.6.2 Non-linear Sensor Response Uncertainty

The oxygen sensor response tended to deviate from a linear response near the extents of the range of gasoline vapour tested. At low gasoline fractions, the linear approximation for the sensor response resulted in an error of 3.5% HC.

REFERENCES

- [1] Anonymous. City Technology Ltd oxygen sensors: General overview. Retrieved March 12, 2006, from <http://www.citytech.com/technology/02-sensors.asp>, 2006.
- [2] Alphasense Ltd. Application note AAN009. 2005.
- [3] D. Wilson. University of alberta Mec E 300 notes and illustrations. 2002.

APPENDIX D

CFX MODEL

D.1 Introduction

CFX 5.7, a commercial computational fluid dynamics package, was used to numerically model flow in a gas tank under leak testing conditions. This model could be used to estimate the total flammable volume formed in a typical fuel tank when leak testing is performed with air.

D.2 Fluid Properties

Most of the fluid properties were taken from the CFX built in library, with the exception of the equilibrium fuel vapour pressure and the binary kinematic diffusivity of the fuel vapour in air. The equilibrium vapour pressure was based on the empirical data collected in the experimental section of this work. The kinematic diffusivity was calculated with the method of Reid.¹

$$D_{AB} = \frac{3}{16} \frac{\sqrt{4\pi k_B T / M_{AB}}}{(P / \bar{R} T) \pi \sigma_{AB}^2 \Omega_D} f_D \quad (\text{D.1})$$

Turns¹ gives the method for calculating M_{AB} , σ_{AB} , and Ω_D . The correction factor f_D was taken to be 1.

Figure D.1 shows the diffusivity coefficient for saturated hydrocarbons found in gasoline vapour. The calculated value for hexane diffusivity in air was in close agreement with tabulated data for hexane diffusivity in nitro-

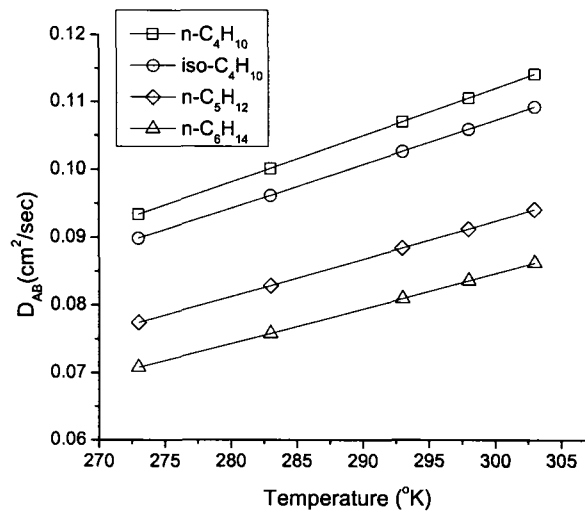


Figure D.1: Binary diffusivity of saturated hydrocarbons typically found in gasoline vapour.

gen.²

D.3 Fuel Species Sensitivity Study

The sensitivity of the model to the fuel vapour properties was examined by completing three model runs using n-butane, n-pentane, and n-hexane properties. Figure D.2 shows the vertical fuel vapour fraction gradient at the edge of the tank for each fuel species. Very little difference was noted after 2.5 minutes of flow. After a flow duration of 10 minutes, hexane and pentane remained essentially identical. Butane produced a maximum difference of 3% fuel vapour relative to pentane.

D.4 Mesh Refinement Study

CFD modelling approximates the solution of the fluid properties at a finite number of points. The number of points chosen to solve a particular problem is always a compromise between accuracy and computational expense.

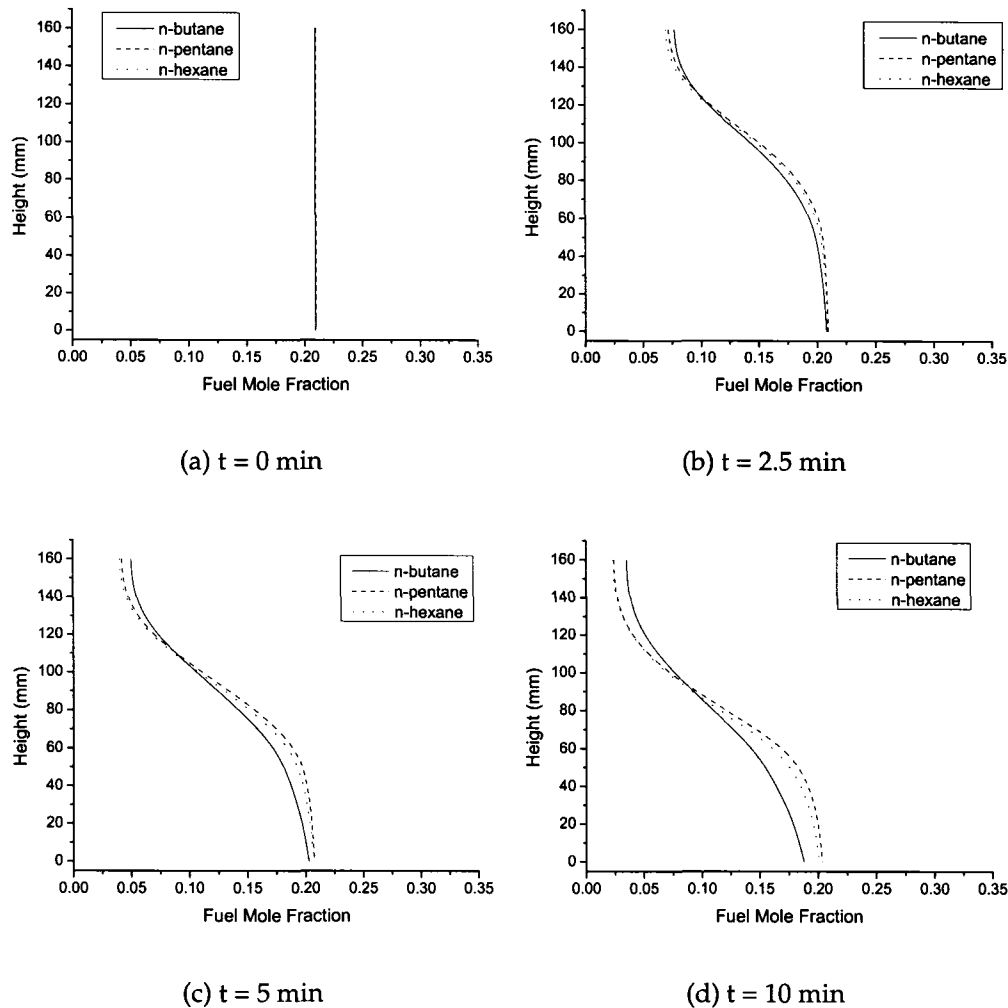


Figure D.2: Sensitivity of model results to fuel species. Typical gasoline vapour components n-butane, n-pentane, and n-hexane were considered.

The computers used for this modeling work were desktop PCs with 2.4 GHz processors and 1 Gb of RAM. A typical simulation of 10 minutes of air flow into the fuel tank using the standard mesh shown in figure D.3 required 5 days to complete using the available computing resources. An additional model run using a finer mesh, shown in figure D.4, was completed to determine the solution sensitivity to the mesh size. The statistics for the standard

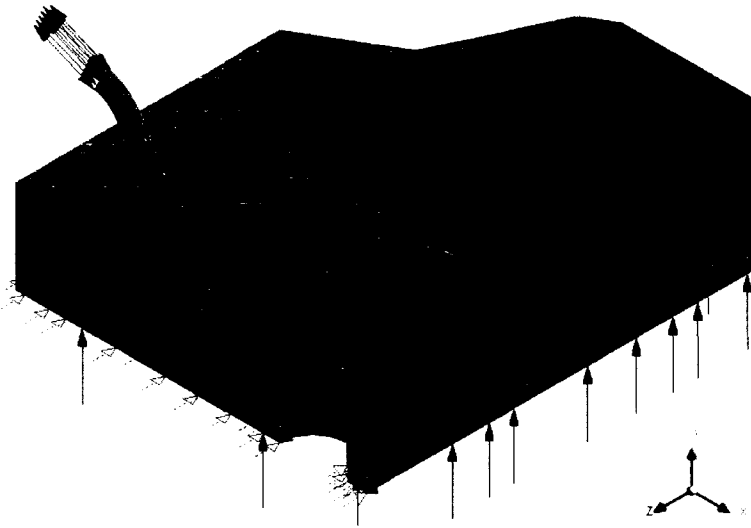


Figure D.3: Coarse mesh of fuel tank model. The vertical dimension in the tank vapour space was resolved with 8 elements.

Number of Nodes	24422
Number of Elements	122152

Table D.1: Coarse Mesh Statistics

Number of Nodes	83866
Number of Elements	439094

Table D.2: Fine Mesh Statistics

coarse mesh and fine mesh are given in table D.1 and table D.2, respectively.

The fine mesh simulation was limited to 5 minutes of air flow time by the available computational resources. At this point, the results for each mesh were compared. Figure D.5 (a) and (b) compare the gasoline vapour concentration gradient in the tank after 2.5 minutes and 5 minutes of flow, respectively.

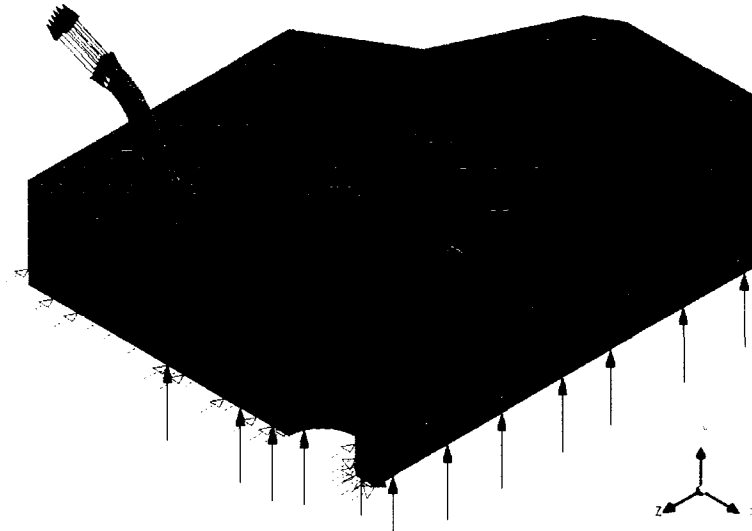


Figure D.4: Fine mesh of fuel tank model. The finer mesh provided double the resolution (16 elements) of the vertical gasoline vapour fraction gradient.

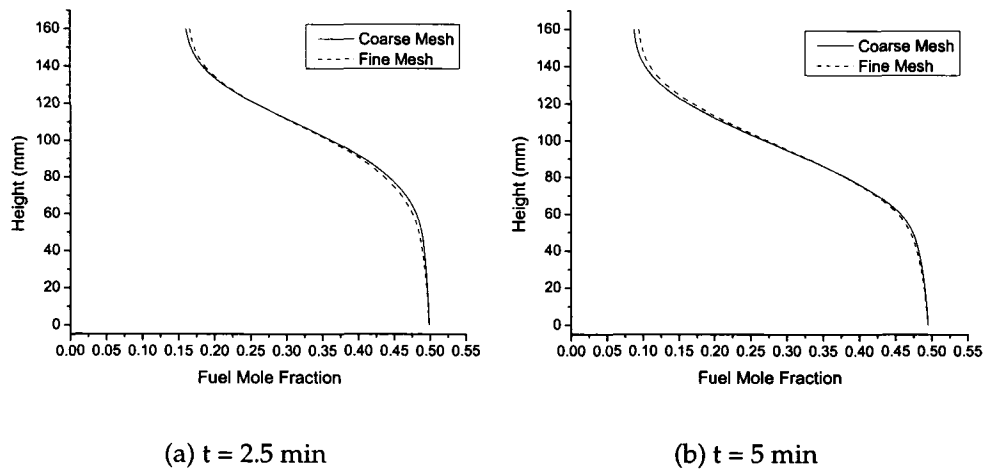


Figure D.5: Sensitivity of model results to mesh size. Increasing the mesh element density by a factor of four did not change the model results substantially.

D.5 Sample CFX Input File

A CCL file for a model run of 10 LPM flow from the service port with an initial fuel mole fraction of .21 is included below. For clarity, the fluid properties for all substances not used in the simulation are removed.

```
# State file created: 2006/06/14 16:00:03
# CFX-5.7.1 build 2004.11.12-23.20

FLOW:
  SOLUTION UNITS:
    Angle Units = [rad]
    Length Units = [m]
    Mass Units = [kg]
    Solid Angle Units = [sr]
    Temperature Units = [K]
    Time Units = [s]
  END
  OUTPUT CONTROL:
    RESULTS:
      File Compression Level = Default
      Option = Full
    END
    TRANSIENT RESULTS:Transient Results 1
      File Compression Level = Default
      Option = Minimal
      Output Variables List = Absolute Pressure,Air Ideal Gas.Mass Fraction,
      Air Ideal Gas.Molar Fraction,C5H12.Mass Fraction,C5H12.Molar Fraction,
      Density,Pressure,Velocity
      Time Interval = 10 [s]
    END
  END
  DOMAIN:Tank
    Coord Frame = Coord 0
    Domain Type = Fluid
    Fluids List = Mixture
    Location = Assembly,Assembly 2
  BOUNDARY:Sym
    Boundary Type = SYMMETRY
    Location = Symmetry,Symmetry 2
  END
  BOUNDARY:Tank Default
    Boundary Type = WALL
```

```
Location = F100.121,F101.121,F102.121,F103.121,F104.121,F105.121,
F106.121,F107.121,F109.121,F110.121,F111.121,F112.121,F113.121,
F114.121,F115.121,F116.121,F118.121,F119.121,F120.121,F122.121,
F123.121,F124.121,F125.121,F28.25,F29.25,F30.25,F32.25,F34.25,
F95.121,F96.121,F97.121,F98.121
BOUNDARY CONDITIONS:
  WALL INFLUENCE ON FLOW:
    Option = No Slip
  END
  WALL ROUGHNESS:
    Option = Smooth Wall
  END
END
DOMAIN MODELS:
  BUOYANCY MODEL:
    Buoyancy Reference Density = 1.18 [kg m-3]
    Gravity X Component = 0 [m s-2]
    Gravity Y Component = -9.81 [m s-2]
    Gravity Z Component = 0 [m s-2]
    Option = Buoyant
  BUOYANCY REFERENCE LOCATION:
    Cartesian Coordinates = -0.637276 [m], 0.103167 [m], 0.0176777 [m]
    Option = Cartesian Coordinates
  END
END
  DOMAIN MOTION:
    Option = Stationary
  END
  MESH DEFORMATION:
    Option = None
  END
  REFERENCE PRESSURE:
    Reference Pressure = 1 [atm]
  END
END
FLUID MODELS:
  COMBUSTION MODEL:
    Option = None
  END
  COMPONENT:Air Ideal Gas
    Option = Constraint
  END
  COMPONENT:C5H12
    Kinematic Diffusivity = Dab
    Option = Transport Equation
  END
  HEAT TRANSFER MODEL:
    Fluid Temperature = 293 [K]
```

```
    Option = Isothermal
END
THERMAL RADIATION MODEL:
    Option = None
END
TURBULENCE MODEL:
    Option = k epsilon
    BUOYANCY TURBULENCE:
        Option = Production
    END
END
TURBULENT WALL FUNCTIONS:
    Option = Scalable
END
END
BOUNDARY:Inlet
    Boundary Type = INLET
    Location = Evap Inlet
    BOUNDARY CONDITIONS:
        COMPONENT:C5H12
            Mass Fraction = 0.0
            Option = Mass Fraction
        END
        FLOW REGIME:
            Option = Subsonic
        END
        MASS AND MOMENTUM:
            Normal Speed = flow
            Option = Normal Speed
        END
        TURBULENCE:
            Option = Medium Intensity and Eddy Viscosity Ratio
        END
    END
END
BOUNDARY:Outlet
    Boundary Type = OPENING
    Location = Filler
    BOUNDARY CONDITIONS:
        COMPONENT:C5H12
            Mass Fraction = 0
            Option = Mass Fraction
        END
        FLOW DIRECTION:
            Option = Normal to Boundary Condition
        END
        FLOW REGIME:
            Option = Subsonic
        END
    END
```

```
MASS AND MOMENTUM:
  Option = Static Pressure
  Relative Pressure = 0.2 [Pa]
END
TURBULENCE:
  Option = Medium Intensity and Eddy Viscosity Ratio
END
END
BOUNDARY:Liquid
  Boundary Type = INLET
  Location = Liquid
  BOUNDARY CONDITIONS:
    COMPONENT:C5H12
    Mass Fraction = VMF
    Option = Mass Fraction
  END
  FLOW REGIME:
    Option = Subsonic
  END
  MASS AND MOMENTUM:
    Normal Speed = Evap
    Option = Normal Speed
  END
  TURBULENCE:
    Option = Medium Intensity and Eddy Viscosity Ratio
  END
END
BOUNDARY:Domain Interface 1 Side Tank Part 1
  Boundary Type = INTERFACE
  Location = F117.121
  BOUNDARY CONDITIONS:
    COMPONENT:C5H12
    Option = Conservative Interface Flux
  END
  MASS AND MOMENTUM:
    Option = Conservative Interface Flux
  END
  TURBULENCE:
    Option = Conservative Interface Flux
  END
END
BOUNDARY:Domain Interface 1 Side Tank Part 2
  Boundary Type = INTERFACE
  Location = F26.25
  BOUNDARY CONDITIONS:
    COMPONENT:C5H12
```

```
        Option = Conservative Interface Flux
    END
    MASS AND MOMENTUM:
        Option = Conservative Interface Flux
    END
    TURBULENCE:
        Option = Conservative Interface Flux
    END
    END
    END
    END
    DOMAIN INTERFACE:Domain Interface 1
        Boundary List1 = Domain Interface 1 Side Tank Part 1
        Boundary List2 = Domain Interface 1 Side Tank Part 2
        Interface Type = Fluid Fluid
    INTERFACE MODELS:
        FRAME CHANGE:
            Option = None
        END
        PITCH CHANGE:
            Option = Automatic
        END
    END
    END
    SIMULATION TYPE:
        Option = Transient
    INITIAL TIME:
        Option = Automatic
    END
    TIME DURATION:
        Option = Total Time
        Total Time = 10 [min]
    END
    TIME STEPS:
        Option = Timesteps
        Timesteps = 4800* .125[sec] %Complete list of timesteps removed for clarity
    END
    END
    INITIALISATION:
        Option = Automatic
    INITIAL CONDITIONS:
        Velocity Type = Cartesian
    CARTESIAN VELOCITY COMPONENTS:
        Option = Automatic with Value
        U = 0 [m s-1]
        V = 0 [m s-1]
        W = 0 [m s-1]
    END
    COMPONENT:C5H12
```

```
    Mass Fraction = VMF
    Option = Automatic with Value
END
EPSILON:
    Option = Automatic
END
K:
    Option = Automatic
END
STATIC PRESSURE:
    Option = Automatic with Value
    Relative Pressure = 0 [Pa]
END
END
END
SOLVER CONTROL:
  ADVECTION SCHEME:
    Option = High Resolution
  END
  CONVERGENCE CONTROL:
    Maximum Number of Coefficient Loops = 9
  END
  CONVERGENCE CRITERIA:
    Residual Target = 0.00001
    Residual Type = RMS
  END
  TRANSIENT SCHEME:
    Option = Second Order Backward Euler
    Timestep Initialisation Option = Extrapolation
  END
END
END

MATERIAL:Air Ideal Gas
Material Description = Air Ideal Gas (constant Cp)
Material Group = Air Data, Calorically Perfect Ideal Gases
Option = Pure Substance
Thermodynamic State = Gas
PROPERTIES:
  Option = General Material
  DYNAMIC VISCOSITY:
    Dynamic Viscosity = 1.831E-05 [kg m-1 s-1]
    Option = Value
  END
  REFRACTIVE INDEX:
    Option = Value
    Refractive Index = 1.0 [m m-1]
  END
  SCATTERING COEFFICIENT:
```

```
Option = Value
Scattering Coefficient = 0.0 [m^-1]
END
ABSORPTION COEFFICIENT:
Absorption Coefficient = 0.01 [m^-1]
Option = Value
END
THERMAL CONDUCTIVITY:
Option = Value
Thermal Conductivity = 2.61E-2 [W m^-1 K^-1]
END
EQUATION OF STATE:
Molar Mass = 28.96 [kg kmol^-1]
Option = Ideal Gas
END
SPECIFIC HEAT CAPACITY:
Option = Value
Reference Pressure = 1 [atm]
Reference Specific Enthalpy = 0. [J/kg]
Reference Specific Entropy = 0. [J/kg/K]
Reference Temperature = 25 [C]
Specific Heat Capacity = 1.0044E+03 [J kg^-1 K^-1]
Specific Heat Type = Constant Pressure
END
END
END
MATERIAL:C5H12
Material Description = Pentane C5H12
Material Group = Gas Phase Combustion
Option = Pure Substance
Thermodynamic State = Gas
PROPERTIES:
Option = General Material
SPECIFIC HEAT CAPACITY:
Option = NASA Format
Reference Pressure = 1 [atm]
Reference Temperature = 25 [C]
TEMPERATURE LIMITS:
Lower Temperature = 300 [K]
Midpoint Temperature = 1000 [K]
Upper Temperature = 4000 [K]
END
LOWER INTERVAL COEFFICIENTS:
NASA a1 = 0.01877908E+02 []
NASA a2 = 0.04121646E+00 [K^-1]
NASA a3 = 0.01253234E-03 [K^-2]
NASA a4 = -0.03701537E-06 [K^-3]
NASA a5 = 0.01525569E-09 [K^-4]
NASA a6 = -0.02003816E+06 [K]
```

```

        NASA a7 = 0.01877257E+03 []
    END
UPPER INTERVAL COEFFICIENTS:
    NASA a1 = 0.01667798E+03 []
    NASA a2 = 0.02114483E+00 [K^-1]
    NASA a3 = -0.03533321E-04 [K^-2]
    NASA a4 = -0.05742202E-08 [K^-3]
    NASA a5 = 0.01515948E-11 [K^-4]
    NASA a6 = -0.02553670E+06 [K]
    NASA a7 = -0.06372940E+03 []
    END
    END
DYNAMIC VISCOSITY:
    Dynamic Viscosity = 6.7E-06 [kg m^-1 s^-1]
    Option = Value
    END
REFRACTIVE INDEX:
    Option = Value
    Refractive Index = 1.0 [m m^-1]
    END
SCATTERING COEFFICIENT:
    Option = Value
    Scattering Coefficient = 0.0 [m^-1]
    END
ABSORPTION COEFFICIENT:
    Absorption Coefficient = 1.0 [m^-1]
    Option = Value
    END
THERMAL CONDUCTIVITY:
    Option = Value
    Thermal Conductivity = 14.4E-03 [W m^-1 K^-1]
    END
EQUATION OF STATE:
    Molar Mass = 72.15 [kg kmol^-1]
    Option = Ideal Gas
    END
    END
END
MATERIAL:Mixture
    Material Group = Air Data, Gas Phase Combustion
    Materials List = Air Ideal Gas, C5H12
    Option = Variable Composition Mixture
    END
CEL:
    EXPRESSIONS:
        Dab = 8.85E-6 [m^2 s^-1]
        Evap = (VMF-
            (areaAve(C5H12.Mass Fraction)@Domain Interface 1 Side Tank Part 1))*const

```

```
VMF = 0.3984
const = Dab/((1-VMF)*length)
flow = inletv - inletv*step((t - flowtime)/1 [s])
flowtime = 10 [min]
inletv = 6.4 [m s^-1]
length = 0.02 [m]
END
END
END

REGION ATLAS:GTM atlas
  REGION MAP:Primary map
    REGION:Default 2D Region 2
      Region List = F28.25,F29.25,F30.25,F32.25,F34.25
    END
    REGION:Interface 2
      Region List = F26.25
    END
    REGION:Liquid
      Region List = F27.25
    END
    REGION:Symmetry 2
      Region List = F31.25,F33.25
    END
    REGION:Default 2D Region
      Region List = F100.121,F101.121,F102.121,F103.121,F104.121,F105.121,
        F106.121,F107.121,F109.121,F110.121,F111.121,F112.121,F113.121,
        F114.121,F115.121,F116.121,F118.121,F119.121,F120.121,F122.121,
        F123.121,F124.121,F125.121,F95.121,F96.121,F97.121,F98.121
    END
    REGION:Evap Inlet
      Region List = F99.121
    END
    REGION:Filler
      Region List = F108.121
    END
    REGION:Interface
      Region List = F117.121
    END
    REGION:Symmetry
      Region List = F126.121
    END
  END
END

COMMAND FILE:
  Version = 5.7
END
```

REFERENCES

- [1] S. R. Turns. *An Introduction to Combustion: Concepts and Applications*. McGraw Hill, Inc, 2nd edition, 2000.
- [2] R. H. Perry and D. W. Green. *Perry's Chemical Engineers' Handbook*. McGraw Hill, Inc, 7th edition, 1997.

APPENDIX E

FUEL TANK FLAMMABLE MIXTURE IGNITION: FIELD TESTING

E.1 Introduction

A flammable mixture ignited in a fuel tank has the potential to do damage to the fuel system components, start secondary fires, and injure service personnel. A field test was completed to directly confirm the creation of flammable mixtures, and indicate the extent of damage possible in an ignition event after performing a leak detection procedure.

E.2 Equipment and Procedure

A typical steel "thin profile" gasoline fuel tank from a 1997 Chevrolet Cavalier with approximately 4 L of low volatility, 60 kPa RVP gasoline was connected to an air line. The ambient temperature at the time of testing was 15°C. The air flow was metered with an OMEGA FMA2200 flow meter, and controlled with a 1/4" needle valve. An exploding wire ignition system was used to ignite the mixture in the tank. The exploding wire was inserted near the top of the fuel sending unit, one of the possible ignition locations for an in-service gasoline tank. A remote switch was used to trigger the exploding wire.

The gasoline vapour in the tank was allowed to reach equilibrium before starting air flow. After air was allowed to flow into the tank at 10 LPM for

a duration of 15 minutes, the exploding wire was activated. The ignition event was captured on digital video.

E.3 Results

Figure E.1 shows the results of the flammable mixture ignition. The fuel pump insert/sending unit was launched and the tank experienced a large amount of deformation. Flames were noted at the base of the sending unit as it exited the fuel tank.

The sending unit proved to be the weak point in this steel tank configuration and once it was expelled from the tank, the remaining combustion products were able to vent from the large opening left in the tank. Plastic tank configurations may experience different results, but were not tested.

The liquid level in the tank was very low and all the fuel in the sending unit components, (such as the fuel send line, return line, and pump), was drained before the test was run. In a normal operating vehicle configuration, these components will contain fuel, possibly under pressure. In the event that the sending unit fails during an explosion, liquid fuel could be spilled and start a secondary fire. At any rate, this test shows that fuel system components can be explosively propelled if flammable vapours in the tank are ignited.

E.4 Conclusions

A fuel tank containing low volatility gasoline at normal ambient temperature was exposed to a typical air flow used during leak testing. The flammable vapours formed in the tank were ignited from an internal source to see the extent of damage that would be caused. The fuel tank experienced significant deformation and the fuel sending unit was propelled out of the tank.

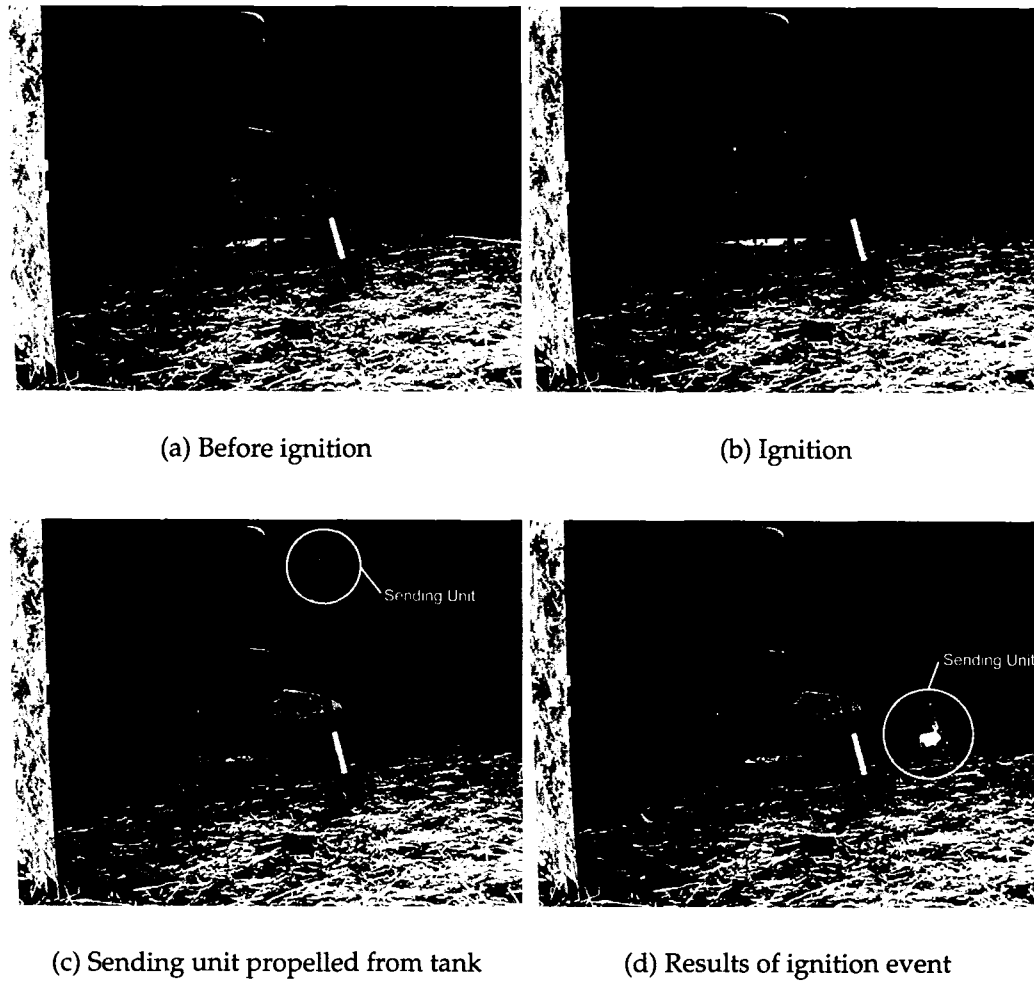


Figure E.1: The flammable mixture formed in a fuel tank under typical leak testing conditions is ignited. Flow rate: 15 LPM, Flow duration: 15 minutes.